The role of Snail and Slug in invasion and cancer stem cell maintenance in glioblastoma multiforme

Inauguraldissertation

eingereicht im Fachbereich Medizin
in Erfüllung der Anforderungen zur Erlangung des akademischen Grades Ph.D.
der Fachbereiche Veterinärmedizin und Medizin
der Justus-Liebig-Universität Gießen

Vorgelegt von Sarah Goos
aus Herborn

Gießen 2015

Aus dem Institut für Neuropathologie

(Direktor: Prof. Dr.med. Till Acker)

des Fachbereichs Medizin

Erster Gutachter und Mitglied der Prüfungskommission: Prof. Dr. Till Acker
Zweiter Gutachter und Mitglied der Prüfungskommission : Prof. Dr. Amparo Acker-Palmer

Weitere Gutachter in der Prüfungskommission:

Tag der Disputation:

Declaration

I declare that I have completed this dissertation single-handedly without the unauthorized help of second party and only with the assistance acknowledged therein. I have appropriately acknowledged and referenced all text passages that are derived literally from or based on the content of published or unpublished work of others, and all information that relates to verbal communications. I have abided by the principles of good scientific conduct laid down in the charter of the Justus Liebig University of Giessen in carrying out the investigations described in the dissertation.

Table of content

1. Summary

Glioblastoma multiforme (GBM) is the most common tumour of the central nervous system. Despite some progress in the therapy of the disease, patients still have a poor prognosis and a median survival of approximately 15 months. The biggest obstacle for successful surgical removal of glioblastoma is the high infiltration of invasive cancer cells throughout the brain. This makes it impossible to remove the complete tumour tissue, eventually resulting in relapse. Recent evidence suggests that glial-to-mesenchymal transition (GMT), a cellular program comparable to epithelial-to-mesenchymal transition (EMT), could play a major role in controlling the invasiveness of glioma cells. The transcription factors Snail and Slug are known to be major regulators of EMT in epithelial cancers. We therefore hypothesized that they may act as key components of GMT in glioma. Analysis of the expression of Snail and Slug in GBMs of different molecular subclasses revealed that these two EMT regulators are mainly expressed in the mesenchymal GBM subclass. By profiling a panel of signature markers we demonstrate that the combined loss of Snail and Slug impaired the TGFβ1-induced transition from a glial/proneural phenotype to a mesenchymal phenotype in GBM cells. Furthermore, we show that Snail and Slug play a crucial role in controlling glioblastoma stem cell properties, such as self-renewal and the expression of cancer stem cell markers. In line with their role in GMT, Snail and Slug silencing led to a severely impaired invasive behaviour of GBM cells in vitro. Importantly, we found that Snail and Slug silenced GBM cells showed significantly reduced tumour growth in an orthotopic mouse xenograft model. Detailed analysis revealed that the reduced growth did not result from changes in proliferation and apoptosis due to the silencing of Snail and Slug. Instead, the invasiveness of Snail and Slug silenced cells was drastically reduced. In summary, this work demonstrates that Snail and Slug are major regulators of GMT in glioma, controlling the transition from a glial/proneural to a mesenchymal phenotype. Importantly, the mesenchymal phenotype is closely connected to the adoption of invasive and stem cell properties indicating that these are the major mechanisms through which Snail and Slug regulate GBM growth. This improved understanding of GMT in glioma could help to optimize existing GBM treatments and provide a basis for the development of novel therapeutic strategies.

2. Zusammenfassung

Glioblastoma multiforme (GBM) ist der häufigste Tumor des zentralen Nervensystems. Trotz großer Fortschritte in der Therapie der Erkrankung haben Patienten immer noch eine schlechte Prognose und eine mittlere Lebenserwartung von 15 Monaten. Das größte Hindernis bei der chirurgischen Entfernung des Tumors ist die hohe Infiltration des Gehirns durch invasive Krebszellen. Dadurch ist es nahezu unmöglich das vollständige Tumorgewebe zu entfernen und viele Patienten leiden unter einem Rezidiv. Neueste Erkenntnisse legen nahe, dass gliale zu mesenchymale Transition (GMT), ein zelluläres Programm vergleichbar mit epithelialer zu mesenchymaler Transition (EMT), eine wichtige Rolle bei der Kontrolle der Invasivität von Gliomzellen spielt. Es ist bekannt, dass die Transkriptionsfaktoren Snail und Slug EMT-Hauptregulatoren in epithelialen Tumoren sind. Daher nehmen wir an, dass diese Transkriptionsfaktoren ebenfalls Schlüsselkomponenten von GMT in GBM sind. Eine Analyse der Expression von Snail und Slug in GBMs in verschiedenen molekularen Unterklassen zeigte, dass diese beiden Regulatoren vor allem in der mesenchymalen GBM-Unterklasse exprimiert werden. Wir zeigen anhand der Expression einiger Signaturmarker, dass der gleichzeitige Verlust von Snail und Slug den TGFβ1-induzierten Übergang von einem glialen/proneuralen Phänotypen hin zu einem mesenchymalen Phänotypen verhindert. Darüber hinaus demonstrieren wir, dass Snail und Slug eine entscheidende Rolle bei der Kontrolle der Glioblastom-Stammzelleigenschaften wie Selbsterneuerung und der Expression von Krebsstammzellmarker spielen. Der Verlust von Snail und Slug führte des Weiteren zu einer starken Beeinträchtigung des invasiven Verhaltens der Krebszellen in vitro. Wichtig ist, dass reduzierte Snail und Slug Expression in GBM Zellen zu einem signifikant reduzierten Tumorwachstum in einem orthotopischen Maus-Xenograft-Modell führte. Detaillierte Analyse der Tumore zeigte, dass das reduzierte Wachstum nicht von Veränderungen der Proliferation und Apoptose der Zellen herrührte. Stattdessen konnten wir durch eine in vivo Invasionanalyse belegen, dass der Verlust von Snail und Slug die Invasionsfähigkeit der Zellen signifikant verringert. Zusammenfassend zeigt diese Arbeit, dass Snail und Slug wichtige GMT-Regulatoren sind die den Übergang von einem glialen/proneuralen zu einem mesenchymalen Phänotypen kontrollieren. Wichtig ist, dass der mesenchymale

Phänotyp sehr eng mit der Invasivität und dem Erwerb von Stammzell-Eigenschaften der Gliomzellen verknüpft ist. Das legt nahe, dass dies wichtige Mechanismen sind durch die Snail und Slug das Tumorwachstum von GBM kontrollieren. Dieses verbesserte Verständnis von GMT könnte dazu beitragen bestehende Behandlungsformen von GBM zu verbessern und neue therapeutische Ansätze zu finden.

3. Introduction

Primary tumours of the central nervous system consist of a quite heterogeneous group of benign and malignant neoplasias (Soeda et al.). The majority of CNS tumours are of glial origin and termed glioma (Ohgaki and Kleihues, 2005). Initially glioma were classified according to the original glial cell type that the tumour arose from: astrocytic, oligodendrocytic, ependymal or mixed forms (Louis et al., 2007). However, recent evidences obtained from human and animal studies also suggest neural stem cells as alternative cells of origin of gliomas (Canoll and Goldman, 2008; Caussinus and Gonzalez, 2005; Dirks, 2006; Galli et al., 2004; Singh et al., 2003).

Glioblastoma multiforme belongs to the most common glial neoplasia and shows the highest malignancy and aggressiveness in the group of gliomas. Patients diagnosed with GBM have a median survival of fifteen months (Norden and Wen, 2006). In the last years research improved the therapeutic approaches to treat the patients, but the prognosis is still poor. The most common therapy is the surgical removal of the primary tumour combined with radio-and or chemotherapy. Unfortunately it is nearly impossible to remove and eliminate all cancer cells, primarily due to the high invasive capacity of the tumour cells into the surrounding brain parenchyma already prior to the surgery. Secondary tumours arise from these remaining and invading cells and reduce the survival of the patients.

3.1 Classification of malignant glioma

The World Health Organization (WHO) classified gliomas in terms of malignancy into grade I, II, III and IV (published in the 3rd edition by Kleihues and Cavenee in 2000, complemented by Louis and Kleihues in 2007, Table 3.1). These grades are based on histological facts like cell differentiation, cell and cell core polymorphism, cell density, proliferation rate, proliferation of endothelium and tumour necrosis.

Tumours classified as grade I glioma, such as pilocytic astrocytoma and subependymal giant cell astrocytoma, show a high extent of differentiation and a slow proliferation with a good survival prognosis for the patient.

Grade II gliomas, such as diffuse astrocytoma, pleomorphic xanthoastrocytoma or pilomyxoid astrocytoma, are characterized by diffuse infiltration of the brain parenchyma, weak proliferation and patients often suffer from relapse of the tumour. The median survival of patients with grade II tumours is between three to eight years.

Anaplastic astrocytoma and anaplastic oligodendroglioma are examples for grade III tumours. Characteristics for this tumour type are atypical cell core morphology, high rate of proliferation and single cell necrosis. Patients have a median survival of two to three years (Norden and Wen, 2006).

Grade IV tumours show high proliferation, necrotic areas, hyper proliferating endothelium and high polymorphism. Glioblastoma multiforme (GBM) is the most abundant tumour type in this class. Patients diagnosed with GBM have a median survival of fifteen months. The median age of patients diagnosed with glioblastoma is 64 years.

WHO-Grade	Tumour Type
I	Pilocytic astrocytoma, subependymal giant cell astrocytoma
II	diffuse astrocytoma, pleomorphic xanthoastrocytoma, pilomyxoid astrocytoma
III	Anaplastic astrocytoma, anaplastic oligodendroglioma,
IV	Glioblastoma

Table 3.1 Examples of grade I-IV gliomas, based on the WHO classification of tumours of the central nervous system (Louis et al., 2007)

Nearly 70% of all diagnosed primary malignant brain tumours in the USA are gliomas. Every year more than 14.000 new cases are reported. That means that 5 people out of 100.000 are diagnosed with glioma. Approximately 60 to 70% of malignant gliomas are glioblastoma, 10 to 15% are anaplastic astrocytoma, anaplastic oligodendroglioma and anaplastic oligoastrocytoma account for 10%. The

rest are the less common anaplastic ependymoma and anaplastic ganglioglioma (Wen and Kesari, 2008)

3.1.1 Molecular subclasses of glioma

With the development of new molecular techniques the classification of gliomas was refined to include information related to the expression of specific genetic signatures.

With the help of microarray gene expression profiling it was possible to identify molecular subtypes of gliomas as well as genes associated with tumour grade, progression, and patient survival (Godard et al., 2003; Rickman et al., 2001; van den Boom et al., 2003). While GBM and anaplastic astrocytomas are still defined by histological criteria, several reports showed that expression profiles predict patient outcome better than a histological examination (Freije et al., 2004; Nutt et al., 2003). This led to the hypothesis that neoplasms defined morphologically as anaplastic astrocytoma and GBM could represent a mix of molecular genetic subtypes.

In 2006 Phillips et al. (Phillips et al., 2006) showed prognostically relevant molecular subclasses of high grade glioma, especially high grade astrocytoma. These subclasses resemble known stages in neurogenesis. They divided their expression profiling in three subgroups: proneural, proliferative and mesenchymal.

The proneural subclass showed a better prognosis in patient outcome and expressed genes that are associated with normal brain and the process of neurogenesis (for example Olig2 (oligodendroglial marker 2) and MAP2 (microtubule associated protein 2)). For the proliferative subclass the authors reported increased expression of genes involved in cell proliferation (for example PCNA (proliferating cell nuclear antigen) and TOP2A (topoisomerase II alpha). The mesenchymal subclass was defined by the enrichment of cells of mesenchymal origin with the upregulation of respective genes like CD44 (transmembrane glycoprotein) or YKL40 (human chitinase 3 like protein 1) as well as the stem cell marker CD133 (transmembrane glycoprotein). Both classes showed a poor overall survival of the patients. Interestingly recurrent tumours were observed to shift in their expression profile to the mesenchymal subclass.

Based on the study described above and on data from The Cancer Genome Atlas (TCGA) glioblastoma cohort in 2010 Verhaak et al. (Verhaak et al., 2010) defined four subclasses of tumours (proneural, neural, classical, mesenchymal) all morphologically diagnosed as GBM.

The proneural subtype showed an amplification of PDGFRA (platelet derived growth factor receptor A) and very frequently a point mutation in IDH1 (isocitrate dehydrogenase 1) as well as a mutation and the loss of heterozygosity in p53. Furthermore a high expression of oligodendrocytic development genes such as PDGFRA and Olig2 was characteristic for this subclass.

In accordance to the study of Phillips et al. the expression of YKL40 and CD44 was elevated in the mesenchymal subclass. Furthermore they found a frequent hemizygous deletion of NF1 and a co-occurring mutation of NF1 (neurofibromin 1) and PTEN (phosphatase and tensin homologue). Components of the TNFα and the NF-κB pathways were highly upregulated as a consequence of higher necrosis and associated inflammatory infiltrates in the mesenchymal class.

The neural subclass was difficult to distinguish from normal brain because of the high expression of neuron markers like NEFL (neurofilament), GABRA1 (gamma-aminobutyric acid (GABA) A receptor alpha 1), SYT1 (synaptotagmin I) and SLC12A5 (potassium/chloride transporter), but all samples were histologically identified as GBM.

The classical subtype showed an amplification of chromosome 7 and a loss of chromosome 10, no mutations in p53 and amplification and a high mutation rate of EGFR (epidermal growth factor receptor). Co-occurring with the amplification of EGFR was a homozygous deletion of CDKN2A (cyclin-dependent kinase inhibitor 2A). In this subclass a high expression of neural precursor and stem cell marker nestin was found, as well as a high activation of the Notch and sonic hedgehog pathways.

Shortly after the analysis by Verhaak et al. another possibility to get a deeper insight in the molecular differences of GBM was published. The method of choice was to identify promoter DNA methylation alterations of 272 GBM tumours in the TCGA cohort (Noushmehr et al., 2010). It was found that a distinct subset of samples displays a concerted hypermethylation at a large number of loci. This could indicate

the existence of a glioma CpG-island methylator phenotype (G-CIMP), as previously described for colorectal cancer (Toyota et al., 1999). G-CIMP tumours belong to the proneural subgroup and are more prevalent in lower-grade glioma. Interestingly, the G-CIMP phenotype seems to be tightly associated with IDH1 mutations. Patients with G-CIMP tumours are younger at the time of diagnosis and have an improved outcome.

3.2 Invasion and migration of tumour cells

One of the main characteristics of GBM is the high invasive and migratory capacity of tumour cells. Single cells or groups of cells are able to leave the primary tumour mass and invade along the white matter, myelinated fibres or along blood vessels in the surrounding brain parenchyma even until the contralateral hemisphere where they are the basis for recurrent tumours. Recurrence is usually still observed even after surgical removal of the primary tumour and chemo- or radiotherapy. The infiltrating tumour micro-satellites or small groups of cells are hard to visualize and to discriminate from healthy brain tissue during surgery or in MRI (Black, 1997; Claes et al., 2007; Giese and Westphal, 1996; Louis et al., 2007).

The very common necrotic areas in glioblastoma are often surrounded by pseudopalisades with a higher cell density. These pseudopalisades consist of cells which show low proliferation and a higher apoptosis rate than cells that are not in close proximity to necrotic areas. The reason for this higher cell density in perinecrotic areas seems to be an enhanced migration of tumour cells out of the necrotic tissue. These migratory cells are believed to be selected for a more aggressive, more malignant and more resistant phenotype (Brat et al., 2004; Claes et al., 2007).

Despite the high invasiveness of glioma cells distant metastasis outside neural tissues is observed very rarely (Subramanian et al., 2002). The reasons for that are still not fully understood. Possible contributing factors could be the blood-brain barrier which prevents the cells to leave the brain, the lack of lymphatic drainage or the special microenvironment of the brain which is not found in other organs and makes it

more difficult for cancer cells from the brain to adapt in distant organs and establish metastasis.

3.2.1 Mechanisms of invasion and migration

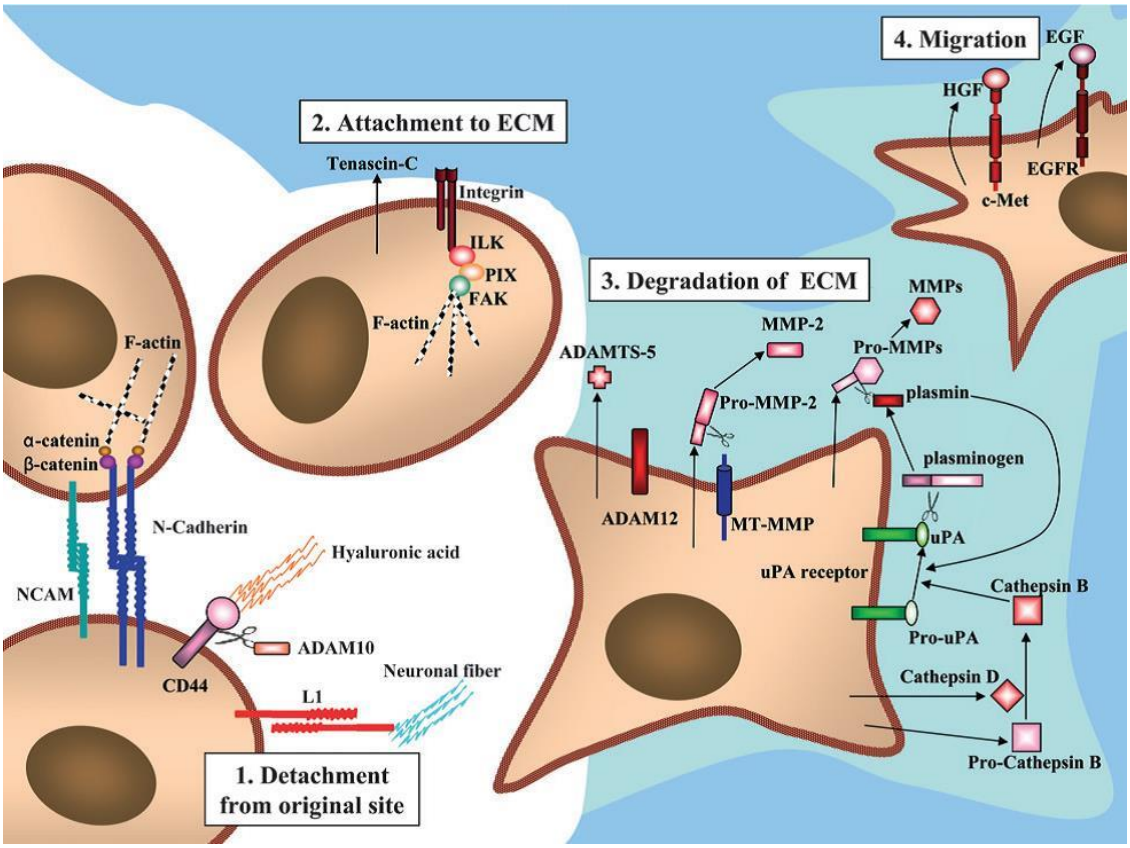

Fig. 3.2 Schematic illustration of the principal mechanisms of glioma invasion. Principally, glioma invasion can be divided into 4 steps: 1. Detachment from the tumour mass. 2. Attachment to the ECM. 3. Degradation of the ECM and 4. Migration to a distant side. The involved signalling pathways and cellular components are described in the text. (Image taken from Nakada, 2007)

The molecular principles of tumour cell invasion are based on changes in the mechanisms of cell adhesion to the extracellular matrix (ECM) components and loss of direct cell-cell contact. For the detachment of tumour cells from the main tumour mass cell adhesion proteins have to be cleaved or their expression has to change (Nakada et al., 2007). A good example for cleavage of adhesion molecules in GBM is the transmembrane glycoprotein CD44. It interacts with hyaluronic acid in the ECM and gets cleaved by proteinases ADAM10 and 17 (Nagano et al., 2004; Okamoto et al., 1999) (Fig. 3.2). During the loss of cell adhesion especially in GBM the

expression of the neural cell adhesion molecule NCAM is also reduced (Sasaki et al., 1998). Furthermore calcium depending adhesion molecules like cadherins (N-cadherin and E-cadherin) are changed in their expression during the process of invasion. A reduced E-cadherin expression and an induced expression of N-cadherin are important for the cell motility and migration (Cavallaro and Christofori, 2004; Thiery, 2003). The particular role of these two proteins in invasiveness of tumour cells will be elaborated later in detail in context of epithelial-to-mesenchymal transition (see section 3.3).

In the brain the ECM works as a scaffold to guide invasive cells. To make way for the migrating tumour cells the ECM gets degraded by proteolytic proteins. In glioma it is known that especially the proteinases MMP-2 and -9 (matrix metalloproteinases), ADAM10, 12m and 17, the serine proteinase uPA (urokinase-type plasminogen activator) and its receptor uPAR as well as cysteine proteinases (cathepsin B, L, S) play an important role during the degradation of the ECM (Nakada et al., 2007) (Fig. 3.2).

The motility of the cells depends furthermore on many more paracrine and autocrine signalling pathways. Through several signalling molecules the cell morphology changes, the cell gets polarized and starts to form protrusions like pseudopodia, lamellipodia and filopodia to be able to invade and migrate. Invasive glioma cells show an upregulation of Tenascin-C which stimulates via the RhoA signalling pathway the development of actin-rich filopodia (Mahesparan et al., 2003; Wenk et al., 2000). Also the interaction of ECM components like fibronectin, collagen, laminin and vitronectin with the intracellular actin-cytoskeleton via integrins is an important requirement for cell motility. In invasive glioma cells it was observed that especially integrin-β1 is upregulated (Hynes, 2002; Perego et al., 2002) (Fig. 3.2).

The final step in the mechanism of migration is the formation of membrane anchors which enables the cell to move forward through contractions of the cytoskeleton (Nakada et al., 2007) (Demuth and Berens, 2004) (Fig. 3.2).

3.3 Epithelial-to-mesenchymal transition

During tumour development from a benign to a malignant or metastatic tumour the tumour cells have to undergo morphological and phenotypical changes. In case of epithelial cancer types the cells develop from highly differentiated epithelial cells to less differentiated, migratory and invasive cells with a mesenchymal phenotype. This specific change is called epithelial-to-mesenchymal-transition or shortly EMT.

Originally this transition program is known from embryonic development. It is very important for the positioning and differentiation of particular cell types and for the development of complex structures of many tissues and inner organs during gastrulation and the formation of the neural crest (Thiery, 2003).

An epithelial cell layer is characterised by close cell-cell contacts between neighbouring cells through adherens junctions, tight junctions and desmosomes. During EMT these close connections are abrogated to enable the detachment of the cells from the basal membrane and to leave the cell layer due to a higher motility (Fig. 3.3). For that a morphological change of the cells is necessary and the cytoskeleton gets rearranged. Epithelial cells have a rounder shape than mesenchymal cells which show a more spindle-shaped structure and more protrusions like filopodia which are typical for migratory and invasive cells.

During tumorigenesis, epithelial cancer cells are also capable of undergoing changes analogous to EMT, including the hallmarks of EMT: repression of epithelial specific proteins like E-cadherin and upregulation of mesenchymal proteins like N-cadherin, vimentin and fibronectin (Peinado et al., 2007; Thiery, 2002; Yilmaz and Christofori, 2009). The loss of E-cadherin is one of the key events during EMT and can be correlated with increased tumour progression and metastatic incidence in carcinoma (Birchmeier and Behrens, 1994; Perl et al., 1998). In tumour cells E-cadherin is transcriptionally repressed by a group of EMT repressor genes. These repressor genes are mainly Zinc-finger transcription factors of the Snail-family (SNAI1 (Snail), SNAI2 (Slug)) (Batlle et al., 2000; Bolos et al., 2003; Cano et al., 2000), and the ZEB-family (ZEB1, ZEB2) (Comijn et al., 2001; Eger A et al., 2005; Peinado et al., 2007) (Fig. 3.3). All these transcription factors bind the E-box consensus sequence CANNT(G) in the promoter region of E-cadherin and repress the transcription of the gene (Batlle et al., 2000; Cano et al., 2000). SNAI1/2 and ZEB1/2 are also involved in

the epigenetic regulation of E-cadherin by recruiting chromatin-remodelling complexes (HDAC2 complex) to the E-cadherin gene (Peinado et al., 2004; Peinado et al., 2007)

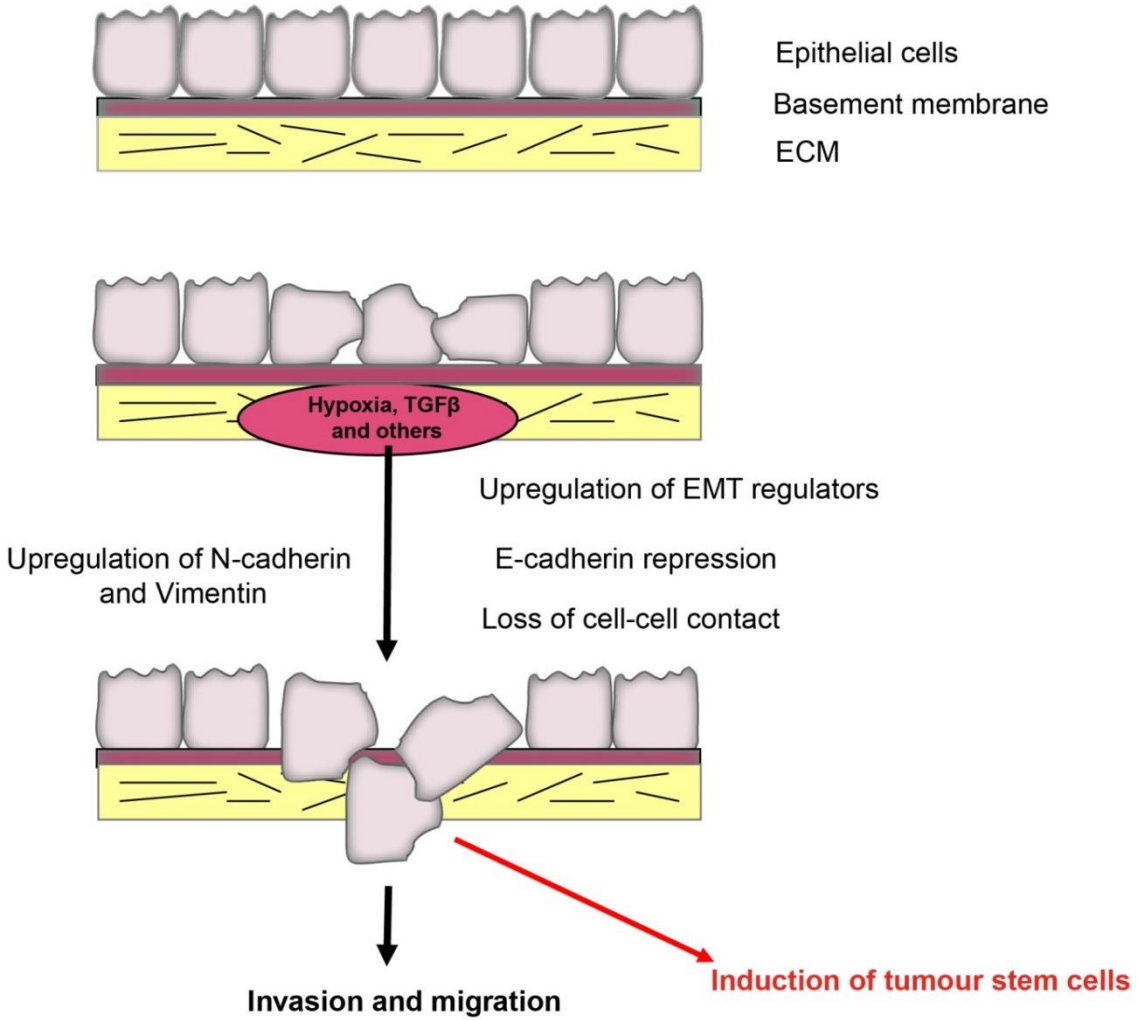

Fig. 3.3 Schematic illustration of EMT. Due to microenvironmental triggers like hypoxia or TGFβ signalling transcriptional inducers like Snail and Slug get activated and the expression of E-cadherin is repressed. The cells lose tight cell-cell contact and start to leave the epithelial cell layer. Subsequently, the expression of mesenchymal markers like vimentin and N-cadherin is elevated. Cells which gain a mesenchymal phenotype start to migrate and invade. Furthermore, EMT can promote the acquisition of a cancer stem cell phenotype. Adapted from (Pouyssegur et al., 2006).

Several signalling pathways involved in tumour cell migration or cell growth/proliferation are in turn influenced by the loss of E-cadherin, for example the canonical Wnt pathway and the remodelling of the actin-cytoskeleton by Rho-family GTPase dependent pathways (Cavallaro and Christofori, 2004; Perego et al., 2002).

Many EMT repressors are mainly expressed at the invasive front of tumours but also in necrotic/hypoxic areas and are known to be regulated by many pro-tumorigenic pathways like HIF, TGFβ, STAT3, NF-κB as well as by other autocrine growth factors like HGF, EGF or FGF (Janda et al., 2002; Kang and Massague, 2004; Lu et al., 2003; Peinado et al., 2003; Spaderna et al., 2006; Thiery et al., 2009; Yook et al., 2005). These growth factors are either produced by the tumour cells themselves or by the neighbouring stromal cells. TGFβ is also known as the most potent inducer of SNAI transcription, discussed below (see section 3.3.3).

There is growing evidence that a program comparable to EMT can also be observed in non-epithelial cancers like gliomas. In this context it can rather be termed GMT (glial to mesenchymal transition) due to distinctive features of glial cells, as compared to epithelial ones. Interestingly the same repressive transcription factors and pathways could play an important role in glioma as well, but so far there is only little known. Previous studies gave some of the first evidence that the EMT factors Snail and Slug are very important regulators of this transitions (see section 3.3.2 and 3.3.3). But also other EMT regulators like TWIST1 and ZEB1 can play a functional role in GBM growth, invasion and therapy resistance related to a transition to a mesenchymal phenotype (Siebzehnrubl et al., 2013) (Mikheeva et al., 2010)

3.3.1 Induction of EMT by Hypoxia

Cellular responses to low oxygen tension (hypoxia) are mediated by the hypoxia inducible factors (HIF). Under hypoxic conditions the HIFα subunit (HIF1α or HIF2α) gets stabilised and interacts with the HIFβ subunit to form a heterodimer. Subsequently the HIF dimer binds to hypoxic responsive elements (HREs) in the promoter regions of hypoxia regulated genes to induce their expression. Normoxic conditions lead to the proteasomal degradation of HIFα through ubiquitination by VHL (von Hippel-Lindau) and no expression of hypoxia responsive genes.

Hypoxia is reported as a potent inducer of EMT by elevating the expression of the respective transcriptional regulators. The importance of HIF to induce EMT in epithelial cancers is reported for pancreatic ductal adenocarcinoma (Liu et al., 2014a), hepatocellular carcinoma (Liu et al., 2014b), ovarian carcinoma (Du et al., 2014) and lung cancer (Shaikh et al., 2012). In non-epithelial cancers like GBM it is reported that tumours with a mesenchymal gene signature show a high level of necrotic/hypoxic areas (Verhaak, 2010). Furthermore it is known that cells surrounding such necrotic zones (pseudopalisading cells) and therefore lacking a sufficient oxygen supply show a high expression of the mesenchymal transcription factors C/EBP-β and C/EBP-δ together with a poor prognosis for patients with this class of tumours (Cooper et al., 2012). In this context a recent study reported that in necrotic/hypoxic areas EMT is mainly promoted by the hypoxic induction of the EMT regulator ZEB1 which facilitates the expression of mesenchymal markers and impacts the invasiveness of the cancer cells (Joseph et al., 2015).

3.3.2 Induction of EMT by TGFβ

TGFβ is, like hypoxia, a master inducer of mesenchymal transition and invasion of cancer cells. Latent TGFβ is immobilized to the ECM through its components fibronectin and fibrillin by interaction with latent TGFβ-binding proteins (LTBP) like LTB1-4. To activate TGFβ, it needs to be released by limited proteolysis mediated by MMPs or furins which are activated and released by activated stromal cells (Mu et al., 2002). As an alternative way to make ECM bound TGFβ accessible for its receptors is that integrins bind to latent TGFβ-binding protein complexes and pull to induce a conformational change (Wipff et al., 2007). Also TNFα can upregulate the transcription of TGFβ (Sullivan et al., 2009) and subsequently accelerate TGFβ-induced EMT dramatically (Bates and Mercurio, 2003).

Nevertheless, TGFβ has a dual role in carcinogenesis. In early lesions it is considered to be a master anti-inflammatory cytokine which prevents uncontrolled proliferation of the cells (Siegel and Massague, 2003). But many more advanced tumours show a resistance towards the growth-inhibitory effects of TGFβ, instead it is able to act as an activator of prometastatic pathways like EMT (Jakowlew, 2006).

Taken together TGFβ can act on the one hand as a tumour suppressor at early stages of cancer progression but on the other hand contribute later to the malignant progression by promoting invasion and metastasis and help to induce oncogenic EMT (Massague, 2008) (Galliher et al., 2006).

TGFβ induces EMT through two distinct pathways, the Smad-dependent pathways and the Smad-independent pathway (Kalluri and Weinberg, 2009). The Smad-dependent pathway includes the binding of TGFβ by the TGFβ receptors type I and II which form tight complexes. The activation of the receptors lead to phosphorylation of Smad2 and Smad3 and the receptor-related Smad (R-Smad) proteins (Massague and Wotton, 2000). Phosphorylated Smads form heteromeric complexes with Smad4 and translocate into the nucleus to regulate transcription of EMT associated target genes like Snail, Slug and ZEBs (Derynck and Zhang, 2003). The Smad independent pathway is characterised by the direct activation of several non-Smad signalling pathways through TGFβ including Ras/ERK, c-Jun and JNK (Myazono, 2009; Ozdamar et al., 2005).

After single tumour cells or groups of cells leave the primary tumour mass and when the invading cells reached the surrounding tissue or their specific side of metastasis the EMT program is reversible. Through interaction with the new microenvironment the cells can turn back to their initial epithelial phenotype. This backwards conversion is called MET (mesenchymal to epithelial transition) (Spaderna et al., 2006; Thiery, 2003; Thiery et al., 2009). It seems that EMT in cancer is only transiently activated and may be locally limited to the invasive front and heavily regulated by complex orchestrated environmental cues.

3.3.3 The Snail super-family of transcription factors and their role in E(G)MT

Snail transcription factors were first discovered in the fruit fly *Drosophila melanogaster.* In this organism they are essential for the development of the mesoderm (Alberga et al., 1991; Grau et al., 1984). In vertebrates there are three Snail family members: Snail1 (Snail), Snail2 (Slug) and Snail3 (Smuc). Interestingly, in contrast to the other two Snail proteins, Snail3 is a non-essential protein in embryogenesis of mice which shows a tissue specific expression in thymus and

skeletal muscles (Bradley et al., 2013) and seems to have only poor abilities to induce EMT (Gras et al., 2014).

Snail is a protein with a very short half-life. Its turn-over in the nucleus is decreased but in the cytoplasm it gets rapidly degraded by proteasomes (Zhou et al., 2004). All members of this transcription factor family encode transcriptional repressors. They all share a highly conserved domain organisation. The C-terminal domain contains four to six C_2H_2 type zinc fingers and binds target gene promoters at the E-box consensus motif 5´-CANNTG-3´ and is responsible for the repressive activity of Snail (Nieto, 2002). The N-terminus of all Snail members harbours the conserved SNAG domain. This domain is essential for the binding of co-repressor complexes to transcriptionally and epigenetically influence the expression of target genes. Such co-repressor complexes include the Sin3A, histone deacetylase 1/2 (HDAC1/2) complex (Peinado et al., 2004), the Polycomb repressive complex 2 (PRC2) (Herranz et al., 2008), the protein arginine methyltransferase 5 (PRMT5)/Ajuba complex (Hou et al., 2008) or the lysine-specific demethylase 1 (LSD1)/coREST complex (Lin et al., 2010) (Fig. 3.4).

In the centre of the Snail proteins one can find a serine-rich domain (SRD) where most sites for post-translational modifications are located and a nuclear export sequence (NES), which are important for protein stabilisation, activation, localisation and degradation of the gene product (Dominguez et al., 2003). In the SRD many phosphorylation sites are found which get phosphorylated mainly through GSK3β but also PAK1 phosphorylates serine 246 and enhances the accumulation of Snail in the nucleus and promotes subsequently its repressive activity in the nucleus (Yang et al., 2005) (Fig. 3.5). The small C-terminal domain phosphatase (SCP) removes such phosphorylations through interaction with Snail to stabilize the protein (Wu et al., 2009b). Nevertheless, phosphorylated Snail interacts with β-TrCP and gets degraded subsequently (Zhou et al., 2004). Especially, the F-box E3 ubiquitin ligase FBXL14 promotes the ubiquitination and proteasomal degradation of Snail. Furthermore lysyl oxidase-like 2 (LOXL2) binds to the SNAG domain of Snail and antagonises the interaction between Snail and β-TrCP or FBXL14, which leads to stabilisation of Snail (Vinas-Castells et al., 2010). Recently it was described in breast cancer that the E3 ligase SCF-FBXO11 targets Snail for ubiquitination and degradation. The authors could show that the degradation of Snail by FBXO11 is dependent on Ser-11 phosphorylation by protein kinase D1 (PKD1). This degradation process inhibits

Snail-induced EMT, tumour initiation and metastasis in various breast cancer models (Zheng et al., 2014).

Direct regulators	Interaction location	Upstream pathway(s)
LOXL2/3	SNAG domain; K98 and K127	Notch/Lox
NF-κB	Promoter: -194 to -78 bp	TNFα, RANKL, PI3K/Akt
HIF-1α	Promoter: -750 to -643 bp	Hypoxic conditions
SMADs	Promoter: -631 to -506 bp	TGF-β1, Ras
IKKα	Promoter: -631 to -506 bp (concurrent with SMADs)	TGF-β1, Ras, PI3K/Akt
HMGA2	Promoter: 2 regions within -131 to -92 bp	TGF-β1
YY1	3′ Enhancer	NF-κB
Egr-1	Promoter: 4 sites between -450 and -50 bp	HGF, MAPK
PARP-1	Promoter: SIRE	ILK
Gli1	There are 4 candidate GLI binding sites (consensus sequence for binding: 5'-GACCACCCA-3')	Shh, Wnt
STAT3	Promoter	IL-6/JAK, HB-EGF/EGFR/MEK/ERK (mice)
MTA3	Promoter	ER
PAK1	S^{246}	
GSK-3β	Motif 1 (S^{96}, S^{100}, S^{104}) and Motif 2 (S^{107}, S^{111}, S^{115}, S^{119})	Wnt, PI3K/Akt, FGF
Snail1	Promoter: E box within SIRE	Binds to own promoter

Fig. 3.4 Regulation of Snail expression. Summary of direct regulators of Snail and their interaction locations and respective pathways (Kaufhold and Bonavida, 2014).

Snail expression or induction in cancer depends on many signalling molecules from the tumour microenvironment. Growth factors like HGF, FGF or EGF activate signalling through receptor tyrosine kinases (RTKs) via the RAS-MAPK or PI3K-Akt pathway which leads to an induction of Snail expression (Ciruna and Rossant, 2001; Lu et al., 2003). TGFβ and the SMAD pathway play an important role in inducing Snail expression, which in turn helps to overcome the tumour suppressing effects of TGFβ. Snail mediates resistance to TGFβ initiated apoptosis and shifts the response to promotion of tumour progression (Franco et al., 2010). TGFβ increases also Notch signalling via SMAD3 which leads to elevated expression of Jagged1 and HEY1 and subsequently promotes expression of Slug which leads to an EMT phenotype (Leong et al., 2007). But Notch also controls Snail expression via two synergistic mechanisms: direct transcriptional activation of Snail or a more indirect mechanism through lysyl oxidase (LOX). Under hypoxic conditions Notch recruits HIF1α to the promoter of LOX, which increases LOX expression, stabilises the Snail protein and leads to EMT (Grego-Bessa et al., 2004; Sahlgren et al., 2008). A very important

signalling pathway in tumour progression is the Wnt-pathway. Activation of this pathway inhibits GSK3β-mediated phosphorylation of β-catenin and Snail (two of its main targets) and stabilises the two proteins in the nucleus (Barrallo-Gimeno and Nieto, 2005; Kim et al., 2002; Liebner et al., 2004).

Another important regulator of Snail expression is the NF-κB pathway. Snail gets regulated by this pathway transcriptional and post-translational. NF-κB binds to the human Snail promoter (at positions -194 and -78) (Fig.3.5) and elevates the expression of Snail (Barbera et al., 2004). The post-translational regulation of Snail works via activation of NF-κB through AKT signalling, which leads to phosphorylation of IKKα and the upregulation of Snail (Julien et al., 2007; Ozes et al., 1999; Romashkova and Makarov, 1999; Zhou et al., 2000).

Inflammatory pathways also provide important microenvironmental cues during tumour progression. TNFα, a major inflammatory cytokine, stabilises functional Snail. By disrupting the binding of Snail with GSK3β and β-TrCP, TNFα inhibits the phosphorylation and ubiquitination of Snail (Fig. 3.6) (Wu et al., 2009a).

In addition to the microenvironmental associated pathways Snail and Slug are also able to autoregulate their own expression. Both bind to the own promoter and repress their expression through an autoregulatory loop (Fig. 3.5) (Peiro et al., 2006).

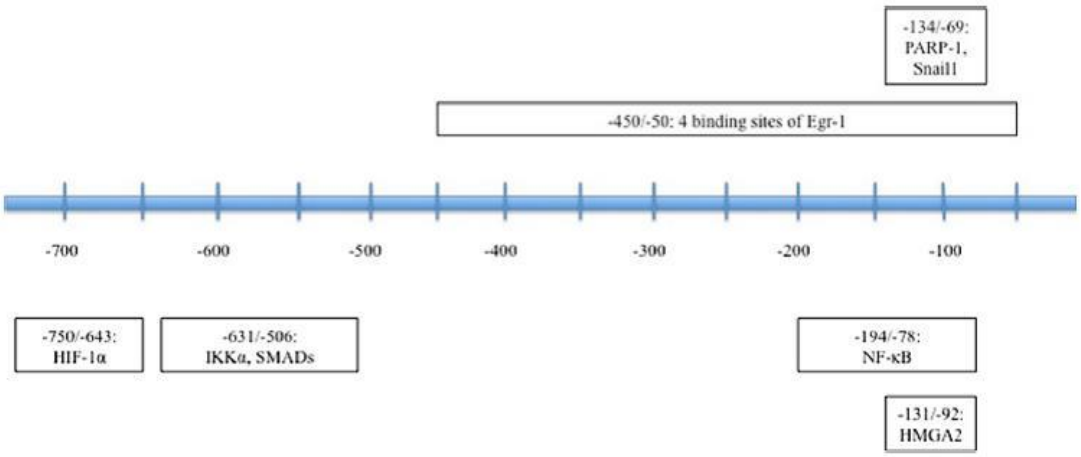

Fig. 3.5 Regulatory elements in the SNAI promoter. Overview showing different regulatory elements and the respective transcriptional regulators of the Snail promoter (Kaufhold and Bonavida, 2014).

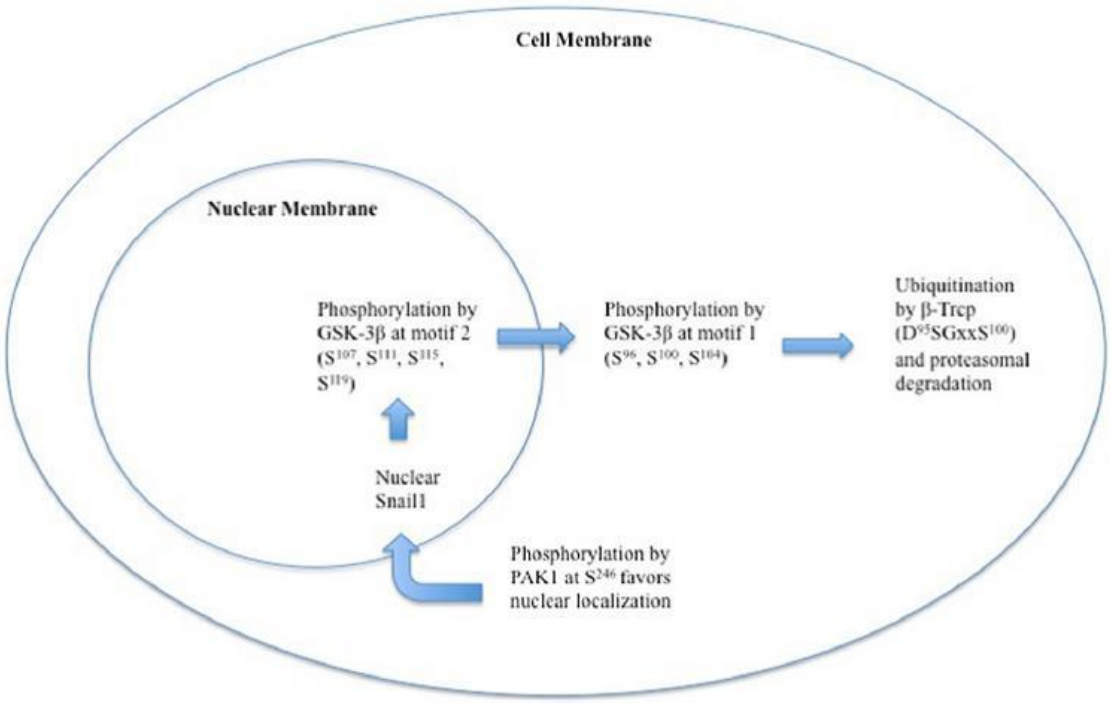

Fig. 3.6 Localisation and stabilisation of Snail. Schematic overview of translational modifications changing the localisation and the stability of Snail (Kaufhold and Bonavida, 2014).

3.4 Cancer stem cells

Since many years it is a main goal in cancer research to explain the origin of cancer and to use this knowledge for therapeutic approaches. It is known that cancer arises from a series of mutations in a few cells or even in a single cell which can be called founder cell. Such cells could gain unlimited and uncontrolled expansion potential and a long life-span (Hanahan and Weinberg, 2011). To explain these observations two hypothetical models are currently under discussion. The first is the stochastic model in which it is assumed that all cells of the tumour have the same tumorigenic potential and can account for tumour growth (Reya et al., 2001). The second one is the hierarchical model, according to which only a small subpopulation of tumour cells have the capacity to self-renew and maintain the tumour growth, while the bulk of the tumour cells are differentiating or terminally differentiated cells (Fig. 3.7) (Reya et al., 2001; Visvader and Lindeman, 2008, 2012).

The hierarchical model, also referred to as the cancer-stem-cell or the tumour-initiating-cell model, was described first in human myeloid leukaemia(Bonnet and Dick, 1997; Lapidot et al., 1994). Later the concept was extended to human solid

tumours like breast cancer(Al-Hajj et al., 2003; Cho et al., 2008; Ginestier et al., 2007), prostate cancer (Collins et al., 2005) and brain tumours as well (Harris et al., 2008; Singh et al., 2003; Son et al., 2009)

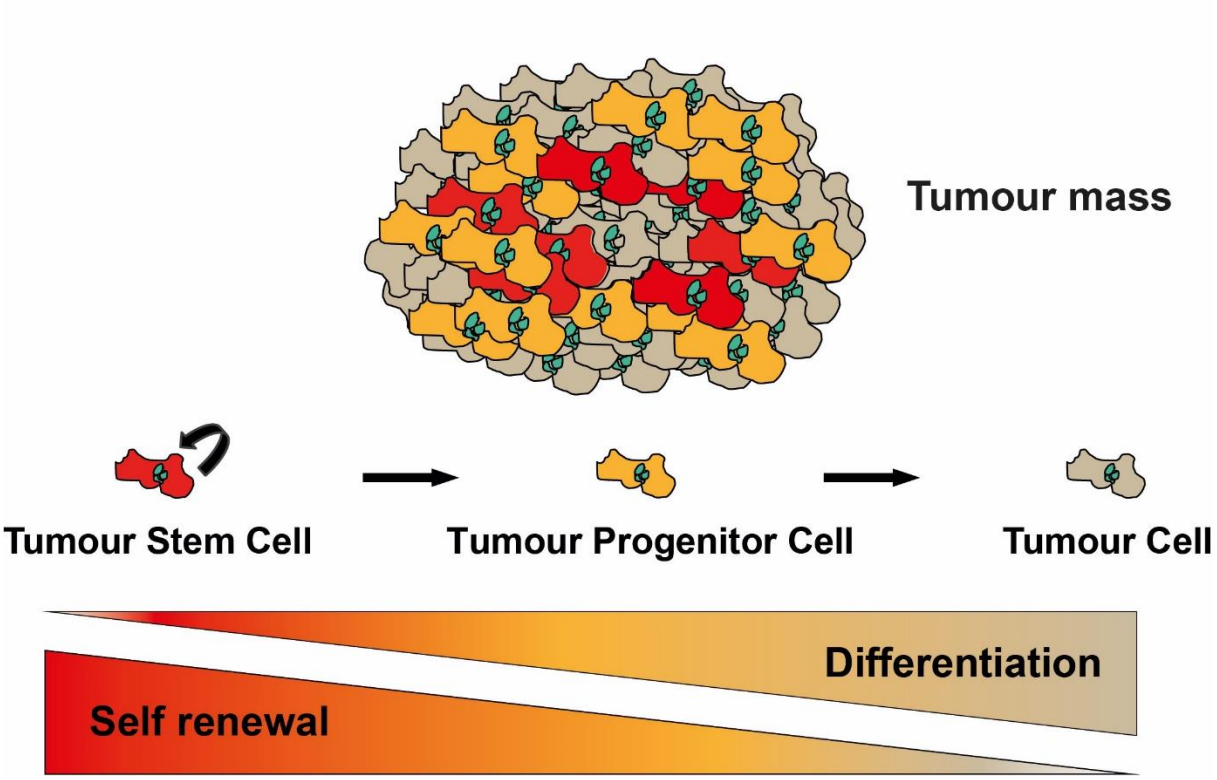

Fig. 3.7 Schematic illustration of the cancer stem cell model. The tumour mass consists of three cell types with a different state of differentiation. A few cells in the tumour mass exhibit a high capacity of self-renewal and a very undifferentiated cell status. These tumour stem cells are able to give rise to more differentiated progenitor cells and to new stem cells (self-renewal). Progenitor cells can give rise to differentiated tumour cells, which form the main tumour cell population (modified from Till Acker).

Cancer stem cells (CSC) are a small minority of tumour cells which show characteristics comparable to normal stem cells, such as differentiation potential and self-renewal. In addition, CSCs show a high resistance to chemo-and radiotherapy (Bao et al., 2006a). Another important fact in the context of normal stem cells and CSCs is the homeostatic control, the maintenance of the stem cell pool (Reya et al., 2001; Sell, 2004, 2006; Sell and Pierce, 1994; Wicha et al., 2006). When stem cells divide they give rise to one daughter cell which remains in the stem cell state, whereas the other daughter cell can enter the process of differentiation (Fig. 3.7).

3.4.1 Cancer stem cells in glioma

Within solid tumours gliomas were among the first tumour entities in which the CSC model was experimentally validated (Venere et al., 2011)

Like in other cancer types several markers are used to identify and characterise brain tumour stem cells (BTSCs). One of the most prominent markers in brain tumour stem cells is the surface protein CD133. It was shown that FACS sorted CD133 positive cells can initiate new brain tumours when transplanted into the striatum of immunodeficient mice whereas CD133 negative cells were not able to form a tumour (Singh et al., 2003) (Galli et al., 2004; Singh et al., 2003). The obtained tumours showed the classic features of GBM like extensive migration and infiltration and also the histological features were comparable. It was also possible to re-isolate stem like cells from theses tumours and in a second transplantation experiment with these cells GBM tumours were obtained, demonstrating the self-renewal and tumour-initiating ability of these cells in vivo. Other markers that are often used to identify BTSCs are integrinα6 (Lathia et al., 2010), CD15 (Son et al., 2009), EGFR (Jin et al., 2011), A2B5 (Ogden et al., 2008), L1CAM (Bao et al., 2008), CD44 (Anido et al., 2010) and the chemokine CXCR4 (Ping et al., 2011). Through a side-population approach further stem cell signature genes, ASPHD2 (aspartate beta-hydroxylase domain-containing protein 2), NFATc2 (nuclear factor of activated T cells 2, part of the calcineurin pathway) and MAML3 (mastermind-like protein 3, part of the Notch pathway) were identified. All these side population genes are hypoxia-inducible through the activation of HIF2α (Seidel et al., 2010).

The regulation of brain tumour stem cells shows the same key mechanisms like normal neuronal progenitor cells, found in the subventricular zone (SVZ). Self-renewal in adult neural stem cells relies predominantly on the Notch pathway (Hitoshi et al., 2002; Shen et al., 2004), overexpression of Notch receptors and their ligands Delta-like 1 and Jagged1 are correlated with proliferation of human glioma cells (Purow et al., 2005). Additionally, self-renewal in normal neural stem cells and tumorigenesis of the central nervous system is positively regulated through the repression of INK4a and the tumour suppressor ARF (Molofsky et al., 2003).

Furthermore, the regulation and maintenance of neural stem cells, progenitor cells and cancer stem cells relies not only on specific intrinsic genetic mechanisms but

also on interaction with several microenvironmental cues. Within malignant brain tumours like GBM two distinct microenvironmental niches can be found which play an important role for induction, regulation and maintenance of brain tumour stem cells, the perivascular niche and the hypoxic niche.

The tumour tissue in close proximity to blood vessels is called the perivascular niche. Due to the vasculature this niche is well supplied with oxygen and nutrients. It was shown that the perivascular niche contains cells associated to blood vessels with stem cell like phenotypes and stem cell marker expression (Calabrese et al., 2007). GBMs are fast growing highly proliferating tumours and have strong metabolic needs which cannot sufficiently served by the existing vasculature. It was shown that BTSCs of GBM can support neo-angiogenesis. Interestingly, blood vessels and brain tumour stem cells rely on a bidirectional regulation. BTSCs secrete VEGF (vascular endothelial growth factor) which induces angiogenesis (Bao et al., 2006b) and endothelial cells secrete themselves mitogens which activate the Notch pathway to maintain the brain tumour stem cell pool (Charles et al., 2010). The perivascular niche could be also a therapeutic target to indirectly eliminate BTSCs. Especially anti-angiogenic treatments could help to starve out the stem cell population due to lack of nutrients and oxygen. An anti-VEGF treatment which is already in clinical use, Avastin (Bevacizumab), showed only limited clinical success because tumours of patients treated with this drug showed a more invasive behaviour than before (Paez-Ribes et al., 2009) (Chinot et al., 2014; Gilbert et al., 2014; Haines and Gabor Miklos, 2014).

Regions of low oxygen tension due to severe necrosis or inefficient vasculature are not only histological hallmarks of GBMs but also a second niche for BTSCs (Pries et al., 2010). The molecular response to low oxygen availability is mainly regulated by HIFs (Hypoxia-inducible factors, HIF1α and HIF2α) (Bar, 2011; Li et al., 2009; Soeda et al., 2009). These factors are very important to maintain BTSCs and are closely linked to induction of angiogenesis. In particular, HIF2α promotes the expression of stem cell maintenance markers like Oct4 and Nanog, CD133, MAML3, ASPHD2 (Covello et al., 2006; Heddleston et al., 2009; Seidel et al., 2010). Several experiments could show that the stabilisation of the HIF2α protein under hypoxic conditions or through expression of a non-degradable HIF mutant increased self-renewal of BTSCs and enhanced the tumour formation in vivo, even in tumour cells

which showed no stem cell characteristics before (Heddleston et al., 2009) (Li et al., 2009; Pietras et al., 2009; Seidel et al., 2010). HIF1α is known to induce the expression of the stem cell marker CD133 and increase the self-renewal of BTSCs (Soeda et al., 2009).

In addition to the microenvironmental niches the TGFβ signalling pathway plays an important role in the regulation of CSCs. Despite the fact that TGFβ signalling is commonly found in tumours, so far there is only little known how TGFβ can influence CSCs. Nevertheless, some recent reports showed that in glioma TGFβ signalling is important for the maintenance of stem-like cells through the induction of the direct TGFβ target Sox4 which leads to accelerated expression of the stem cell marker Sox2 (Ikushima et al., 2009). Furthermore, it was reported that the self-renewal capacity of BTSCs in glioma relies on the induction of the cytokine LIF (leukaemia inhibiting factor) via TGFβ signalling (Penuelas et al., 2009). Through inhibition of the TGFβ pathway it was shown that this resulted in a decrease of the CD44(high)/Id1(high) population which is thought to represent BTSCs in glioma as well (Anido et al., 2010).

Many of the above described signalling pathways, especially TGFβ and hypoxia, are also important for the induction of EMT. Interestingly, a number of recent studies suggest EMT is linked not only to the induction of mesenchymal features, but also to the acquisition of a CSC phenotype (Fig. 3.8). The strongest evidence was found in epithelial cancers like breast cancer. The cellular processes observed in cells undergoing EMT during cancer metastasis are analogous to the processes of tissue reconstruction by adult stem cells (Kondo et al., 2003). As an experimental approach naturally occurring stem cells isolated from immortalized human mammary epithelial cells, normal mouse mammary tissues and human reduction mammoplasty tissues were shown to express EMT markers. Moreover, induction of EMT through overexpression of Snail or Twist generated stem cell-like cells from differentiated transformed mammary epithelial cells stem-like cells can be generated in vitro, suggesting an important role of EMT in CSCs induction (Mani et al., 2008).

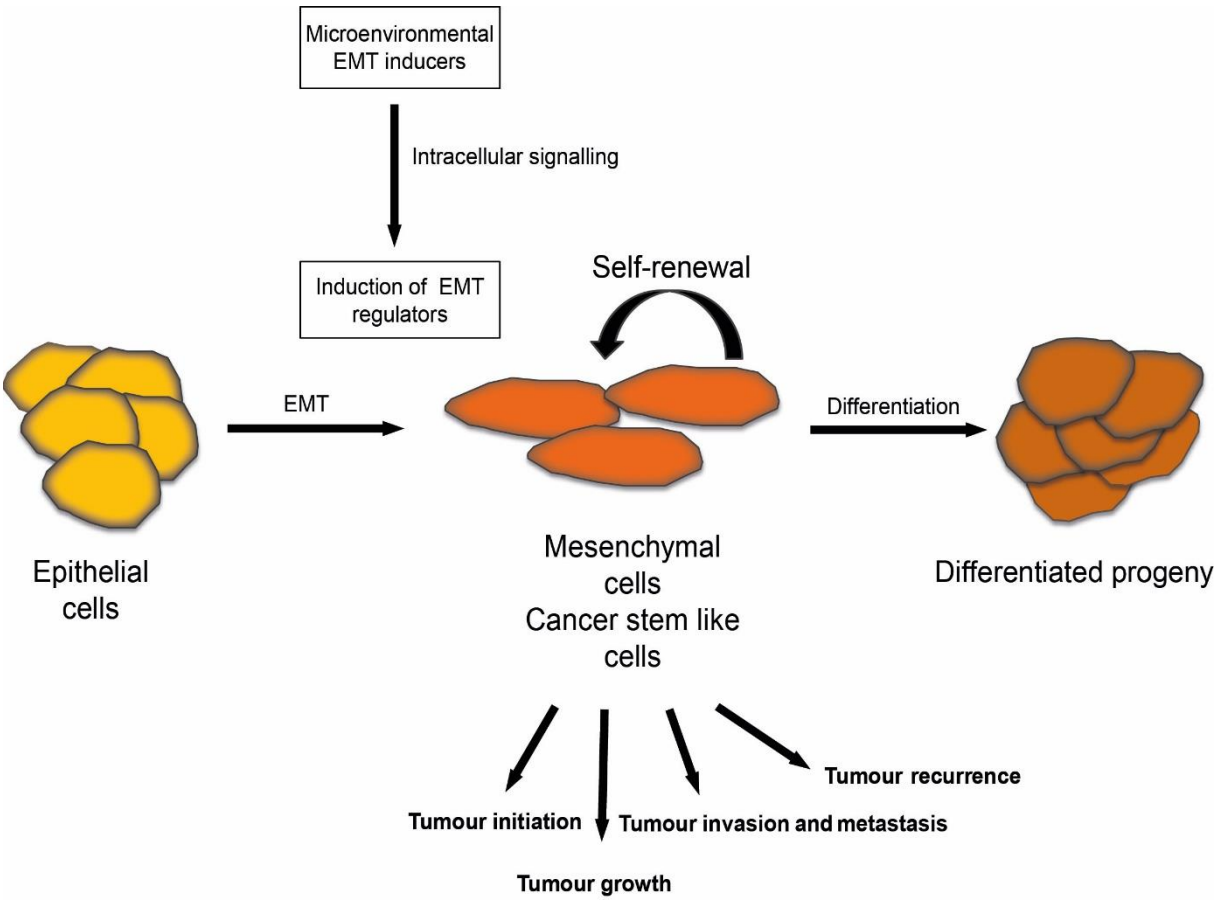

Fig. 3.8 Schematic model of CSC maintenance by EMT. Cells with an epithelial phenotype undergo EMT and are transformed into cells with mesenchymal expression patterns which share cancer stem cell traits. These CSC are able to initiate tumour formation, enhance tumour growth, invasion and migration of tumour cells to form distant metastasis and also contribute to tumour recurrence. Based on (Ouyang et al., 2010).

3.6 Aim of the study

The importance of EMT regulators in invasion as a critical step in malignancy is very well elucidated in epithelial cancers but the mechanisms of glial to mesenchymal transition in solid tumour of the CNS, like glioma, is so far only partly understood. In this work we wanted to assess the role of GMT in tumour growth, invasion and the induction and maintenance of CSCs. Furthermore, we wanted to find out what role microenvironmental cues, such as hypoxia and TGFβ signalling, play in the induction of GMT.

We first determined a set of markers suitable for the analysis of GMT. Next we examined the role of hypoxia and TGFβ signalling in controlling the expression of the key EMT factors of the Snail family. To address the functional significance of the EMT factors in the control of GMT we performed Snail/Slug loss of function experiments. Using stably transduced polyclonal pools of silenced cells we assessed the GMT phenotype by marker expression and by examining the invasive capacity of the cells. The involvement of the GMT regulators in tumour growth and invasion was examined by in vivo xenograft transplantation experiments. In addition, we investigated the functional role of Snail and Slug in the regulation of the cancer stem cell phenotype.

4. Results

4.1. Expression of Snail and Slug in the different molecular subclasses of glioblastoma

To examine the specific expression of EMT regulators Snail and Slug (SNAI1,SNAI2) in the molecular subclasses of glioblastoma we carried out a bioinformatic analysis of glioblastoma expression datasets from “The Cancer Genome Atlas” (TCGA). The mRNA expression data of the EMT regulators was downloaded from the publicly available datasets for GBM with neural, proneural, mesenchymal and classical gene signature (TCGA, 2008; Verhaak, 2010). The analysis showed that Snail and Slug, in line with their known function in other cancers, are significantly upregulated in tumours with a mesenchymal gene signature and downregulated in proneural, neural and classical subtypes (Fig. 4.1).

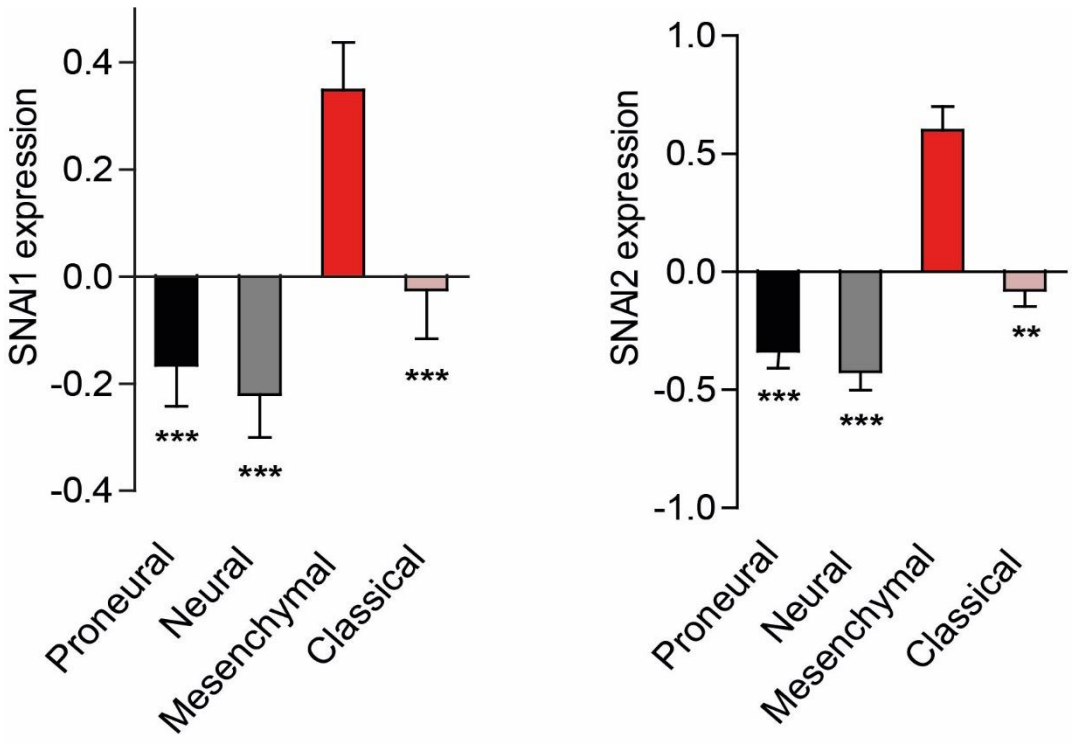

Fig.4.1 SNAI1 and SNAI2 are overexpressed in the mesenchymal glioblastoma subtype. mRNA expression of SNAI1 and SNAI2 in GBM with proneural, neural, mesenchymal and classical gene signature. The significances were calculated versus the mesenchymal subclass. **p < 0.01, ***p < 0.001

4.2 Regulation of Snail and Slug expression and induction of GMT by environmental signals

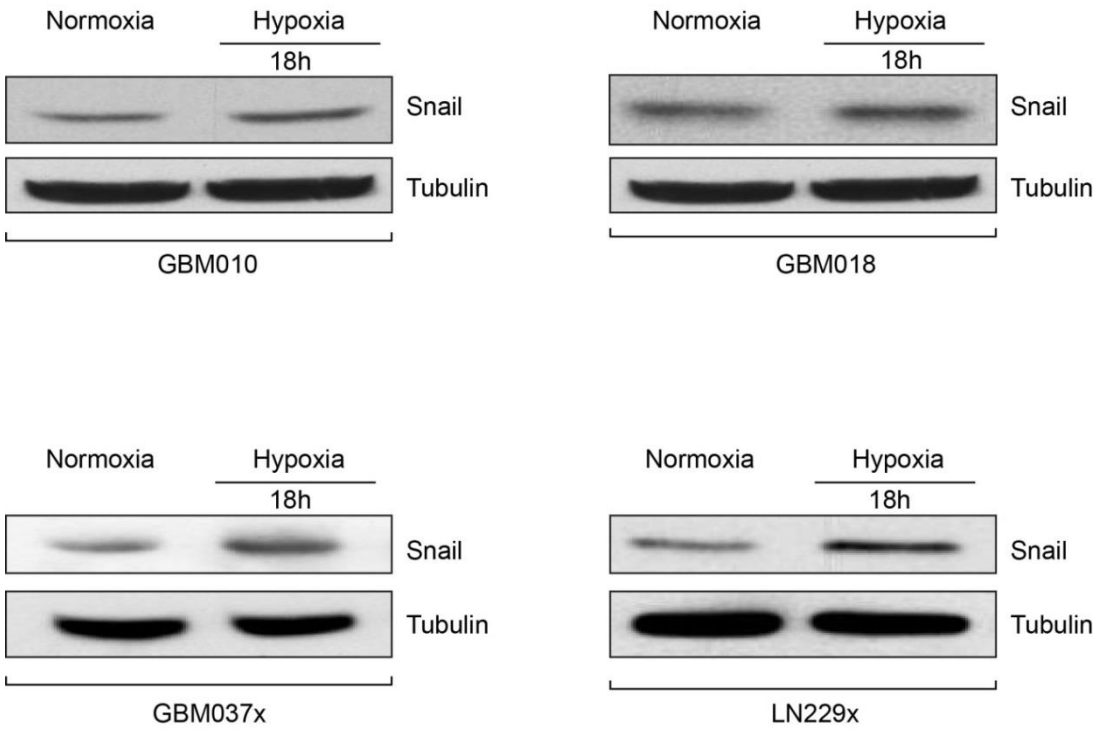

Fig. 4.2 Hypoxic induction of Snail Western blot analysis of different glioma cell lines, showing induced Snail expression when exposed to 1% oxygen for 18 h, compared to normoxic (21% oxygen) controls.

EMT/GMT is regulated by environmental cues, such as hypoxia and TGFβ. These triggers lead to an upregulation of transcriptional regulators like Snail and Slug as well as markers like vimentin and N-cadherin, accompanied by a downregulation of markers like E-cadherin, as a part of the induction of the EMT programme.

To find out if the expression of Snail is induced by low oxygen concentrations several glioblastoma cell lines were cultured either under normoxic (21% O_2) or hypoxic (1% O_2) conditions for 18 hours (Fig. 4.2). We used GBM10, GBM18 and GBM37x primary cell lines isolated from patient tumour samples, as well as LN229x, an established human glioma cell line that was re-isolated from a mouse xenograft. The analysis of protein levels by Western blotting showed a hypoxic induction of Snail, in comparison to the normoxic control, in several glioblastoma cell lines (Fig. 4.2). However the common markers for EMT like vimentin and N-cadherin showed no

regulation, upon hypoxic treatment in the glioblastoma cells used (data not shown). Furthermore E-cadherin showed no expression in our GBM lines. These results show that though hypoxia induces EMT regulator Snail this is not sufficient for the induction of typical EMT markers in glioblastoma.

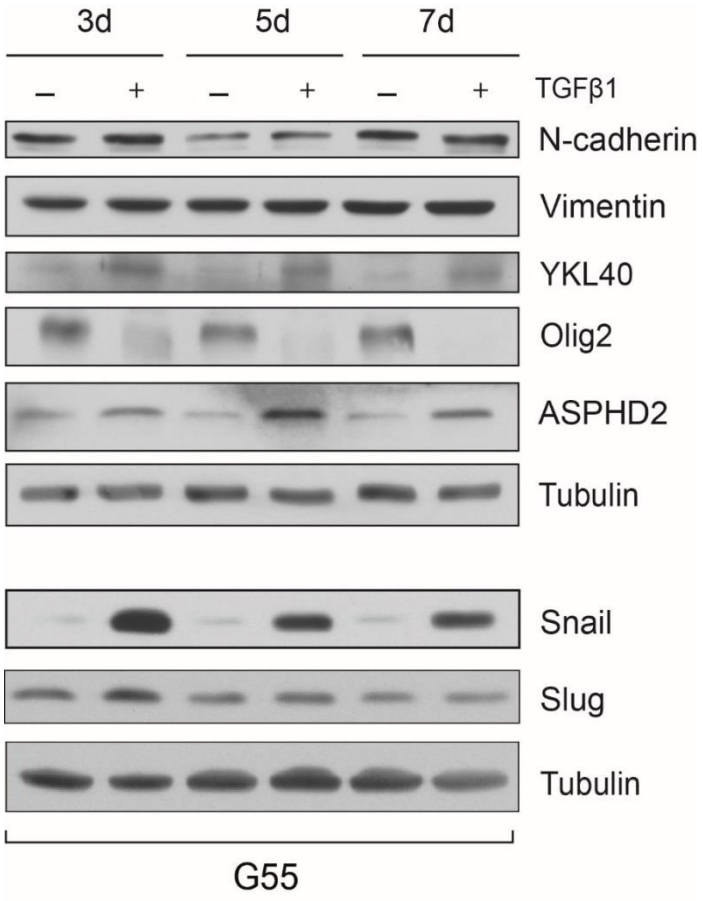

Fig. 4.3 Regulation of Snail and Slug expression and induction of GMT by environmental signals. TGFβ treatment (2.5 ng/ml for 3,5 or 7 days) induced Snail and Slug expression and regulated a set of markers corresponding to the transition from a proneural to a mesenchymal phenotype.

We next sought to determine the effect of TGFβ, the classical inducer of EMT on glioblastoma cells. G55 cells, an established glioma line, were treated with 2.5 ng/ml TGFβ for either 3, 5 or 7 days. As shown in Fig. 4.3 the expression levels of Slug and especially of Snail were strongly upregulated upon TGFβ treatment at all time points. Similarly to our findings following hypoxic exposure, however, the classical EMT markers vimentin and N-cadherin showed no consistent regulation upon TGFβ treatment. Therefore we aimed to determine whether alternative markers could be

found, which could be linked to the transition from a proneural to a mesenchymal phenotype. Based on literature research and expression profiling data (Phillips et al., 2006; Verhaak et al., 2010) we decided to test several possible markers to distinguish if cells are undergoing GMT and if this is accompanied to the acquisition of a cancer stem cell phenotype.

We used YKL40 as a mesenchymal marker, Olig2 as a proneural marker and ASPHD2 as a marker for stemness (Phillips et al 2006, Seidel et al 2010). Indeed, following TGFβ treatment G55 cells showed an upregulation of the mesenchymal marker YKL40 and the stemness marker ASPHD2 (Fig. 4.3). Consistently, Olig2 as proneural marker showed a stable downregulation when cells were treated with TGFβ (Fig. 4.3).

4.3. The loss of Snail and Slug impairs GMT and the establishment of a cancer stem cell phenotype

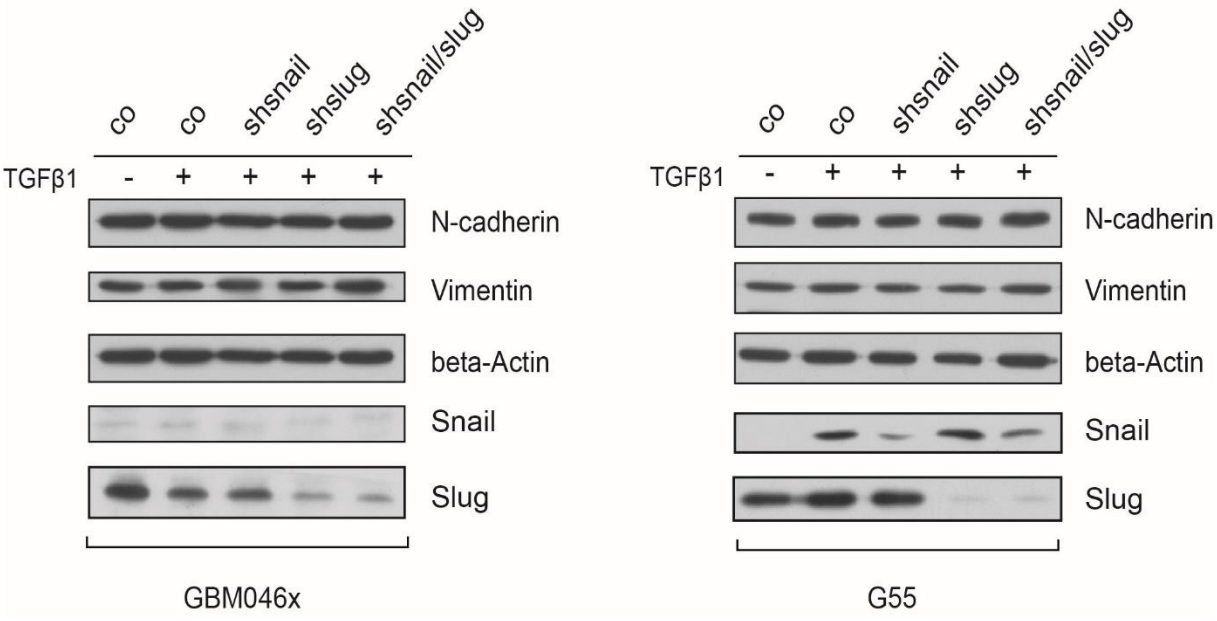

Fig. 4.4 The loss of Snail and Slug does not impair the expression of the classical EMT markers N-cadherin and vimentin. Western blot analysis of Snail and Slug deficient cells demonstrating no changes in the expression of N-cadherin and vimentin. GBM046x and G55 cells were treated with 2.5 ng/ml TGFβ1 for 3 days.

Snail and Slug were highly upregulated by TGFβ during the induction of EMT/GMT, suggesting that they play an important role in this process. To directly test this, we examined the phenotype of Snail, Slug or Snail/Slug deficient cells. GBM046x and G55 cells were stably transduced with lentiviruses carrying a vector containing a shRNA to silence either Snail or Slug or both together (Fig. 4.4). First, we checked the expression of the classical marker N-cadherin and vimentin in these knock-down pools. Consistent with our earlier findings, we could not observe any changes in protein levels of N-cadherin and vimentin following TGFβ treatment or silencing of either Snail, Slug or both (Fig. 4.4).

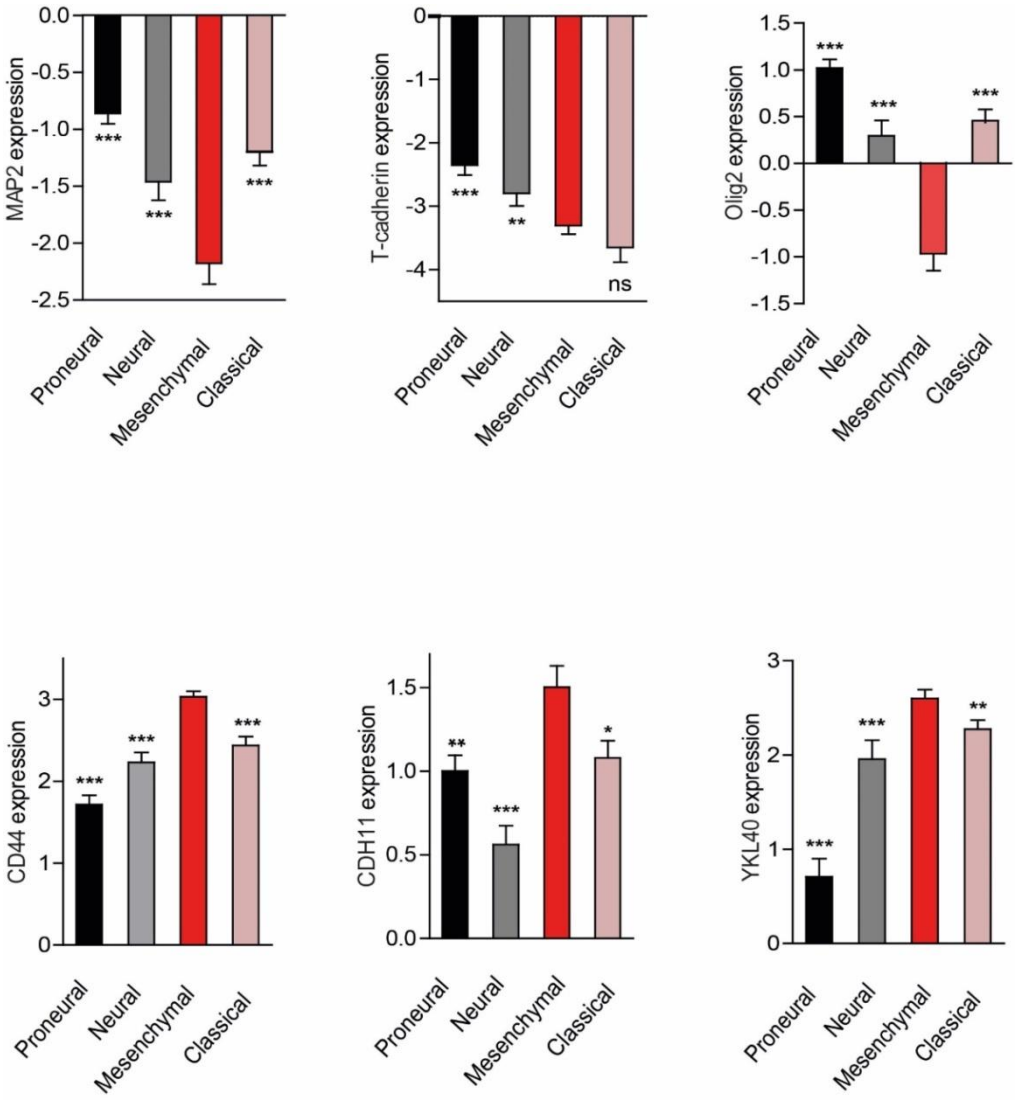

Fig. 4.5 Expression of GMT markers in glioma molecular subgroups. Analysis of the TCGA database showed that the panel of markers used in this work are differentially expressed in the different molecular subclasses of GBM. Significances were calculated versus the mesenchymal subclass. *p < 0.05, ** p < 0.01, ***p < 0.001

We next went on to establish a panel of markers that could be suitable for the distinction between proneural and mesenchymal states in glioblastoma. We focused on markers that have been previously proposed in expression profiling studies including MAP2, Olig2, and T-cadherin as proneural/glial marker, as well as CD44, CDH11 and YKL40 as mesenchymal markers (Phillips 2006, Verhaak 2010, Carro 2010). As a first step we analysed the expression of these markers in the TCGA glioblastoma dataset (Fig. 4.5). We found that MAP2, T-cadherin and Olig2 were significantly reduced in the mesenchymal subgroup compared to the proneural group. CD44, CDH11 and YKL40 showed a significant increase of expression in tumours classified for the mesenchymal subgroup compared to the proneural subgroup (Fig. 4.5)

Immunoblotting (Fig. 4.6) and an analysis of mRNA levels (Fig. 3.7) of the markers in GBM046x and G55 cells showed that they are prominently regulated through the addition of TGFβ1. The proneural markers MAP2, Olig2 and T-cadherin exhibit a reduced expression when control cells were treated with TGFβ1, whereas the mesenchymal markers CD44, YKL40 and CDH11 as well as the stemness marker ASPHD2 showed an upregulation when GMT was induced by TGFβ1 in control cells. Importantly, silencing of Snail and Slug largely reversed the TGFβ1 induced GMT transition (Fig. 4.6). Quantitative real-time PCR showed that the loss of Snail and Slug induced strongly the expression of the proneural marker T-cadherin and reduces the expression of the mesenchymal markers CDH11 and CD44 in GBM046x and G55 cells (Fig. 4.7).

The markers MAP2, Olig2, CD44, ASPHD2 were not altered or changed in a direction corresponding to a transition from a mesenchymal to a proneural state upon single silencing of Snail or Slug, but Snail/slug double knockdown induced a pronounced shift to a proneural phenotype. On the other hand for the mesenchymal marker YKL40 single Snail and Slug knockdowns induced a partial mesenchymal to proneural transition, but the effects of the combined Snail/Slug knockdown were again typically more potent. Thus, while silencing of either Snail or Slug was sufficient to alter the expression of some of the proneural and mesenchymal markers, combined silencing of Snail and Slug had the most profound and robust effects, inducing a shift from a mesenchymal to a proneural state under TGFβ1 stimulation.

Taken together, these results demonstrate that the transcription factors Snail and Slug play a synergistic, partially redundant role in the regulation of GMT and the acquisition of cancer stem cell traits.

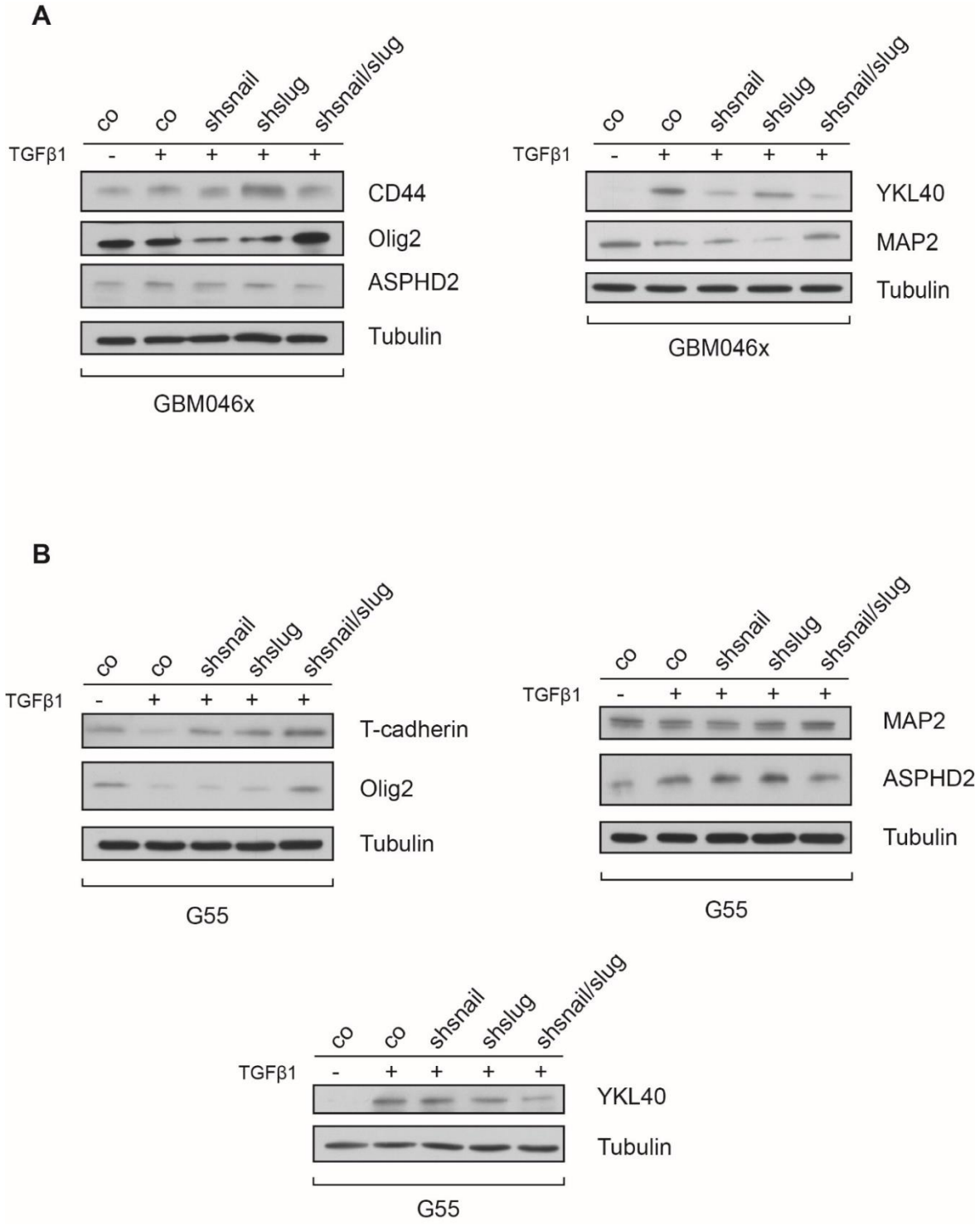

Fig. 4.6 The loss of Snail and Slug inhibits a complete glial to mesenchymal transition. **A+B** Immunoblotting of GMT markers in GBM046x and G55 after TGFβ1 stimulation, showing that cells with silenced Snail and Slug expression are not able to complete the transition from a proneural to a mesenchymal phenotype. (For knock-down efficiency see Fig. 4.4)

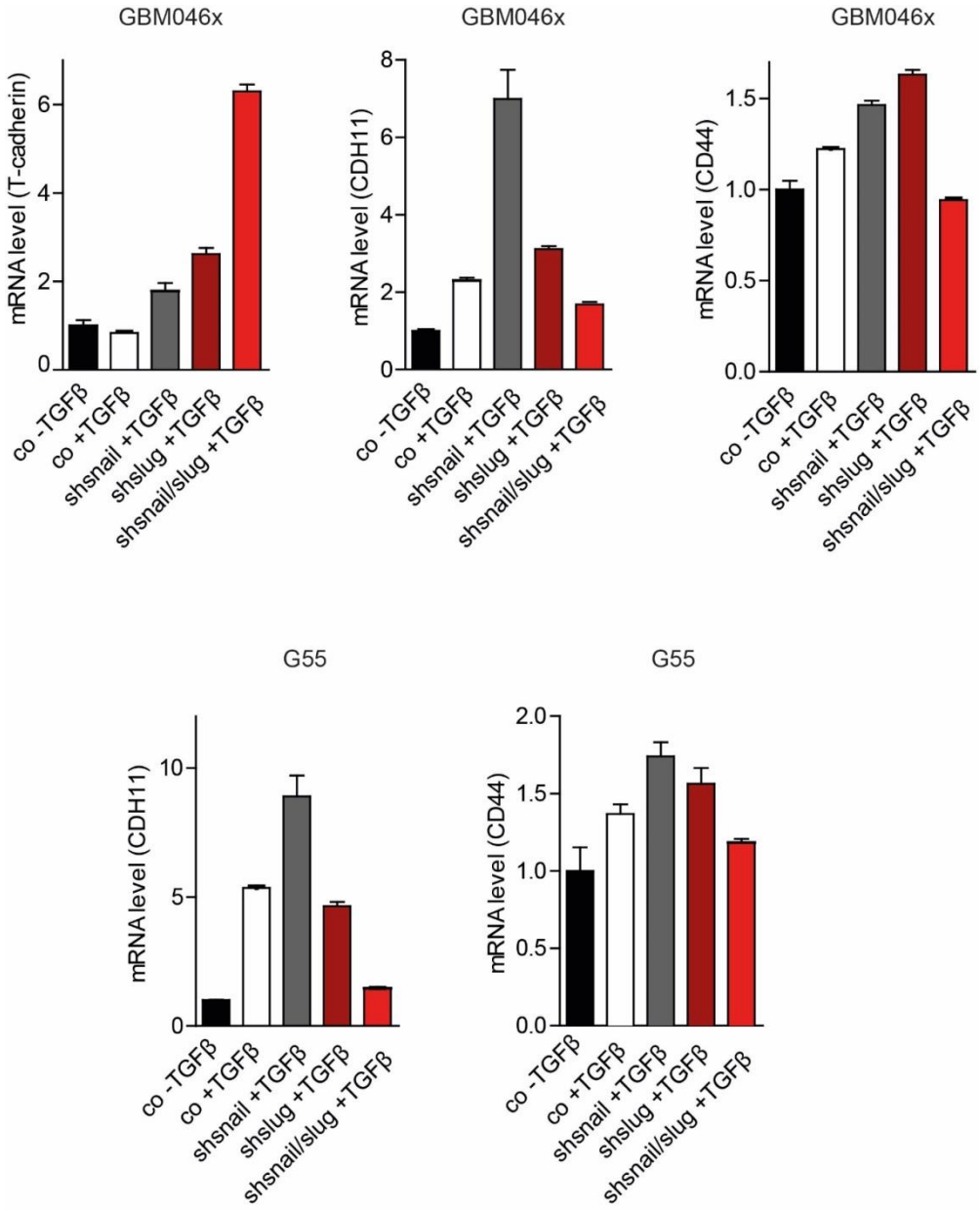

Fig. 4.7 The loss of Snail and Slug impairs the mRNA expression of GMT markers. Analysis of mRNA levels of GMT markers, showing that the loss of Snail and Slug impairs the transition from proneural to mesenchymal phenotype.

4.4 Snail and Slug influence the cancer stem cell phenotype of GBM cells

The regulation of glioma stem cell markers such as ASPHD2 by Snail/Slug silencing (see Fig. 4.6A, B), suggested that Snail and Slug are involved in the control of cancer stem cell expansion or maintenance. To further investigate if cell stemness is connected to the expression of GMT regulators we performed fluorescence activated cell sorting (FACS) to assess the expression of the surface marker CD15 which is

commonly used as a stem cell marker (Read et al., 2009) (Fig. 4.8A). Interestingly, GBM046x cells lacking Snail and Slug showed a significantly smaller population of cells with high CD15 expression in FACS compared to the control cells (Fig. 4.8A). Furthermore Snail/Slug knockdown cells also exhibit a reduced expression of cancer stem cell markers, such as MAML3, SOX2 and OCT4 (Fig. 4.8B).

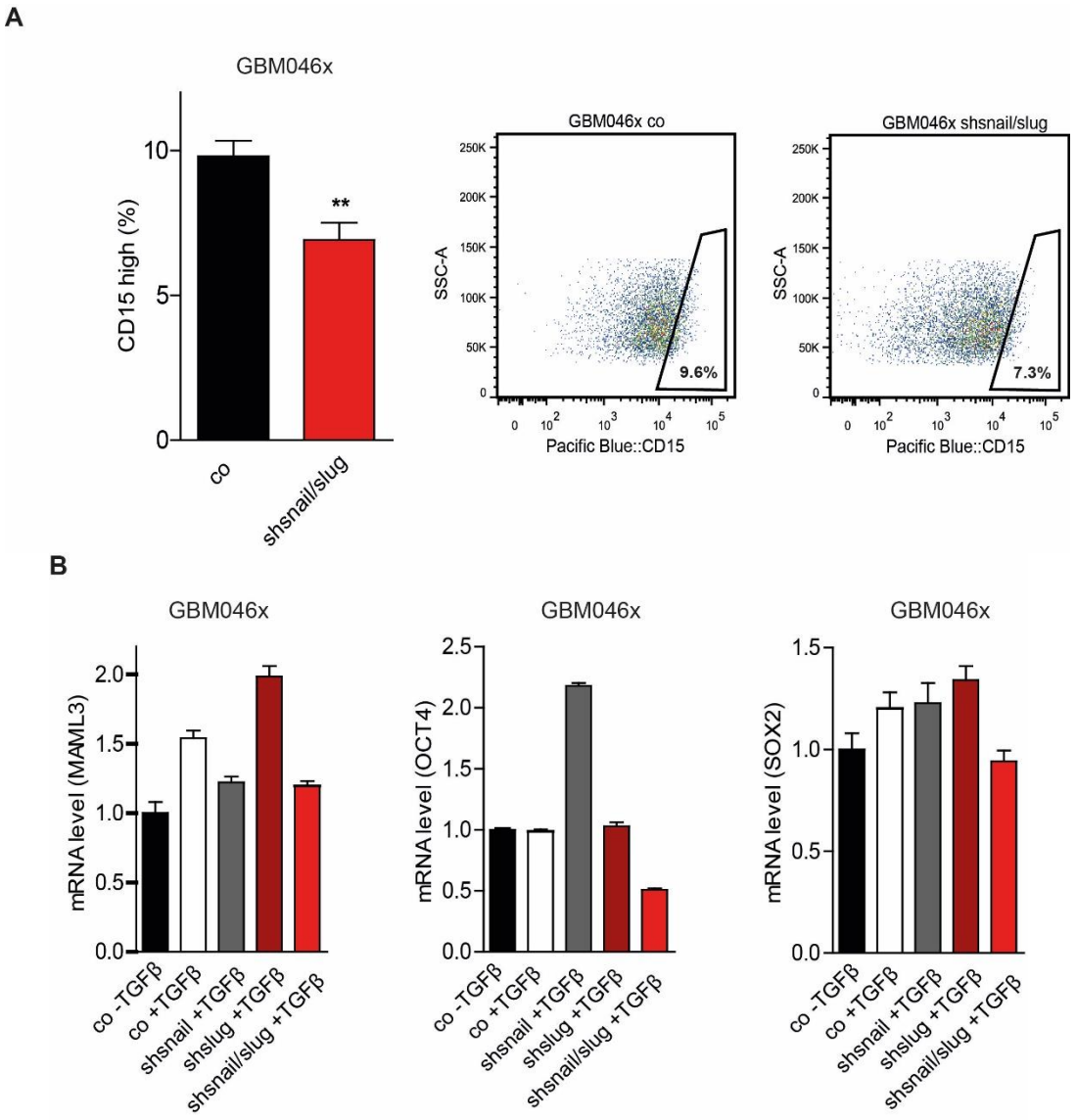

Fig. 4.8 Snail and Slug influence the expression of CSC markers. A FACS analysis of CD15 showed reduced expression in Snail and Slug deficient cells. **B** The expression of the stem cell markers MAML3, OCT4 and SOX2 is reduced in shSnail/Slug cells. **p < 0.01

To functionally confirm that Snail and Slug are involved in stem cell regulation we performed a sphere formation assay for GBM046x and G55 cells (Fig. 4.9). This assay examines the ability of single GBM cells to self-renew and form gliomaspheres

in suspension culture conditions, which is one of the key read-outs for the self-renewal potential of normal and cancer stem cells. Seven days after seeding the single cells, the formed gliomaspheres were counted and the percentage of sphere forming units (SFU) was assessed. These experiments demonstrated that combined silencing of Snail and Slug suppressed the glioma cell self-renewal significantly, with Snail playing an apparently dominant role in GBM046x in this context (Fig. 4.9).

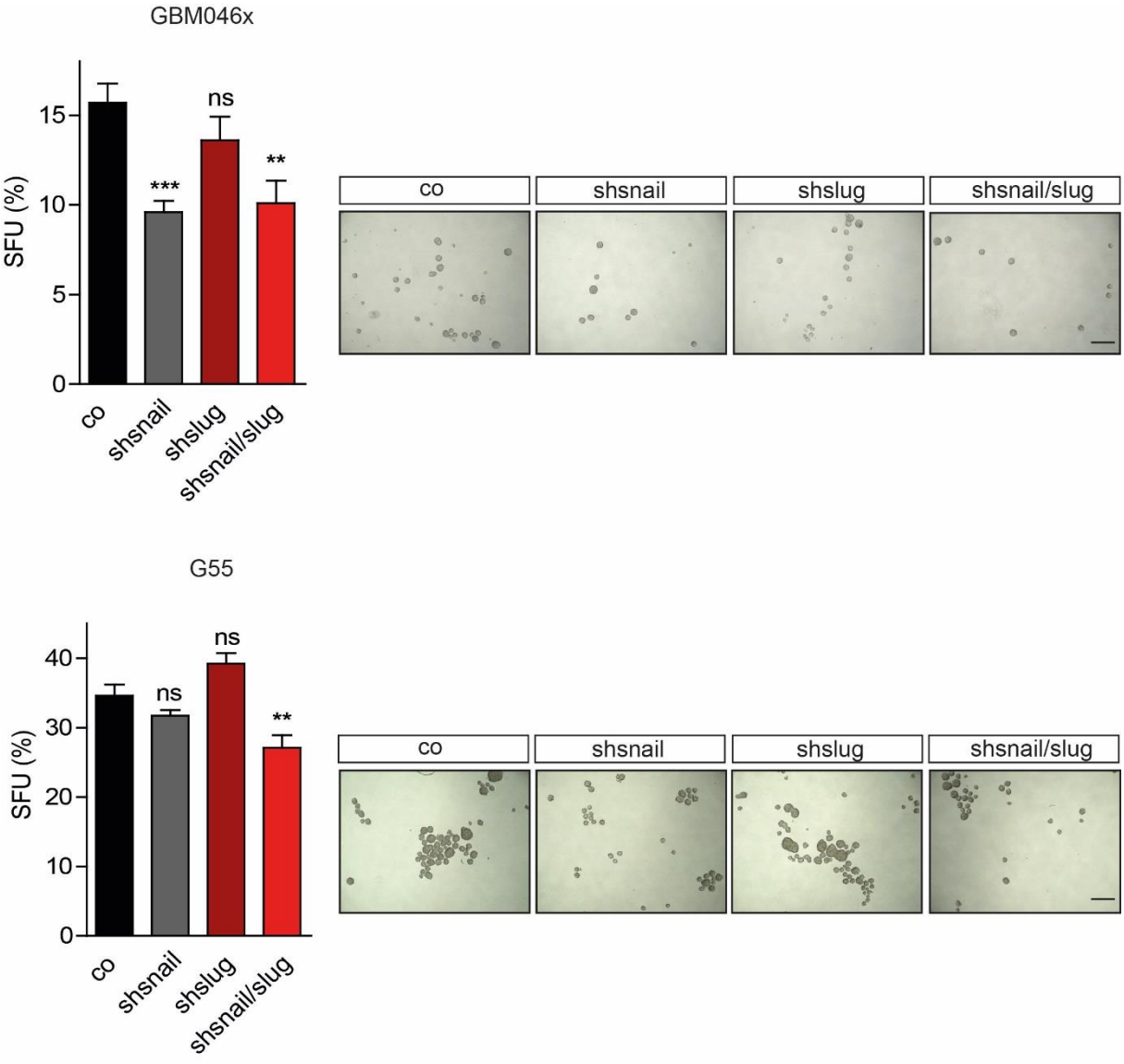

Fig. 4.9 Snail and Slug control the self-renewal ability of glioma cells. Sphere formation assays showing that the self-renewal capacity of Snail/Slug deficient cells is significantly reduced. Scale bars represent 200 µm. **p < 0.01, ***p < 0.001

Taken together, these results show that concomitantly with their effects on GMT, Snail and Slug are important regulators of the glioma stem cell phenotype. As combined silencing of Snail and Slug had more robust and consistent effects on the capacity of glioblastoma cells to undergo GMT and on their stem cell phenotype compared to individual knockdown of Snail or Slug, we focused our further experiments on cells with simultaneous Snail and Slug loss.

4.5 Apoptosis and proliferation of GBM cells in vitro is not impaired by the loss of Snail and Slug

Snail and Slug are also thought to be involved in proliferation and/or apoptosis in vitro as well as in patients (see section 3.3.3). To determine the role of Snail and Slug in cell death and proliferation we performed immunofluorescence stainings of apoptotic cells with the TUNEL assay. Proliferative cells were analysed by staining for BrdU (Bromodeoxyuridine), incorporated in the DNA during S-phase (Fig. 4.10A, B). Quantification of the stainings showed that the loss of Snail and Slug had no significant effect on the amount of apoptotic or proliferative cells in GBM046x and G55 cells (Fig. 4.10A, B).

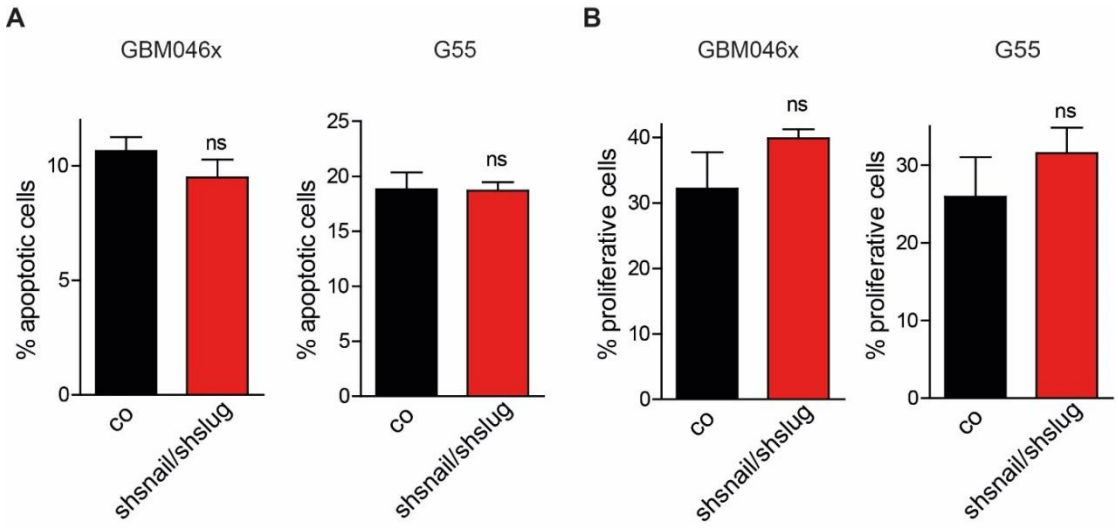

Fig. 4.10 The loss of Snail and Slug does not affect apoptosis and proliferation in vitro. **A** Quantification of TUNEL staining of GBM046x and G55 cells showed no significant differences in the amount of apoptotic cells between control and shSnail/Slug cells. **B** Quantification of BrdU staining of GBM046x and G55 cells showed no significant differences in the amount of proliferating cells between control and shSnail/Slug cells.

4.6. The loss of Snail and Slug impairs the invasiveness of GBM cells in vitro

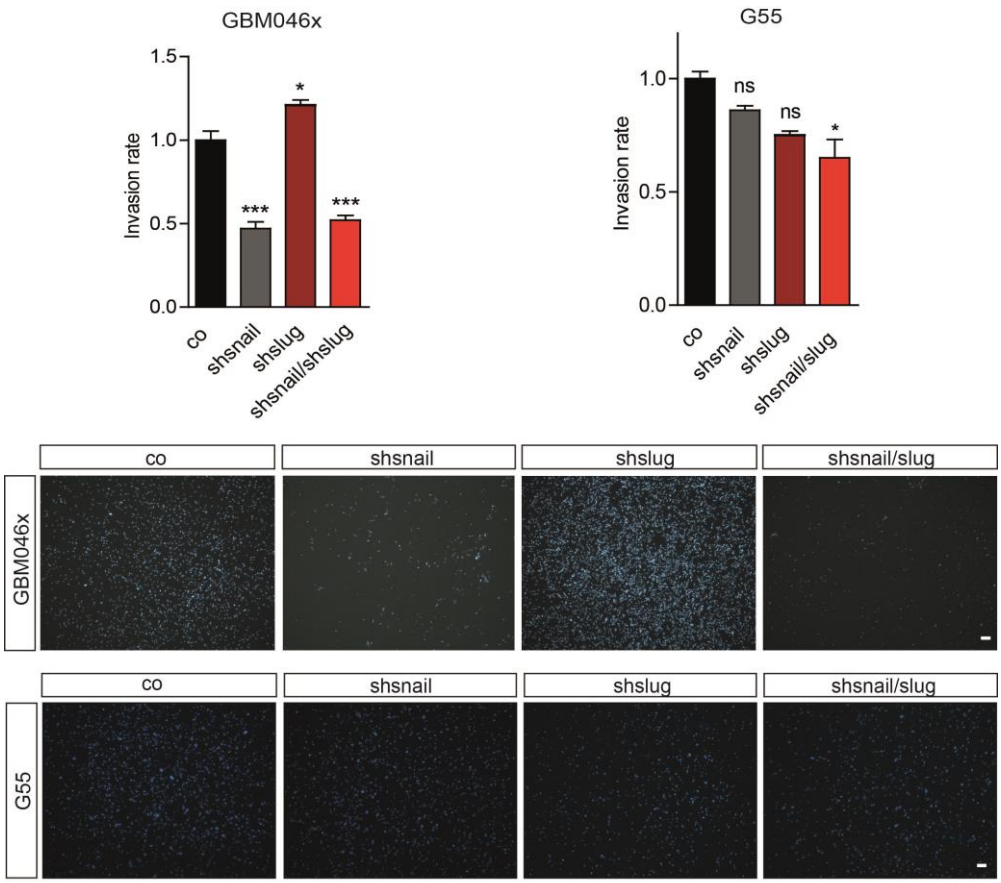

Fig. 4.11 The loss of Snail and Slug impairs the invasiveness of glioblastoma cells through matrigel. Modified Boyden chamber assay showed that GBM046x and G55 cells have a severely reduced ability to invade through a matrigel covered filter when Snail or Snail /Slug are silenced. Scale bars represent 100 µm *p < 0.05, ***p < 0.001

A central characteristic of the mesenchymal phenotype is enhanced cell invasiveness. In the context of GBM this could be reflected by an accelerated infiltration of tumour cells away from the tumour mass into the surrounding brain parenchyma. To assess the role of Snail and Slug in GBM cell invasion we performed in vitro Invasion assays (Fig. 4.11, 4.12). First we used a modified Boyden chamber assay to assess the ability of the cells to invade through a polystyrene filter with a pore size of 8 µm coated with a layer of matrigel, which serves as a model of the

basal lamina. The invasion rate of the cells was examined after 18 hours of invasion. Importantly in both GBM046x and G55 cells silencing of Snail and Slug significantly reduced invasion. Interestingly, in GBM046x cells the single knock-down of Snail seemed to be sufficient to reduce the invasive capacity of the cells in this assay. The observed effect of strongly reduced invasion in the Snail and Slug deficient cells seemed to be presumably due to the silencing of Snail since the knock-down of Slug increased the invasion of the cells (Fig. 4.11). By contrast, in G55 cells the modified Boyden chamber assay showed clearly that only combined Snail and Slug deficiency significantly impaired in invasion through the matrigel layer (Fig. 4.11). Single silencing of Snail or Slug alone had no effect on the invasiveness of the cells.

To provide further support for the role of Snail and Slug in glioblastoma cell invasion we performed an additional assay, namely a collagen invasion assay. This assay resembles the natural conditions of cancer cell invasion through an extracellular matrix. The cancer cells are embedded as a small gliomasphere into a layer of collagen, which is a part of the extracellular matrix, allowing the cells to invade in a three dimensional manner. By capturing microscope images every 24 hours we were able to follow the process of invasion. The ability of the cells to invade into the collagen was quantified using the invasion index formula, invasiveness= $(\text{Perimeter})^2$ / Area (Siebzehnrubl et al., 2013).

The obtained results supported the data of the modified Boyden chamber assay, by demonstrating that silencing of Snail and Slug markedly reduced invasion. In GBM046x cells silencing of Snail was sufficient to impair the invasiveness in collagen after 24 and 48 hours (Fig. 4.12), in accordance with the results from the Boyden chamber assay. In G55 cells, on the other hand the silencing of either Snail or Slug alone had no significant effects on the three dimensional invasion in the collagen matrix. However, combined loss of Snail and Slug strongly impaired the capacity of G55 cells to invade collagen (Fig. 4.12).

Taken together, these finding suggest a prominent role for Snail and Slug in the regulation of invasion in GBM which seems to be closely connected to the regulation of GMT.

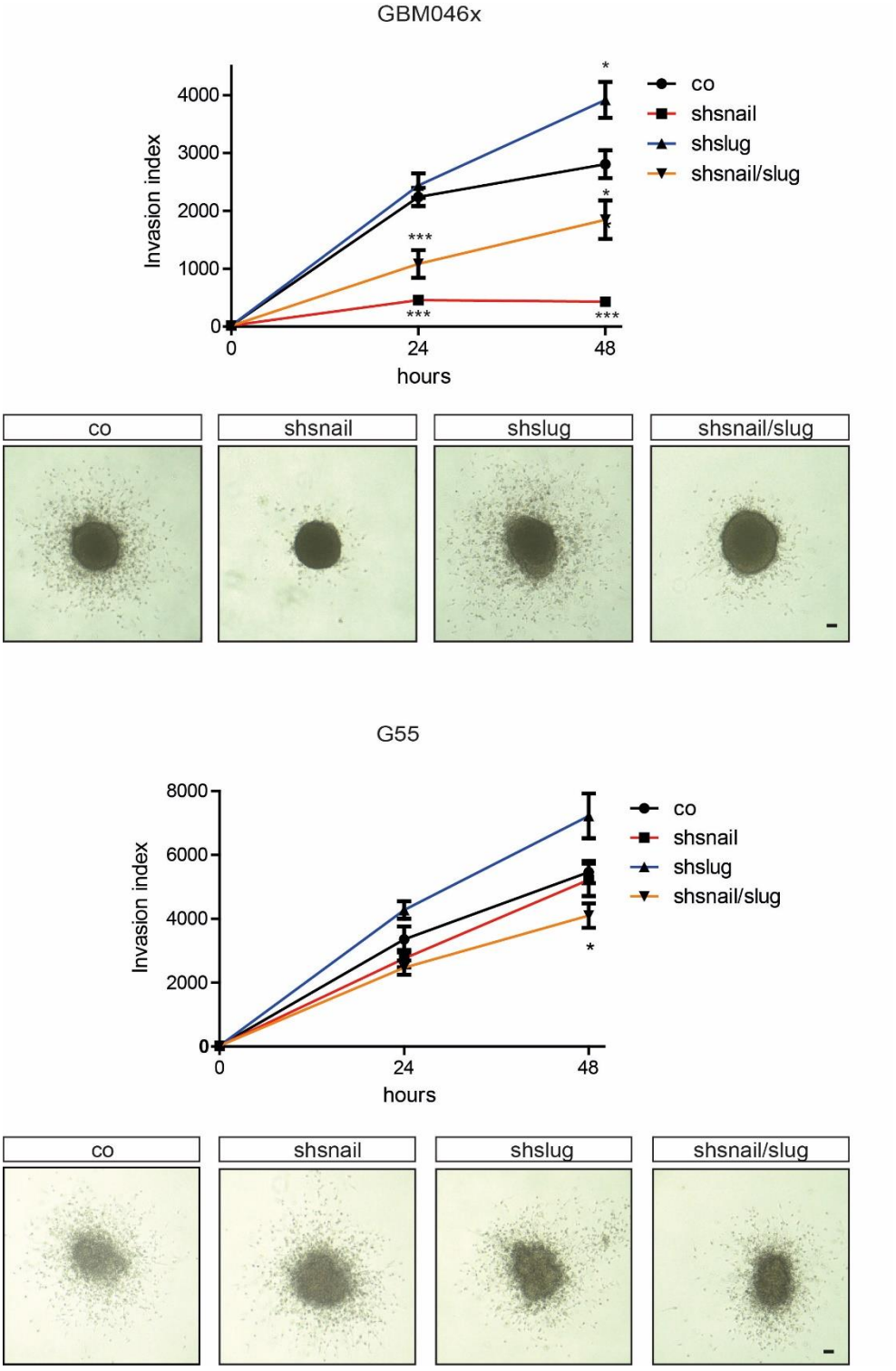

Fig. 4.12 Snail and Slug deficiency reduces the ability of glioblastoma cells to invade into collagen Collagen invasion assay of a tumoursphere showed that the invasion capacity of shSnail and shSnail/Slug cells is highly impaired. Scale bars 100 µm. *p < 0.05, ***p < 0.001

4.7. Snail and Slug deficient cells show reduced tumour growth

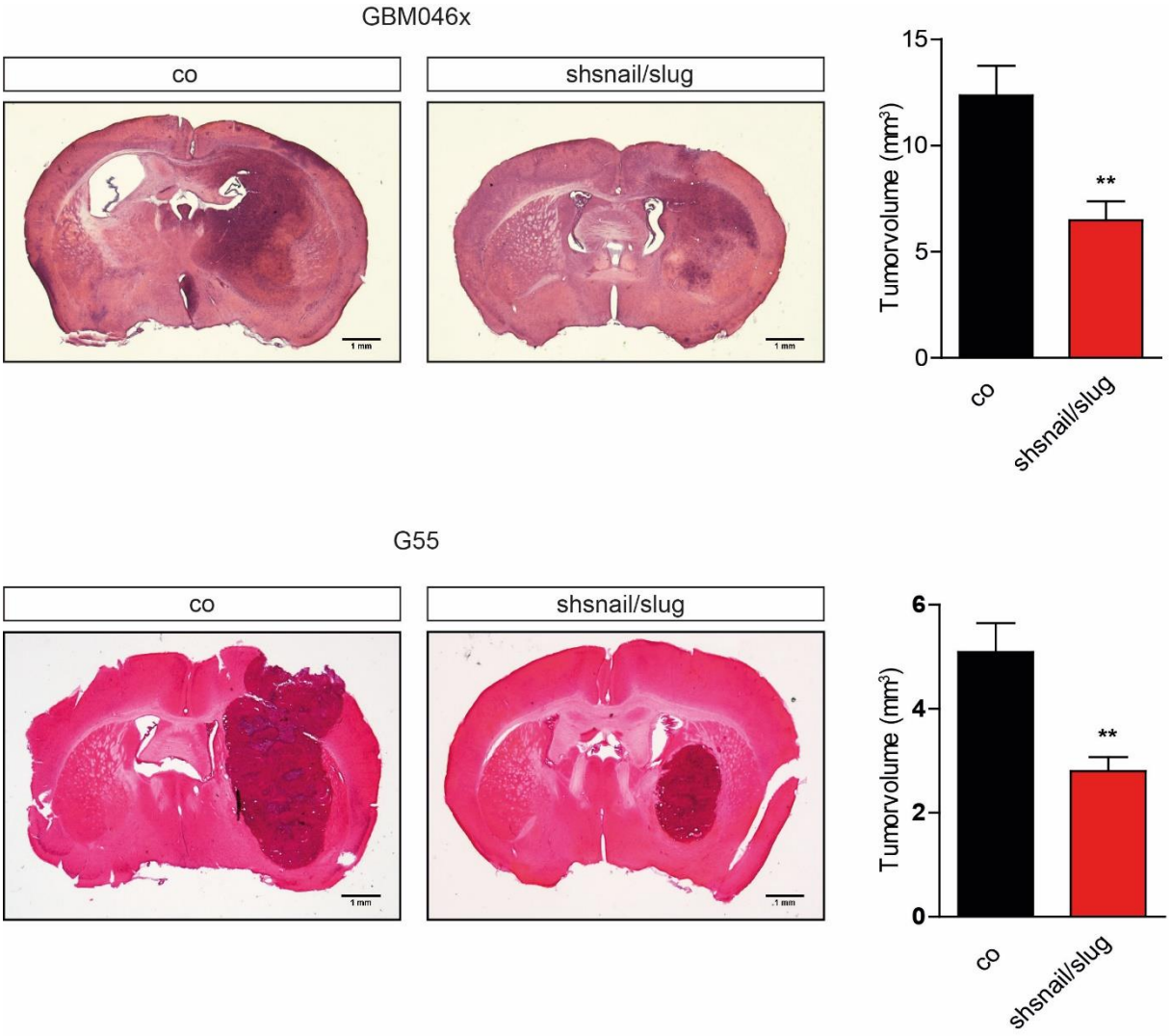

Fig. 4.13 Snail and Slug deficiency reduces intracranial glioma growth. **A** Representative hematoxylin/eosin staining of GBM046x and G55 control and shSnail/Slug tumours (40 µm thick section). Snail and Slug deficient cells showed a significantly reduced tumour volume. Scale bars represent 1mm. **p < 0.01

Given the effects of silencing Snail and Slug on GMT and stemness, we next wanted to assess if Snail and Slug are involved in the control of tumour growth in vivo. The Snail/Slug deficient cells were pretreated with TGFβ1 and then intracranially injected into immuno-deficient nude mice. After the mice started to show neurological symptoms typically associated with brain tumour growth and the development of increased intracranial pressure, they were sacrificed and perfused with 4% PFA to fix the tumour tissue. The tumour growth in the brain was assessed by measuring the tumour volume in hematoxylin and eosin (H&E) staining of serial sections (Fig. 4.13).

The tumours of GBM46x and G55 cells with silenced Snail and Slug showed a significantly smaller size compared to the control group (Fig. 4.13), consistent with our findings of an important functional role of Snail and Slug in GMT and glioma stem cell maintenance.

4.8. The loss of Snail and Slug does not impair apoptosis, proliferation or vascularisation in vivo

To further asses the reasons for the reduced growth of Snail and Slug silenced tumours we also examined the effects on apoptosis and proliferation of tumour cells in vivo as well as the vascularisation of the tumour itself.

To visualize apoptotic cells, 40 µm thick sections of the GBM046x and G55 tumours we used a TUNEL assay (Fig. 4.14). Quantification of the stained cells showed that in both tumours no difference in the number of apoptotic cells per mm^2 was observed between control group and the Snail/Slug double knockdown group (Fig. 4.14). Thus, we could rule out that a higher apoptosis rate in the double knockdown group is the reason for the smaller tumour volume.

Differences in tumour growth can be often explained through effects on cell proliferation. Proliferating cells are detectable when stained for the phosphorylated form of histone 3 on the highly conserved Ser-10 residue. This phosphorylation event is a read out for the onset of mitosis. Staining of tumours from GBM046x and G55 cells for phospho-histone 3 showed no significant difference between control and Snail/Slug silenced tumours (Fig. 4.15), indicating that reduced tumour growth of Snail/Slug double knockdown cells cannot be explained by impaired proliferation.

Another reason for slower growth could be a reduced vascularisation of the tumour. Neovascularisation and co-opted brain vessels are needed by the tumour for suffiencient oxygen and nutritional supply. To asses tumour vascularisation we performed an immunofluorescence staining for endomucin, a protein present on the surface of blood vessel endothelial cells (Fig. 4.16). Quantification of the ratio of area covered by vessels to total analysed tumour area showed that the vascularisation of the tumour was also not affected through the silencing of Snail and Slug (Fig. 4.16).

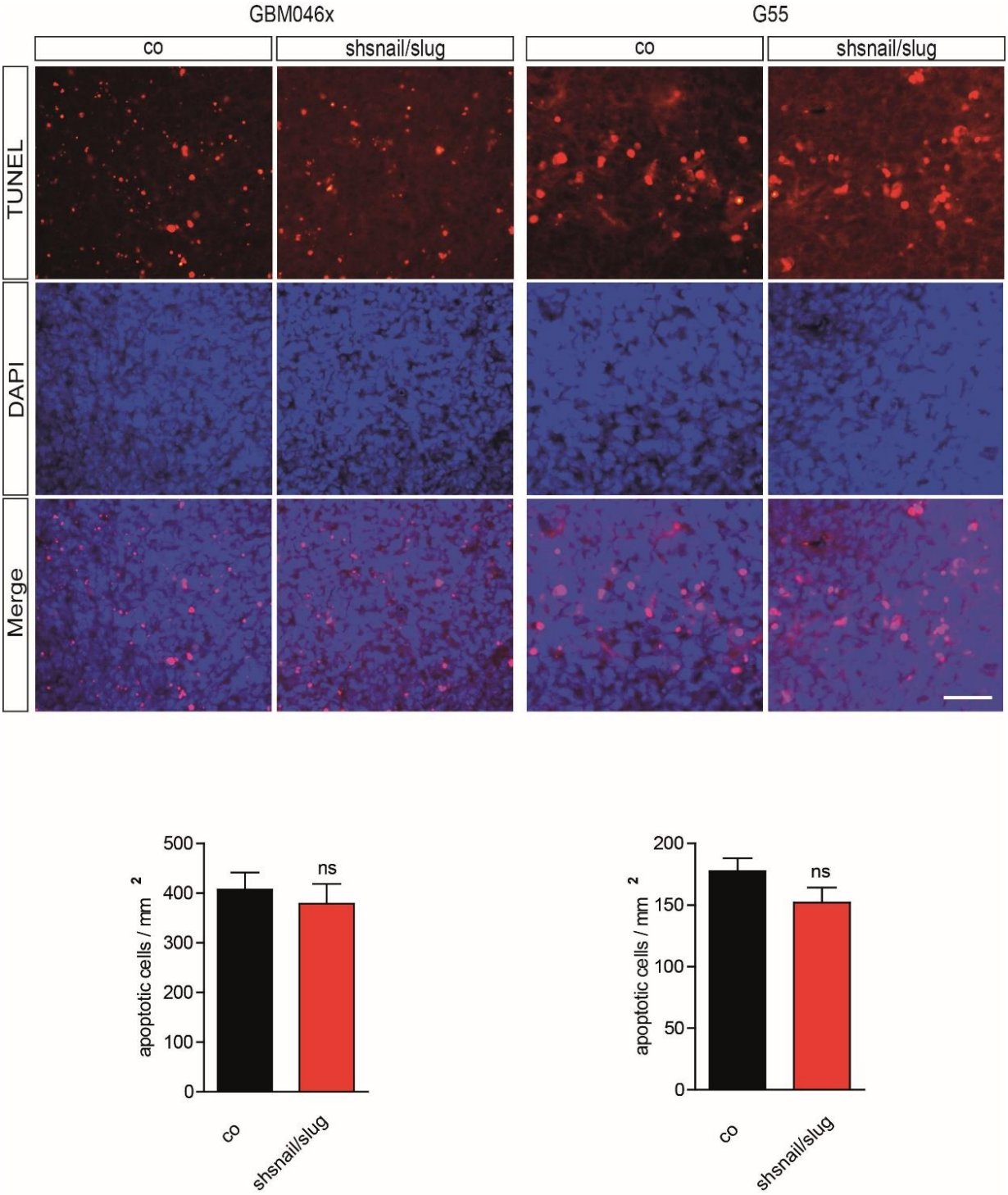

Fig. 4.14 The loss of Snail and Slug does not impair apoptosis of tumour cells. 40 µm tumour sections were stained for apoptotic cells using a TUNELassay. Positively stained cells/mm^2 were quantified. Scale bar represents 100 µm.

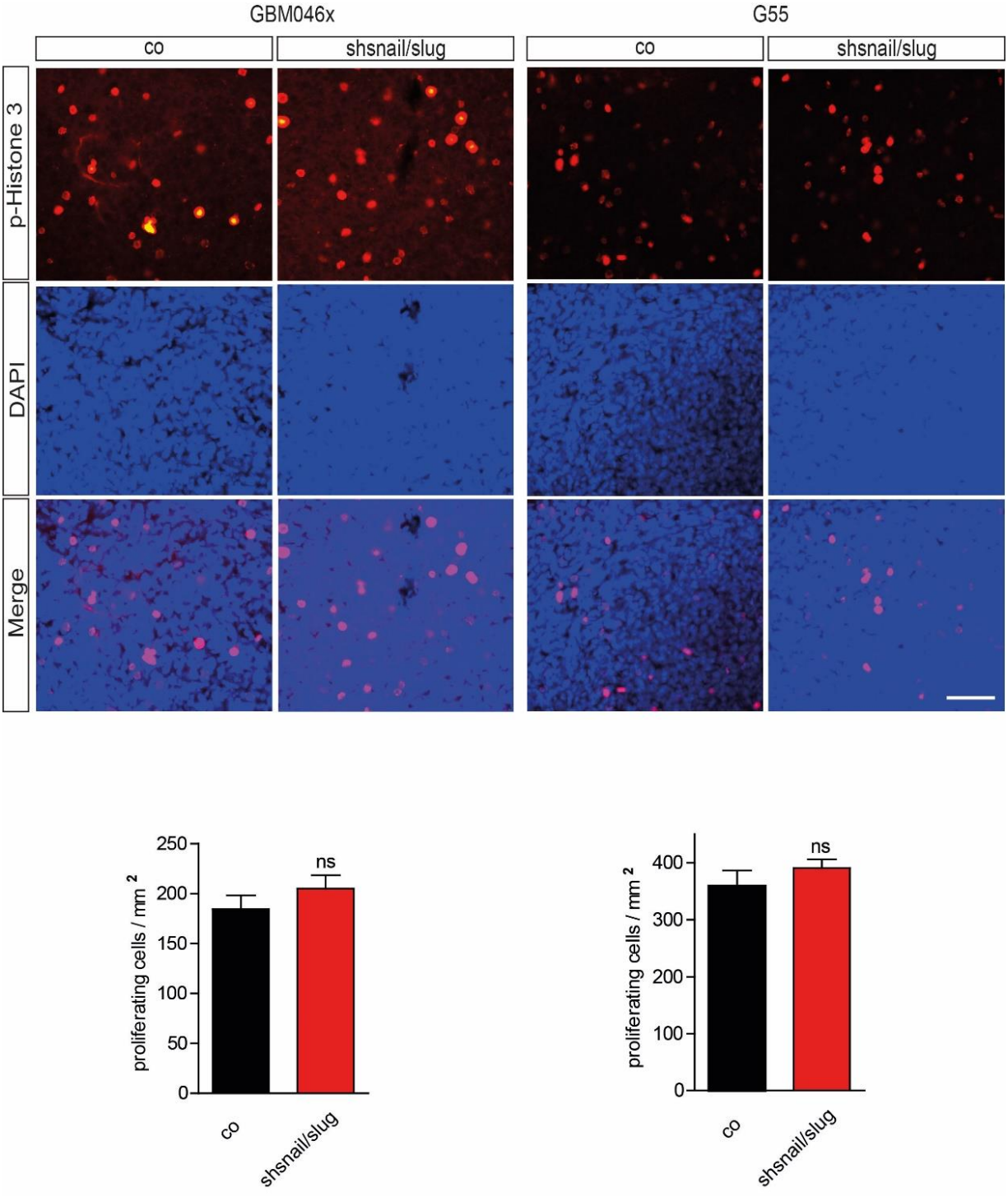

Fig. 4.15 The loss of Snail and Slug does not impair proliferation of tumour cells. 40µm thick tumour sections were stained for proliferating cells using an antibody against phospho-histone 3. Positively stained cells/mm^2 were quantified. Scale bar represents 100 µm.

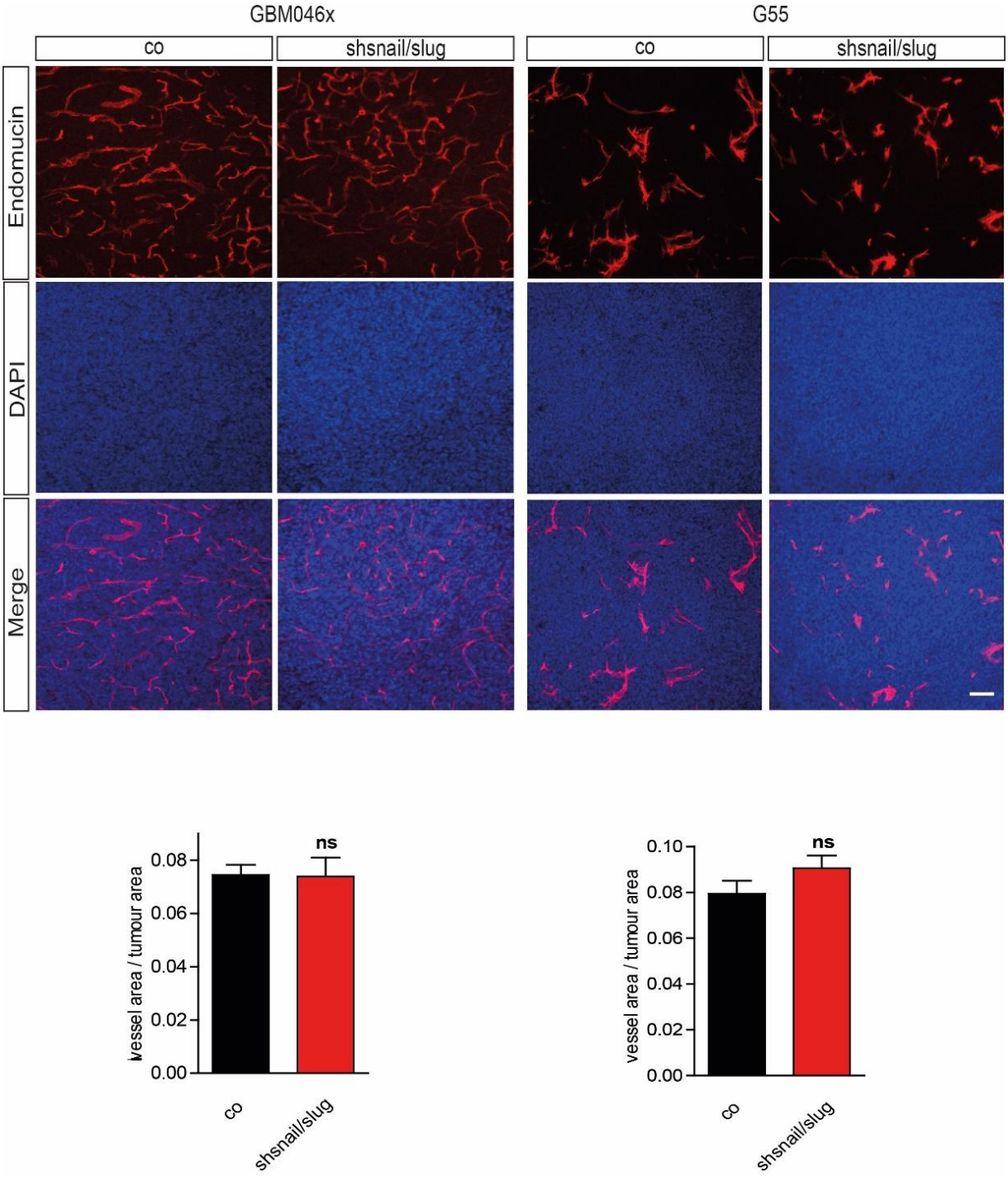

Fig. 4.16 The loss of Snail and Slug does not impair vascularisation of the tumour. 40 µm tumour sections were stained for blood vessels using an antibody against the endothelial protein Endomucin. The stained vessel area was quantified. Scale bar represents 100 µm.

4.9. The loss of Snail and Slug impairs the invasiveness of GBM cells in vivo

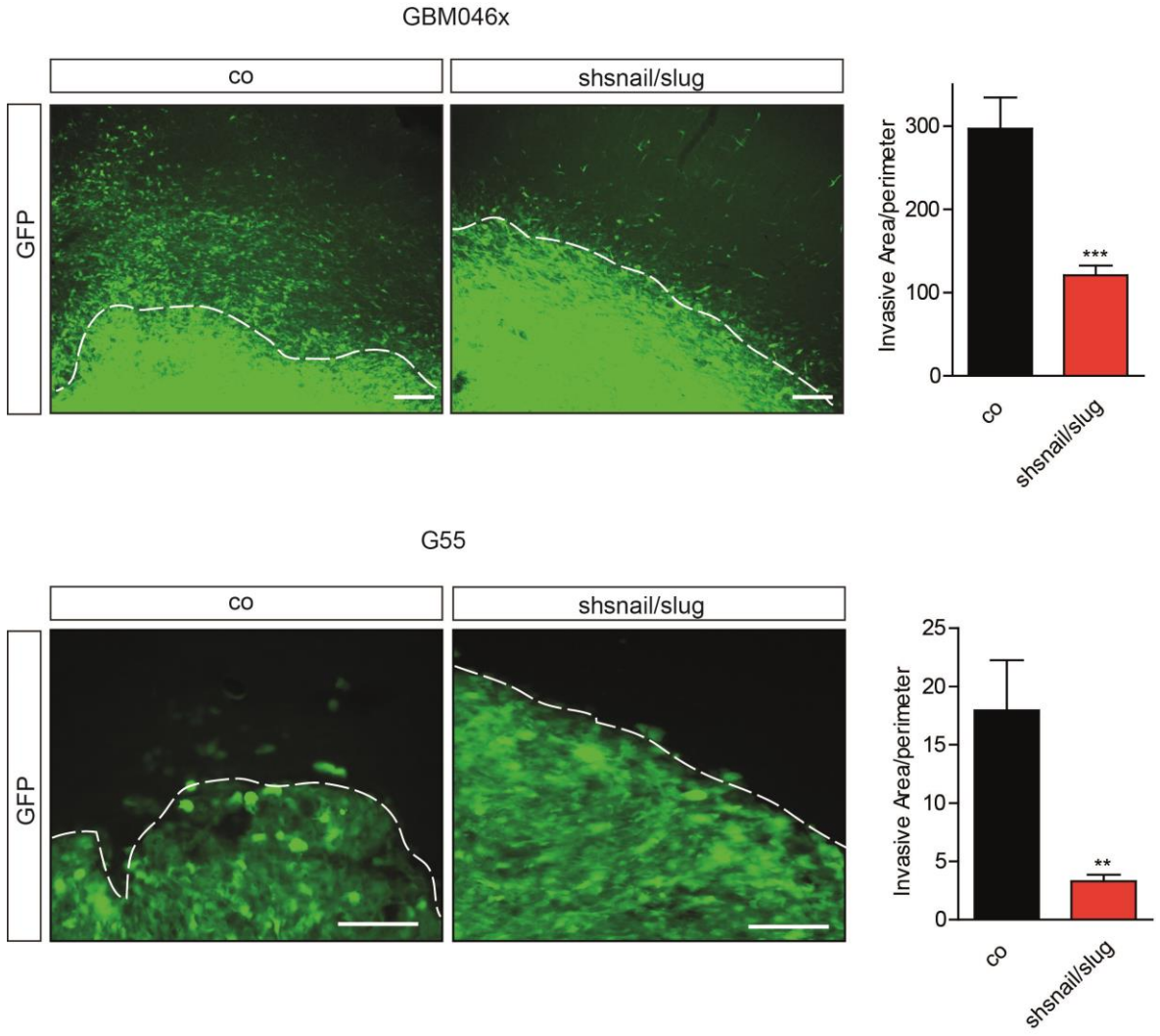

Fig. 4.17 The invasiveness of cancer cells in vivo is significantly reduced by silencing Snail and Slug. GFP expressing control cells or shSnail/Slug GBM046x or G55 cells were orthotopically transplanted into nude mice to monitor the invasive behaviour of the cells. Cells with silenced Snail/Slug expression showed a drastic reduction of invasion into the surrounding brain parenchyma. Pictures of GBM046x tumours were taken with 10x magnification; Pictures of G55 tumours were taken with 20x magnification. Scale bars represent 100 µm. **p < 0.01, *** p < 0.001

In our in vivo experiments we were able to use the GFP signal of the transduced cells to assess the invasive area. 40 µm thick sections of the brain were mounted and pictures were taken with a fluorescence microscope (Fig. 4.17). Both the GBM046x and G55 tumours showed a striking effect on invasion when Snail and Slug were silenced, as apparent through the strong reduction of invading cells leaving the

tumour mass in the double knock-down cells compared to the control cells . Analysis of the invasive area of the tumours showed that the invasion of tumour cells was significantly reduced in the Snail and Slug double knockdown group in comparison to the control tumours (Fig. 4.17).

These findings support our hypothesis that invasion, the key feature of EMT in epithelial cancers is also controlled by the transcriptional regulators Snail and Slug in non-epithelial gliomas.

5. Discussion

In this work we demonstrate that the EMT/GMT regulators Snail and Slug play a crucial role for the transition from a glial to mesenchymal phenotype in glioblastoma. Furthermore, Snail and Slug are involved in the induction or maintenance of cancer stem cells by regulating the self-renewal capacity of the cells, indicating a coupling between mesenchymal and stem cell traits in GBM. Consistently, tumour growth and the invasiveness of glioma cells depend on these EMT/GMT factors. These findings identify common key mechanisms controlling the transition between epithelial/glial and mesenchymal states in epithelial and glial tumours, and highlight the importance of Snail family EMT regulators as potential targets for glioblastoma therapy.

5.1 The molecular subclassification of GBM

The first indications that glioblastoma cells can possess mesenchymal characteristics were based on genome-wide molecular profiling studies that allowed a classification of GBM into distinct subtypes.

The first publication that proposed a classification of GBM in three different molecular subclasses used a microarray based expression analysis of high-grade astrocytoma sample sets (Phillips et al., 2006). It defined three distinct subgroups of tumours by identifying a robust set of signature genes, chromosomal aberrations and possible cells of origin: proneural, mesenchymal and proliferative.

The proneural (PN) subgroup included a mixture of WHO-grade III and IV gliomas with or without necrosis. The specific signature gene set for PN tumours included genes such as the Notch ligand delta.like ligand 3 (DLL3) and brevican (BCAN). Furthermore, markers like Olig2 (oligodendroglial marker 2), MAP2 (microtubule associated protein 2) and the neuronal marker NeuN, which are related to neuroblasts or developing neurons showed an overexpression in this group.

The mesenchymal (Mes) and proliferative (Prolif) subgroup consisted nearly exclusively of WHO grade IV tumours with necrosis. The microarray analysis showed that the Mes group of tumours is characterised by the overexpression of markers like

the chitinase-like protein YKL40, the cell surface glycoprotein CD44 or the transcription factor STAT3 (signal transducer and activator of transcription 3). In this subgroup genes important for angiogenesis, such as VEGF (vascular endothelial growthfactor) and its receptors, as well as the endothelial marker PCAM1, are also upregulated. Interestingly, the mesenchymal subgroup showed also a correlation to the expression of stemness markers like Nestin or CD133. The Prolif group of tumours was classified by the expression of proliferation related markers like proliferating cell nuclear antigen (PCNA) or TOP2A (topoisomerase 2A).

In 2010 a study of gene expression in the glioblastoma cohort of The Cancer Genome Atlas (TCGA) refined the classification of the GBM subtypes (Verhaak et al., 2010). According to this classification GBM is subdivided into 4 molecular groups: classical, mesenchymal, proneural and neural.

In their study the authors classified the classical subtype by genetic aberrations of chromosome 10 and 7, amplification of the EGFR (epidermal growth factor receptor) gene, lack of TP53 mutations and aberrations of components of the RB (retinoblastoma tumour suppressor) pathway (important for DNA replication and transcription). Expression data showed an overexpression of neural precursor and stem cell marker nestin and high expression of components of the notch and sonic hedgehog pathways.

The mesenchymal class was characterised by the deletion of the tumour suppressor NF1 (neurofibromin 1) gene and the strong expression of YKL40 and CD44. Thus the definition of the mesenchymal subtype overlaps with that of (Phillips et al., 2006) which was based on a combination of grade II and grade IV gliomas. Additionally, they show an upregulation of members of the NFκB pathway probably due to higher overall necrosis and associated inflammatory infiltrates in this tumour subtype.

In the proneural subtype they were able to show a high frequency of alteration leading to an overexpression of PDGF (platelet derived growth factor) receptor A (found in all subtypes but the highest percentage is in the proneural class), as well as IDH1 (isocitrate dehydrogenase 1) point mutations. Again in accordance with the previously discussed study (Phillips et al., 2006) they found an elevated expression of oligodendrocytic development genes like DLL3 and Olig2 and others (Verhaak et al., 2010).

The neural subtype is characterised by the high expression of neuronal markers like NEFL (neurofilament light polypeptide), GABRA (gamma-aminobutyric acid (GABA) receptor A), the calcium sensor SYT1 and the potassium/chloride transporter SLC12A5. Interestingly, the different subtypes of GBM show distinct variations in survival benefit of the patients upon different therapies. A common treatment of GBM is the combination of the alkylating agent temozolomide with radiation. Heavily treated patients with tumours of the proneural group showed no beneficial effects on survival, whereas patients with tumours belonging to the classical or mesenchymal subgroup showed delayed mortality.

A further study examined the variation of DNA methylation patterns among different GBM samples of the TCGA collection, revealing additional important features of the distinct tumour subtypes (Noushmehr et al., 2010). The authors showed that a large number of loci are hypermethylated only within the proneural subtype. This indicates the presence of a glioma CpG island methylator phenotype (G-CIMP) as previously described for colorectal cancer (Toyota et al., 1999). Interestingly, G-CIMP tumours showed altered expression of a panel of genes associated with patient outcome, markers of the mesenchyme, tumour invasion and extracellular matrix. In conclusion, the lack of this silencing methylation phenotype could lead to the development of more aggressive tumours, especially in the mesenchymal subtype, which lacks CpG island hypermethylation.

Subsequent work combining methylation, expression and mutational analyses of GBM samples uncovered further subgroups of GBM tumours, highlighting the heterogeneity of these tumours (Sturm et al., 2012). Sturm and co-workers performed a genome-wide methylation pattern analysis but combining adult and pediatric GBM samples. They were able to define six distinct methylation clusters. Based on correlation with mutational status, DNA copy number aberrations and gene expression signatures they classified six biological subgroups as followed: 1. IDH mutated (mostly correlating with the proneural subgroup), 2. Histone 3.3 (H3F3A) K27 mutated (mostly pediatric samples and correlated to proneural subtype), 3. Histone 3.3 (H3F3A) G34 mutated (pediatric GBM), 4. RTK I (typically involving PDGFRA amplification), 5. Mesenchymal, 6. RTK II (correlated with the classical subtype). Interestingly, their definition of the mesenchymal subgroup is not fully comparable to the other studies since they combined in this group all cases that did

not completely fit in one of the other five. The mesenchymal class here consists of samples that showed the highest similarity to normal brain methylation pattern, have a much lower incidence of GBM related copy number aberrations, fewer copy number changes and no characteristic point mutations. Nevertheless, this study could give a deeper insight into how epigenetic mechanisms especially mutation of K27 in Histone 3 could be important to further subclassify GBM tumours.

The first experimental study taking advantage of the classification of GBM subtypes showed that patient derived glioma spheres that resemble either PN or Mes phenotypes (tested by expression of markers and existence of G-CIMP cluster) differ in their biological characteristics (Bhat et al., 2013). After the isolation of the cells most of the samples derived from Mes tumours lost the typical Mes phenotype and shifted toward a PN phenotype following in vitro culturing or transplantation as xenografts. The cells showed a loss of YKL40 and a gain of Olig2 expression, as well as gain of G-CIMP. All this suggesting a lack of microenvironmental signals which are necessary for the maintenance of a mesenchymal phenotype in cell culture conditions and in mouse xenografts. As reported in the previous studies the mesenchymal subclass shows an upregulated activity of the NF-κB pathway, therefore the authors treated the isolated cells with cytokines known to activate the NF-κB pathway. They tested IL6, IL8, IL10, TGFβ and TNFα, showing that only TNFα had a striking effect on the expression of CD44, CD15 and YKL40. Transcriptomic analysis showed that the treatment with TNFα induced a shift from a proneural back to a mesenchymal signature. This analysis also revealed that transcription factors known to induce a mesenchymal signature such as STAT3, C/EBPβ and TAZ were significantly upregulated. Interestingly, transcription factors directly related to EMT, namely Snail1, Slug and TWIST1 showed no differential expression. Furthermore, overexpression of the Mes signature genes CD44 and CD15, as well as the NF-κB activation correlated with poor radiation response and shorter survival in patients.

Taken together these studies demonstrate the utility of GBM subclassification, which can have both prognostic value and therapeutic importance. The studies suggest that different subtypes of GBM may benefit from different types of therapy; therefore assays for the diagnosis of GBM subtype could represent a useful addition to current molecular diagnostic markers for GBM.

5.2 The distinctive features of EMT and GMT

So far there are few reports showing EMT in CNS cancers such as glioma and the terminology related to the study of this process in brain tumours remains a point of debate. Indeed, since the brain is lacking typical epithelium and mesenchyme the use of an alternative terminology is warranted. Therefore we propose the term glial-to-mesenchymal transition (GMT), or proneural-to-mesenchymal transition with regard to the marker expression in the different molecular subclasses of glioma.

Epithelial cell layers outside the CNS are characterized by close cell-cell contacts including tight junctions, adherens junctions and desmosomes. A major component mediating epithelial cell-cell attachment in these structures is E-cadherin. The epithelial cells show an apical and basolateral polarisation and a tight connection to the basal membrane. During EMT in normal development or carcinogenesis the cells change from well differentiated polarized epithelial cells to unpolarised migratory mesenchymal cells with changes in expression of marker genes like vimentin and N-cadherin. To manage these morphological changes a rearrangement of the cytoskeleton and the ECM has to occur as well.

Although glial cells in the brain have a neuroepithelial origin, they are not as strictly organised as epithelial cell layers. They also have cell-cell contacts mediated mainly by cadherins such as N-cadherin and CDH11 as well as NCAM (Sakisaka and Takai, 2005).

In our work we faced the problem that the classical markers often used to determine EMT, such as E-cadherin, N-cadherin or vimentin were either not expressed in glioma cells or did not show any response to EMT induction by major triggers like hypoxia (data not shown) or TGFβ treatment (see Fig. 4.4). Therefore we examined the reports of the molecular subclassification of GBM to find a panel of reliable markers to monitor GMT in our glioma cell lines. After testing many of the proposed signature genes we were able to validate a working set of GMT markers. To determine the mesenchymal state of the cells we used CD44 (also used as marker for stemness), YKL40 and CDH11. The utility of some of these markers was already reported before. YKL40 was shown to play a role in promotion of glioma growth, malignancy, radio-resistance and angiogenesis and is overexpressed in glioma patient with poor prognosis (Francescone et al., 2011). The literature on the calcium

dependent cell adhesion molecule CDH11 is somewhat more controversial. In 2012 and 2013 it was shown that CDH11 can act as a mesenchymal marker, due to its expression in stem-like glioma cells and glioma tissue samples. Furthermore, silencing of CDH11 led to decreased invasion and cell survival in vitro and in vivo (Kaur et al., 2012; Schulte et al., 2013). Nearly at the same time a study was published showing that CDH11 is downregulated at the invasive front in GBM patient samples and that the silencing of CDH11 leads to increased invasion (Delic et al., 2012). In our experiments YKL40 and CDH11 proved as reliable markers for the mesenchymal phenotype, whose expression was reduced upon the loss of Snail and Slug (see Fig.4.7).

As proneural markers we utilised MAP2, T-cadherin and Olig2. For MAP2 it was shown recently that in glioma cells the PKA (protein kinase A) pathway gets activated by upregulated MAP2 expression, which leads subsequently to a reduction of the invasive capacity of the cells (Zhou et al., 2015). T-cadherin was previously used to show in highly invasive VEGF knock-out mouse astrocytoma cells, stimulated with HGF, a transition comparable to EMT. These cells showed an increase in Snail expression and a subsequent decrease of T-cadherin expression upon HGF treatment (Lu et al., 2012). The role of Olig2 in glioma is more ambiguous. Some groups use it as a stem cell marker (Hjelmeland et al., 2011; Trepant et al., 2015) but the molecular classification approaches identified it clearly as a marker for the proneural subclass. In our study Olig2 behaved as a proneural marker that was consistently downregulated by signals that induce EMT/GMT, such as TGFβ (see Fig.4.3). Also the silencing of Snail and Slug restored the reduced Olig2 expression after TGFβ stimulation to an even higher extend than in the untreated control cells (see Fig. 4.5). These results and the molecular subclassification of GBM are clearly arguing for Olig2 as a proneural marker.

Taken together, our results identify and validate a reliable panel of markers to monitor the transition between a proneural state and a mesenchymal state of the cells during TGFβ-mediated GMT.

5.3 The importance of Snail and Slug in GMT in glioblastoma multiforme

As shown in our data Snail and Slug play a crucial role in regulating GMT and stemness in glioma. They do not influence the classical markers N-cadherin and vimentin known from epithelial cancers. However, cells with silenced Snail and Slug show impaired transition from a glial/proneural to a mesenchymal state, as evidenced by changes in the expression of several markers on protein and mRNA level. Interestingly, the relative contribution of Snail and Slug to the regulation of individual markers, such as YKL40 or CDH11, and cellular functions such as self-renewal and invasion appear to be different and in part cell line dependent (see. Fig 4.6; 4.7; 4.9). For example in the primary cell line GBM046x the self-renewal capacity and the invasiveness of the cells is primarily affected by silencing Snail (see Fig. 4.11; 4.12). On the whole, however, GMT, stemness and invasion are more consistently and more robustly suppressed by combined silencing of Snail and Slug than by the loss of either factor individually.

Interestingly, a couple of recent reports show a potential strong involvement of Snail and Slug in invasiveness and stemness of glioma cells but concentrated only on silencing or overexpressing one of the SNAI family members.
A genome-wide expression profiling of human glioma samples showed that tumours with increased in vitro proliferation and invasion had an upregulation of Slug. Slug overexpressing cells exhibited in vivo promoted angiogenesis and elevated tumour growth. Enhanced invasiveness could be abrogated by silencing Slug and subsequent animal studies showed an increased survival of mice bearing Slug silenced tumours (Yang et al., 2010). Two recent reports showed comparable results for Snail. By silencing Snail expression it was observed that the cells showed a reduced expression of vimentin and a subsequent upregulation of E-cadherin together with decreased proliferation, retarded cell cycle and impaired invasion/migration of the cells in vitro(Han et al., 2011; Myung et al., 2014). Furthermore, it was found that Snail supresses the microRNA miR128, a known tumour suppressor involved in regulating the expression of SP1, by binding to the miR128 promoter region. SP1, in turn, regulates the cell cycle, tumour formation and growth, as well as migration of tumour cells (Dong et al., 2014). Another study reported that irradiation leads to elevated levels of Snail in glioma cells, which promotes GMT. Murine tumour specimens taken after irradiation cycles

showed higher migratory and invasive capacity, as well as upregulated Snail expression. Again these effects were reverted by silencing of Snail. Interestingly the irradiated cells showed in addition an elevated expression of the stemness marker SOX2 and a tumour initiating potential (Mahabir et al., 2014).

With our study we are able to confirm for the first time that Snail and Slug together are important to induce a complete transition from a glial/proneural to a more mesenchymal phenotype with concomitant increase in cell invasiveness and stem cell capacity. Furthermore, we also examined in detail the effects of the loss of Snail and Slug on tumour growth in orthotopic intracranial xenografts. We showed that combined silencing of Snail/Slug reduced tumour volume and invasion but did not affect proliferation, apoptosis or vascularisation.

A study in 2013 found that stimulation of glioblastoma cells with BMP7 (bone morphogenetic protein 7), a member of the TGFβ superfamily, induces Snail in a SMAD1/5-dependent manner. They could show that glioma cells overexpressing Snail exhibit elevated invasive behaviour in a xenograft model. Surprisingly, however, overexpression of Snail led to decreased tumour sphere formation in vitro and reduced tumorigenicity, an effect that the authors attributed to the known capacity of BMPs induce differentiation of stem-like cells (Savary et al., 2013). It is conceivable that BMP7-driven Snail expression activates different signalling mechanisms, which leads to a dissociation of the invasive capacity of GBM from the stemness and the tumorigenic potential of the cells. At the same time, it has to be noted that these findings were based on Snail overexpression experiments, which may cause secondary effects in the cells, due to impaired homeostasis of protein synthesis and folding and the activation of pathways that are not induced by normal amounts or through natural triggers of the respective protein. Therefore, we avoided the use of overexpression approaches and instead focused our analysis on studying the effects of loss-of-function of the endogenous protein.

5.4 EMT and the cancer stem cell phenotype

Accumulating evidence over the last years demonstrates a link between the transition from an epithelial to a mesenchymal state and the acquisition of stem cell traits in

cancer cells. Especially the outgrowth of metastases is closely connected to EMT through the generation of more motile cancer cells that invade and disseminate to distant sides. A prerequisite to initiate the growth of cancer cells outside and far away from the primary tumour is the gain of cancer stem cell traits or tumour initiating abilities in particular the ability to self-renew, to generate progeny and to act as founder cells for the formation of micro-and macro-metastasis.

Previously it was discovered that the induction of a mesenchymal state is associated with the induction of a stem cell state in both normal epithelial cells and in carcinomas (Mani et al., 2008). That leads to the assumption that cancer cells take advantage of the conserved EMT cellular program to achieve dissemination and acquire phenotypes that are beneficial for tumour progression. In breast cancer, it was shown that tumours harbour cell populations with stem-cell characteristics. It is possible to distinguish this population from the rest of the tumour cells through the expression of the surface proteins CD44 and CD24. The stem cell population is characterised by the expression pattern $CD44^{high}/CD24^{low}$. Importantly, this subpopulation expresses markers associated with EMT, like reduced E-cadherin expression, higher expression of N-cadherin, vimentin and fibronectin. In addition, the EMT regulators Snail, Twist and FOXC2 (forkhead box protein 2) are induced in this particular cell population (Mani et al., 2008).

A strong connection between EMT and CSCs is suggested by the discovery that the same transcriptional regulators are involved in the control of both features. Zeb1 negatively regulates the expression of the members of the miR-200 family, which function to suppress stemness (Burk et al., 2008; Korpal et al., 2008; Park et al., 2008). Furthermore, miR-200 family members have been shown to suppress the expression of the Bmi-1, component of the polycomb complex 2, which is known to be important to support the stemness in cancer and embryonic stem cells (Shimono et al., 2009; Wellner et al., 2009).

Pathways that are known to participate in self-renewal or stem cell maintenance were also reported to directly influence EMT regulators. For example the Wnt-β-catenin pathway is strongly activated at the invasive front of colorectal cancer where the cells undergo EMT (Brabletz et al., 1998). These and many other studies suggested that Wnt signalling is involved both in the induction of EMT and in the generation of CSCs (Schmalhofer et al., 2009). Additionally, this pathway is important for regulating the

turnover and activity of Snail in breast cancer (Yook et al., 2005) and normal hepatocellular regeneration (Sekiya and Suzuki, 2011). Especially TGFβ, as a major EMT inducer (Kalluri and Weinberg, 2009; Massague, 2008), activates Snail, Slug and Twist in many epithelial cancers and induced the stem cell population $CD44^{high}/CD24^{low}$ in immortalised mammary epithelial cells (Thuault et al., 2006).

5.4.1 The role of Snail and Slug in the maintenance of cancer stem cells in GBM

In non-epithelial cancers like GBM little is known about the role of EMT or GMT in the induction and maintenance of CSCs. In the last few years some evidence arose that a comparable connection, involving similar components and pathways also exists in glioma. Especially TGFβ signalling seems to play a major role in GBM both for the induction of EMT and the maintenance of stem-cell properties (Anido et al., 2010; Ikushima et al., 2009; Penuelas et al., 2009). Recently it was shown that the EMT regulator Zeb1 controls key features of CSCs in glioma and can be used as a marker for invasive cells that is also linked to chemoresistance (Siebzehnrubl et al., 2013). Furthermore, the EMT marker TWIST1 is involved in the promotion of invasiveness and stemness of glioma cells (Mikheeva et al., 2010). There are also a few reports showing that Snail and Slug can induce cellular changes comparable to EMT and that the loss of theses transcription factors reduces invasion and vimentin expression (Han et al., 2011; Myung et al., 2014; Yang et al., 2010). However, a direct connection of GMT regulators of the Snail family to the CSC phenotype has been missing so far.

In our study we were able to show and confirm a direct link of the transcription factors Snail and Slug to GMT and stem-cell features in GBM. The loss of Snail or Snail and Slug impairs not only the transition from a glial to a mesenchymal cell state induced by TGFβ signalling but also the ability of cells to self-renew as functionally shown with a glioma sphere formation assay in two GBM cell lines (see Fig. 4.9). Also, the expression of the established glioma stem cell markers SOX2, OCT4, MAML3 and CD15 is impaired by silencing Snail and Slug (see Fig. 4.8). These results are clearly arguing for a connection of GMT and the induction of a CSC phenotype in glioma.

Surprisingly, we were not able to detect a reduction of the commonly used glioma stem cell marker CD133 upon silencing Snail and Slug; indeed silencing of the two transcription factors led to an induction of CD133 (data not shown). These findings, however, are supported by a very recent report, which analysed co-expression of glioma stem cell markers in publicly available GBM databases. This study found that CD133 is negatively correlated with CD44 and in turn CD44 is positively correlated with the stem cell marker CD15. Moreover, the expression of CD133 overlapped surprisingly with the proneural signature of the samples, whereas CD44 and CD15 clearly overlapped with the mesenchymal phenotype (Brown et al., 2015). This could mean that CD133 is not a suitable marker for stem cell traits induced via GMT and could explain our observations.

5.5 Invasion in GBM

GBM is the most aggressive tumour type of the CNS and most brain tumours are glioblastomas. With a median survival of fifteen month, patients have a very poor prognosis. Despite the development of improved imaging methods, specific surgical techniques and new chemo-and radiotherapies the survival prognosis for patients did not significantly change in the last decades. One of the mayor reasons is the high infiltration of GBM cells throughout the brain, often even to the opposite hemisphere. Upon surgical removal of the primary tumour it is nearly impossible to remove all tumour tissue. Many patients suffer from a relapse with secondary tumours formed by residing invasive cancer cells. Interestingly, therapeutic approaches, such as anti-angiogenic treatment to withdraw oxygen and nutrients from the tumour result in an initial shrinkage of the tumour but enhances the invasiveness of the cells.

It is not fully understood which mechanisms are responsible for the high invasive capacity of GBM. One explanation could be EMT/GMT. The gain of mesenchymal features is in many cancer types closely connected with a higher invasiveness of the cells and a further progression of the disease. Snail and Slug as the major regulators of EMT were shown to have a strong influence on invasion in epithelial cancers. Therefore, studying GMT and invasion in glioma is very important for understanding the mechanisms for the enhanced invasiveness of the cells, which may lead to an improved treatment for patients.

5.5.1 GMT and invasion

In glioma many recent reports showed a connection between EMT/GMT regulators and the invasive capacity of the glioma cells in vitro. In this study we also examined the influence of Snail and Slug on the invasiveness of glioma cells in vitro and in vivo. Interestingly, we found that the precise extent to which GBM cell invasion depended on specific members of the Snail family was cell line dependent. In the modified Boyden chamber assay the primary cell line GBM046x showed that silencing of Snail is sufficient to abrogate the ability of the cells to invade through the matrigel layer. Surprisingly, silencing of Slug alone led to a significant increase of invasion, suggesting a differential role of these two transcription factors in regulating invasive behaviour in this cell line. When both regulators were lost the invasive capacity of the cells was again significantly reduced (see Fig. 4.11). The same results were obtained for GBM046x with a second invasion assay that mimics the three dimensional tumour architecture and allows gliomaspheres to invade a collagen layer in all directions (see Fig.4.12).

In the established cell line G55 the single knock-down of Snail or Slug had no significant effect on the invasion of the cells, either in the matrigel invasion assay or in the collagen invasion assay. Only the loss of both regulators led to a significant decrease of invasiveness in both assays (see Fig. 4.11; 4.12). These findings show that Snail alone can already influence the invasive behaviour in a cell line dependent manner, but taking into account that only the double knockdown of Snail and Slug shows a complete transition from proneural to mesenchymal state in terms of signature gene expression our data support a model in which both regulators can play a crucial role in GMT induced invasion. Therefore we performed in vivo studies with glioma cells lacking Snail and Slug and examined the invasiveness of those cells directly in the brain. We could observe that the loss of Snail and Slug led to severely decreased parenchymal invasion compared to the control cells. It should also be pointed out that some of our markers to determine the state of the cells (proneural or mesenchymal) are also functionally involved in invasion. The cadherin CDH11, as described in section 5.2, is strongly involved in glioma invasion and its loss results in decreased invasion. CD44 is not only a mesenchymal marker but also an adhesion molecule of the cells to the ECM. In this particular case, the amount of CD44 protein may be more important for determining the mesenchymal state of the cells than for

showing a direct connection to the invasive behaviour of the cells because to enhance the invasion of cells CD44 has to be cleaved by ADAM proteases (Nagano et al., 2004; Okamoto et al., 1999). To further study if also the cleavage of CD44 is impaired in Snail and Slug silenced cells one could examine the activity of ADAM 10 and 11a.

In general, additional potential avenues for the further elucidation of the connection between GMT and invasion could involve analysis of the expression levels of genes and proteins closely connected to invasion mechanisms of glioma. For example one could characterise the expression of MMPs or integrinβ1, in particular in tumour samples from our in vivo studies.

5.6 Snail and Slug in tumour growth

A major part in the study presented here is the assessment of the role of Snail and Slug in glioma tumour growth. So far this topic is underrepresented in the published reports. Many of the reports mentioned in section 3.3.3 or 5.4.1 showed no in vivo data to confirm their findings about the role of Snail and Slug (Han et al., 2011) (Myung et al., 2014) (Dong et al., 2014). The rest of the reports often used only subcutaneous injection into mice and no orthotopic intracranial injections into the brain. The biggest limitation here is that important components of the specific microenvironment of the brain are missing so that the subcutaneous tumour model cannot fully mirror the natural situation of brain tumour growth. If intracranial injections were used, the authors only analysed the survival of the mice and did not analyse tumour volume or other features influencing tumour growth, such as invasion, proliferation, apoptosis or vascularisation (Yang et al., 2010) (Savary et al., 2013). Nevertheless, these key features of tumour growth and progression need to be assessed to fully understand the role of Snail and Slug in glioma growth. Therefore, we performed intracranial orthotopic injections into the brains of mice to have a microenvironment comparable with situation in GBM. In these in vivo experiments we assessed the proliferation, apoptosis and the vascularisation of the tumours by immunofluorescence staining. By analysing the volume of the tumours we saw a striking effect of silencing of Snail and Slug. The loss of both transcription factors led to significantly reduced tumour growth (see Fig. 4.13). Surprisingly, we

could not observe any differences in proliferation, apoptosis and vascularisation of the Snail/Slug silenced and control tumours (see Fig. 4.14-16), indicating that Snail and Slug have no major influence on these key features of tumour growth. These results were also confirmed by analysing the proliferation and apoptosis of glioma cells in vitro (see Fig. 4.10). By contrast, analysis of the invasiveness of the tumours obtained from the in vivo experiments showed that the invasive capacity of the glioma cells is severely impaired when Snail and Slug are silenced (see Fig.4.17). Interestingly, the abrogated invasiveness of Snail/Slug silenced tumours seems to be the main reason of the reduced tumour growth. We were also able to confirm these data with two independent in vitro invasion assays (see Fig. 4.11; 4.12). Thus, our work shows for the first time the connection between Snail and Slug and in vivo invasiveness of glioma cells.

5.7 Perspectives

5.7.1 Transcriptomic analysis

To further confirm the specific role of Snail and Slug in GBM and in particular in the molecular subtype transition that possibly occurs also during the progression of the disease in patients, a transcriptome analysis could be a helpful approach. We are currently generating Snail and Slug loss-of-function glioma cells with the CRISPR/Cas9 technique. In collaboration with the German Cancer Research Center (DKFZ) in Heidelberg, we will analyse the changes in the transcriptome following the loss of Snail and Slug, which could further support the role of Snail/Slug in GMT by demonstrating a shift of the expression signature to a proneural one. This analysis may also allow us to gain a deeper insight into the Snail/Slug-dependent mechanisms of GMT, invasion and stemness in glioma. Furthermore, it could also complement the panel of markers we are currently using to determine GMT and the CSC phenotype. Such an approach can also provide important information about pathways and mechanism that could be used as potential therapeutic targets to act directly on Snail and Slug expression or on the downstream pathways controlled by them to prevent GMT and the gain of a more aggressive phenotype in glioma cells.

5.7.2 Snail and Slug as therapeutic targets

In general, transcription factors are challenging drug targets. Nevertheless, there are first attempts to target EMT factors with some initial success. Few chemical compounds act directly on Snail, a more promising approach seems to be the targeting of pathways regulating Snail expression (e.g. through HDAC (histone-deacetylase) or LSD (lysine-specific-demethylase) inhibitors) or the interaction of Snail with E-cadherin or p53 (Fig.5.1) (Kaufhold and Bonavida, 2014).

Name	Inhibits	Effect	Known limitations
GN25, GN29	Snail/p53 interaction	Reduced proliferation, tumor progression; increased tumor regression	Only effective in K-Ras activated cancer cells and on wild-type p53
Co(III)-Ebox	Snail/E-cadherin interaction	Increased E-cadherin expression	
Tranylcypromine	LSD1/LSD2	Decreased Snail's effects on EMT markers	
Trichostatin A	HDAC1/HDAC2	Reversed EMT marker expression	
Pargyline	LSD1	Abrogated Snail-induced EMT	
LBH589	HDAC	Abrogated Snail-induced EMT	
Entinostat	HDAC	Increased E-cadherin and cytokeratin 18 expression, Decreased Twist, Snail, vimentin, N-cadherin; encouraged epithelial morphology; decreased cell migration	

Fig. 5.1 Chemical inhibitors of Snail-induced EMT (taken from Kaufhold et al., 2014)

Other EMT regulators are also affected by inhibition of HDACs. The class I HDAC inhibitor mocetinosat acts on the chemotherapy resistance of colorectal tumours expressing high levels of ZEB1. Mocetinosat acts on the ZEB1 target gene miR203 (a major drug sensitizer repressed by ZEB1) as an epigenetic drug to restore miR203 expression, repress stemness and re-induce sensitivity against standard chemotherapy (Meidhof et al., 2015). Epigenetic reactivation of miR expression is technically easier to realize than a targeted delivery of miRNAs directly to a tumour. Comparable strategies could be helpful also for the treatment of GBM. In glioma it was recently shown that in multi-drug resistant cells, which had undergone GMT, ectopic expression of miR203 reversed the resistance phenotype by the downregulation of Slug. Unfortunately, the effects on Snail following overexpression of miR203 were not assessed (Liao et al., 2015). Collectively, this work combined with a transcriptome analysis, as described above, for getting a better understanding

of the mechanisms and pathways regulated by Snail and Slug, has an important potential for new approaches for the design of therapeutic strategies against Snail/Slug-induced GMT, invasion and stemness.

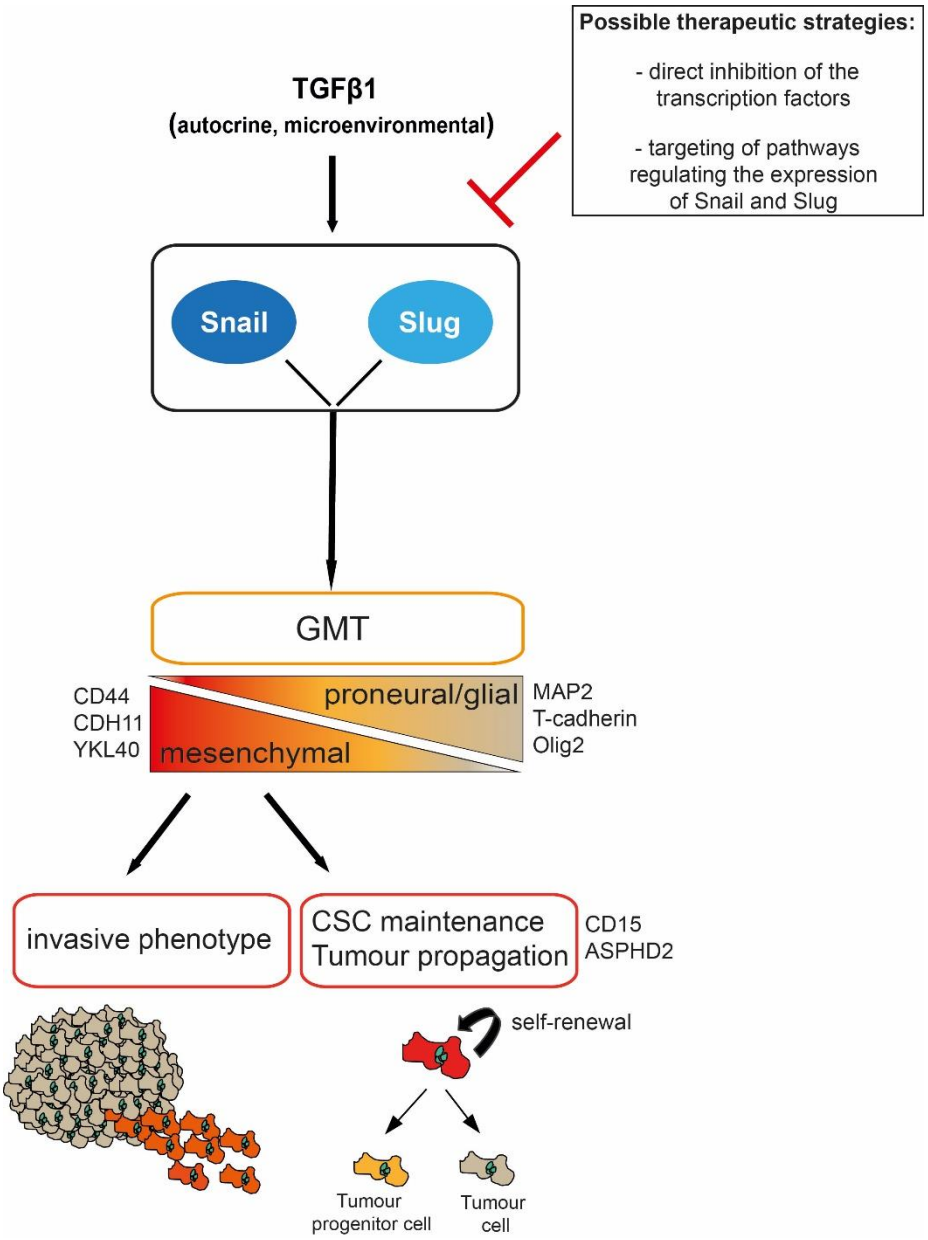

Fig. 5.2 Graphical summary TGFβ1 induced GMT via Snail and Slug leads to an invasive phenotype, CSC maintenance and tumour propagation.

6. Materials and Methods

6.1 Materials

6.1.1 Antibiotics

Name	Stock concentration	Final concentration
Ampicillin (#A-9518, Sigma)	100 mg/ml in aqua dest.	100 µg/ml
Kanamycin (#T832.1, Roth)	100 mg/ml in aqua dest.	100 µg/ml

Table 6.1 Antibiotics for selection of bacterial cells

Name	Stock concentration	Concentration for maintenance of transgene expression
Blasticidin (#R210-01, Invitrogen)	6 mg/ml in PBS	6 µg/ml
Puromycin (#P9620, Sigma-Aldrich)	10 mg/ml ready to use solution	G55: 4 µg/ml GBM46x: 0.4 µg/ml

Table 6.2 Antibiotics for selection of mammalian cells

6.1.2 Antibodies

6.1.2.1. Primary antibodies

Antigen	Species	Dilution	Company
Snail	Rat (monoclonal)	1:500 for WB	#4719, Cell Signaling
Slug	Rabbit (monoclonal)	1:500 for WB	#9585S, Cell Signaling

CD133	Mouse (monoclonal)	1:500 for WB	#130-092-395, Miltenyi
CD44	Mouse (monoclonal)	1:5000 for WB	#3570S, Cell Signaling
YKL40	Goat (polyclonal)	1:200 for WB	#AF2599, R+D Systems
Olig2	Rabbit (polyclonal)	1:1000 for WB	#18953, IBL
T-cadherin	Mouse (monoclonal)	1:1000 for WB	#SC166875, Santa Cruz
MAP2	Mouse (monoclonal)	1:1000 for WB	#M9942, Sigma
ASPHD2	Rabbit (polyclonal)	1:500 for WB	#HPA000820 ,Sigma
Tubulin	Mouse (monoclonal)	1:8000 for WB	#DLN09992, Dianova

Table 6.3 Primary antibodies for western blots

Antigen	**Species**	**Dilution**	**Company**
Endomucin	Rat (monoclonal)	1:500	#14-5851, eBioscience
Phospho-histone 3	rabbit	1:200	#IHC-00061, Bethyl lab
BrdU	Mouse (monoclonal)	1:200	#M0744, Dako Cytomation
Human nuclei	Mouse monoclonal	1:500	#MAB4383, Millipore

Table 6.4 Primary antibodies for stainings

6.1.2.2. Secondary antibodies

Antigen	Dilution	Company
Peroxidase-conjugated AffiniPure goat anti rabbit IgG	1:2500 for Western Blot	#111-035-144, Dianova
Peroxidase-conjugated AffiniPure donkey anti goat IgG	1:2500 for Western Blot	#705-035-147, Dianova
Peroxidase-conjugated AffiniPure goat anti mouse IgG	1:2500 for Western Blot	#115-035-146, Dianova
Peroxidase conjugated f(ab')$_2$ fragment goat anti rat IgG	1:2500 for Western Blot	#721-1333, Rockland
Alexa Fluor®568 goat anti rat IgG	1:200 for Immunofluorescence staining	#A11077, Life Technologies
Alexa Fluor®568 goat anti rabbit IgG	1:200 for Immunofluorescence staining	#A11036, Life Technologies
Alexa Fluor®568 goat anti mouse IgG	1:200 for Immunofluorescence staining	#A11031, Life Technologies

Table 6.5 Secondary antibodies

6.1.3 Human cell lines

LN-229x: human glioblastoma cell line

G55: established human glioblastoma cell line

GBM10: primary glioblastoma cell line, isolated from human tumour material

GBM18: primary glioblastoma cell line, isolated from human tumour material

GBM37x: primary glioblastoma cell line, isolated from human tumour material

GBM46x: primary glioblastoma cell line, isolated from human tumour material

HEK293T: human embryonic kidney cell line: This cell line is transformed with sheared human adenovirus type 5 DNA. The E1A adenovirus gene is expressed in these cells and participates in the transactivation of some viral promoters allowing the cells to produce large amounts of viral particles when transfected with suitable plasmids. This cell line was purchased from Invitrogen.

6.1.4. Knock-down cell pools generated in this work

Name	Construct/Lentivirus	MOI	Selection
G55 nsc	non silencing control (Thermo Scientific)	80	Puromycin
G55 shSlug	pGIPZ-shSlug #2 (Thermo Scientific)	80	Puromycin
G55 shSnail	pGIPZ-shSnail #19 (Thermo Scientific)	80	Puromycin
G55 shSnail/shSlug	pGIPZ-shSnail #19/ pGIPZ-shSlug #2 (Thermo Scientific)	Each 40	Puromycin
GBM46x nsc	non silencing control (Thermo Scientific)	10	Puromycin
GBM46x shSlug	pGIPZ-shSlug #2 (Thermo Scientific)	10	Puromycin
GBM46x shSnail	pGIPZ-shSnail #19 (Thermo Scientific)	10	Puromycin
GBM46x shSnail/shSlug	pGIPZ-shSnail #19/ pGIPZ-shSlug #2 (Thermo Scientific)	Each 5	Puromycin

Table 6.6 Generated knock-down cell pools

6.1.5. Plasmids

pCL-VSV-G lentiviral packaging plasmid, expresses the envelope protein glycoprotein-G (#1733 Addgene, Garry Nolan)

pS-PAX2 lentiviral packaging plasmid (#12260 Addgene, Didier Trono)

pGIPZ non silencing control (Delic et al.) lentiviral expression vector (non targeting)

Hairpin sequence nsc (non silencing control):

TGCTGTTGACAGTGAGCGATCTCGCTTGGGCGAGAGTAAGTAGTGAAGCCACA GATGTACTTACTCTCGCCCAAGCGAGAGTGCCTACTGCCTCGGA 22mer sense: ATCTCGCTTGGGCGAGAGTAAG22merantisense: TACTCTCGCCCAAGCGAGAG

pGIPZshSnail mir (human) lentiviral expression vector to silence SNAI1

Hairpin sequence shRNA Snail (V2LS_199873)

TGCTGTTGACAGTGAGCGCAAAGGTACACTGGTATTTATATAGTGAAGCCACAG ATGTATATAAATACCAGTGTACCTTTATGCCTACTGCCTCGGA

pGIPZ shSlug mir (human) lentiviral expression vector to silence SNAI2

Hairpin sequence ShRNA Slug (V2LHS_153126)

TGCTGTTGACAGTGAGCGACGAAGCCAAATGACAAATAAATAGTGAAGCCACAG ATGTATTTATTTGTCATTTGGCTTCGGTGCCTACTGCCTCGGA

Hairpin sequence color code: miR-30 derived sequence, mature sense, loop, mature antisense, miR-30 derived sequence (as given from the manufacturer)

6.1.6 Sequences (Primers)

CDH11

forward:TGGGCGGACTCTCAGGGACA

reverse: TTCCTCCCCAGGGACGGCTG

T-cadherin

forward: AGCGATGGCGGCTTAGTTG

reverse:CCCCGACAATCACGAGTTCTG

CD44

forward: TGGCACCCGCTATGTCCAG

reverse: GTAGCAGGGATTCTGTCTG

MAML3

forward: CAGCAGGTCAATCAGTTTCAAG

reverse: GGTTCTGGGAGGGTCCTATTC

OCT4

forward: GCTCGAGAAGGATGTGGTCC

reverse: CGTTGTGCATAGTCGCTGCT

SOX2

forward: GCCGGCGGCAACCAGAAAAACAG

reverse: CCGCCGGGGCCGGTATTTAT

HPRT1 (housekeeping gene)

forward: TATGGCGACCCGCAGCCC

reverse: GCAAGACGTTCAGTCCTGTCCAT

6.1.7 Growth factors

Reagent	Stock concentration	Final concentration
EGF (epidermal growth factor) (#C-10015-SS Peprotech)	200 µg/ml	20 ng/ml
bFGF (fibroblast growth factor) (#C-10018-BF Peprotech)	200 µg/ml	20 ng/ml
TGFβ1 (transforming growth factor β1) (-21C Peprotech)	10 mg/ml	2.5 ng/ml

Table 6.7 Growth factors

6.1.8 Protein/DNA ladders

6.1.8.1 Protein ladders

For proteins with low molecular weights PageRuler Prestained Protein ladder (#26616, Thermo Scientific) was used.

For proteins with high molecular weights Spectra Multicolor High Range Protein ladder (#26625, Thermo Scientific) was used.

6.1.9 Media, Buffers and other reagents

6.1.9.1 Animal experiments

Anaesthesia: 9 ml 0.9 % NaCl solution, 2 ml ketamine 10% (#FS1670041 bela-pharm GmbH), 0.5 ml xylazine 2 % (CEVA Tiergesundheit GmbH)

4% Paraformaldehyde: 80 g PFA were solved in aqua dest.

0.5M PB pH7.4: 115 mM NaH_2PO_4 x H_2O, 385 mM Na_2PO_4 x H_2O., pH was adjusted to 7.4

Cryoprotection solution (CPS): 500 ml 0.1 M PB (pH 7.4), 250 ml Ethylene glycol (#9516.1, Roth) and 250 ml Glycerol (#3783.1, Roth), solution was stored at RT

30% sucrose in 0.1M PB pH7.4: 0.1 M D (+)-Sucrose (#84099, Fluka), solution was sterile filtered and stored at 4 °C

6.1.10 Bacterial cultures

LB-Agar: 32 g of ready to use powder were dissolved in 1l aqua dest., the solution was autoclaved at 121 °C for 15 min, cooled down to 40-50 °C and the appropriate antibiotics were added. Afterward the LB-Agar was poured into 10 cm dishes. The plates were stored at 4 °C.

LB-Medium: 20 g of LB powder were dissolved in 1 l aqua dest., and autoclaved at 121 °C for 15 min. The medium was stored at 4 °C.

6.1.11 Cell culture

Accutase: #A11105-01 Gibco

2.5M $CaCl_2$: dissolved in aqua dest., sterile filtered and stored at 4°C

10mM Chloroquine: dissolved in aqua dest., sterile filtered an stored at 4°C

CO_2-independent Medium without L-Glutamine: #18045-054, Gibco

Cryo-Medium SFM: #C-29910, Promocell

Dimethyl sulfoxide (DMSO): #A994.1, Roth

D-MEM/F12 (1:1) (with GlutaMAX): #31331-028, Gibco

D-MEM (Dulbecco´s Modified Eagle Medium High Glucose (with GlutaMAX, 4.5 g/l D-Glucose, Sodium Pyruvate): #31966-021, Gibco

FCS (Foetal Calf Serum): # 10270-106, Gibco

General cell culture medium for adherent cells: 500 ml DMEM, 10 %FCS

2xHBS: 281 mM $NaCl_2$, 100 mM HEPES, 1.5 mM Na_2HPO_4 in aqua dest., pH 7.12, sterile filtered and stored at -20°C

HEPES: #1563-056 Gibco

Tumoursphere medium: 500 ml DMEM/F12, 10ml B27 serum-free supplement (#12587-010, Gibco), 5 ml amphotericin B (#A2942, Sigma), 2.5 ml 1M HEPES, 0.5 ml gentamicin (50 mg/ml) (P11-005, PAA Laboratories GmbH)

1xPBS: #10010-056, Gibco

Polybrene: 6 mg/ml in aqua dest., sterile filtered and stored at -20 °C

Poly (2-hydroxyethyl methacrylate) (pHEMA): 10 mg/ml pHEMA (#P3932-25g, Sigma-Aldrich) was dissolved in 95 % ethanol, sterile filtered and stored at RT

Trypsin/EDTA: #L11-004, PAA Laboratories GmbH

Collagen solution (10 ml): 5.1 ml bovine collagen (Biomatrix), 3.5 ml TSM, 1.36 ml HEPES

FACS Staining buffer: 1x PBS, 0.5 % BSA, 2 mM EDTA, pH 7.2

Papain stock solution: 100 mg papain (LS004194; Worthington) in 5 ml EBSS (14155.048, Invitrogen)

DNase I solution: 100 mg DNase I in 5 ml sterile 0.15 M NaCl, stored in 50 µl aliquots at -20 °C (#DN25-100mg, Sigma)

Solution 1 for primary cell isolation: 50 ml HBSS (#14180-046, Invitrogen) , 9 ml D-Glucose (300 mg/ml), 7.5 ml 1 M HEPES; adjust pH to 7.5, fill up with H_2O to 500 ml; activate before use 30 min at 37 °C, add freshly 200 µl papain and 50 µl of DNase I solution

Solution 2 for primary cell isolation: 100 ml solution 1, 70 mg collagenase I (LS004194, Worthington), 70 mg hyaluronidase (#H3884-100mg, Sigma), 100 mg trypsin (#T9935-100mg, Sigma), stored at -20 °C in 5 ml aliquots, add freshly 50 µl DNase I solution

6.1.12 Western Blot

Ammonium persulfate (APS): 1 g of powdered APS solved in 100 ml aqua dest. and stored in 1 ml aliquots at -20 °C (9592.1, Roth)

Lower-buffer: 0.5 M Tris base, set pH to 8.8, add 0.4 % SDS, fill up with H_2O

Lysis buffer (Laemmli): 10 mM Tris HCl, 2 % SDS, 2 mM EGTA, 20 mM NaF, filled up with aqua dest.

Blocking buffer: 5 % milk powder in 1x PBS-Tween-20 (0.1 %)

20x PBS: 140 mM NaCl, 2.7 mM KCl, 10 mM $Na_2HPO_4x2\ H_2O$, 1.8 mM KH_2PO_4, filled up with aqua dest., set pH to 7.4

10x Running buffer: 250mM Tris base, 2M glycine, 1% SDS, filled up with aqua dest.

Sample buffer: 40 ml 10 % SDS, 16 ml 1 M Tris pH 6.8, 20 ml glycerol, 19 ml aqua dest., stored in 800 µl aliquots, for usage mixed with 200 µl 1% bromphenol blue and 50 µl β-mercaptoethanol

8% separating gel: 2.7 ml 30 % poly-Acrylamide, 2.6 ml lower buffer, 4.5 ml aqua dest., 100 µl APS (10%), 10 µl TEMED

12% separating gel: 4 ml 30 % poly-Acrylamide, 2.6 ml lower buffer, 3.5 ml aqua dest., 100 µl APS (10 %), 10 µl TEMED

Stacking gel: 0.65 ml 30 % poly-Acrylamide, 1.3 ml upper buffer, 4.5 ml aqua dest., 100 µl APS (10 %), 10 µl TEMED

TEMED: Tetramethylenediamine #A1148, Applichem

10x Wet Transfer buffer without SDS: 200 mM Tris base, 1.5 M glycine, filled up with aqua dest.

Upper buffer: 0.5M Tris base, 0.4 % SDS, filled up with aqua dest.

Stripping buffer: 200 mM glycine, 0.05 % Tween-20, filled up with aqua dest.

Washing buffer (PBS-T): 1x PBS, 0.1 % Tween-20, filled up with aqua dest.

6.2 Solvents/Chemicals

Solvents and chemicals were, if not mentioned differently, purchased from Sigma-Aldrich, Roth, Merck and Applichem

6.3 Methods

6.3.1 Working with RNA

6.3.1.1 RNA extraction

Cells were plated in 10 cm dishes (800.000-1.000.000 cells, depending on the duration of the experiment). Cells grown as spheres were centrifuged and washed with PBS afterwards the cells were lysed with 350 µl RLT buffer (RNeasy Mini Kit, #74106, Qiagen; 1 ml RLT buffer+10 ml beta-mercaptoethanol). Cells grown adherent were washed with PBS and lysed with 350 µl RLT buffer and scraped off the dish with a cell lifter RNA extraction was performed following the manufacturer's instructions of the Qiagen RNeasy Mini Kit. The optional on-column DNase digestion was performed using the RNAse-Free DNase Set (#79254, Qiagen) in order to remove residual DNA. The concentration of the RNA was determined by NanoDrop (Peqlab) photometric measurement at a wavelength of 260 nm.

6.3.1.2 Reverse transcription

1 µg of RNA filled up with DEPC-water to 11 µl together with 1 µl random hexamer were incubated for 5 min at 70 °C and cooled down immediately on ice. This procedure unfolds the secondary structures of the RNA. 7 µl of a mix containing 4 µl 5x reverse transcriptase reaction buffer (#EP0451,Thermo), 2 µl dNTP-Mix (10 mM) (#NO447L, NEB) and 1 µl RNase-Inhibitor (#03335402001, Roche) were added and the whole mixture was centrifuged briefly followed by an incubation of 5 min at RT. 1 µl of Revert Aid H Minus M-MuLV Reverse transcriptase (#EP0451, Thermo) was added the whole reaction centrifuged briefly and incubated for 10 min at RT followed by 60 min incubation at 42 °C. The enzymatic reaction was inactivated for 10 min at 70°C. The mixture was cooled down on ice and 1 µl RNase H (#10786357001, Roche) was added. Again the reaction was centrifuged and incubated for 20 min at 37 °C. The cDNA was diluted with 180 µl DEPC-water.

6.3.2 Working with DNA

6.3.2.1 Plasmid isolation

The isolation of larger amounts of plasmid was carried out according to the protocol of the Isolation Kit PureLink HiPure Plasmid Maxiprep Kit (#K2100-07, Invitrogen)

6.3.2.2 Measuring DNA/RNA concentrations

Concentration of DNA or RNA was measured with NanoDrop (Peqlab) at a wavelength of 260 nm.

6.3.2.3 Sequencing

All sequencing reactions were performed by SeqLab.

6.3.2.4 Quantitative real time polymerase chain reaction (qRT-PCR)

Quantitative real time PCR allows amplification and simultaneously quantification of the amount of DNA/cDNA molecules of interest in the sample either as absolute number of copies or as relative amount to a normalizing gene. Quantification is based on the detection of fluorescent signals, which are produced during PCR cycles. In this work the SYBR Green method was used. The fluorescent dye SYBR green intercalates with double- stranded DNA and emits light when excited. The PCR reactions were performed with the Absolute QPCR SYBR Green ROX Mix (ABgene # AB-1162/a) on a StepOne Plus system (ABgene, Thermo-Scientific).

Reactions were performed in triplicates with 20 ng of cDNA, 100 nM forward (fw) primer, 100 nM reverse (rev) primer, 12,5 µl 2X ABsolute™ QPCR SYBR Green Mix and DEPC-water. in a total volume of 25 µl. The amount of target mRNA was determined using the comparative cycle threshold method and normalized relatively to the amount of the housekeeping HPRT mRNA.

Step	Temperature	Time	Number of cycles
Enzyme activation	95°C	15 min	1
Denaturation	95°C	30 sec	45
Annealing	60°C	30 sec	
Extension	72°C	30 sec	
Denaturation	95°C	1 min	1
Annealing/Extension	60°C	1 min	1
Melt curve	55°C	15 sec	0.5°C stepwise increse in temperature
End	4°C	hold	

Table 6.8 Routinely used qPCR program.

6.3.3 Working with proteins

6.3.3.1 Protein extraction

Plates with adherent cells were placed on ice and washed with cold PBS. After aspiration of all PBS the cells were lysed with 100-250 µl Laemmli-buffer (see section 6.1.12) and scraped off the dish with a cell scraper. The proteins were collected in Eppendorf-cups.

Cells grown as spheres were span, washed with cold PBS. After aspiration of all PBS the cell pellet was resuspended in 80-200 µl Laemmli-buffer. The proteins were collected in Eppendorf-tubes. Proteins were stored at -20 °C.

6.3.3.2 Determination of protein concentration

The concentration of proteins was determined with the colorimetric DC Protein Assay Reagents Package (#500-01116, BIO-RAD). The main principle behind this method is a combination of the reactions of copper ions with the peptide bonds under alkaline conditions (the Biuret test) with the oxidation of aromatic protein residues which leads to colour development which can be determined by absorbance measurement between 650 and 750 nm. Protein concentration was determined using the colorimetric DC Protein Assay Reagents Package (BIO-RAD # 500-0116). The alkaline copper tartrate solution (Reagent A), the diluted Folin Reagent (Reagent B) and Reagent S were prepared according to the manual. In an ELISA plate 25 µl of the mixture of reagent B and S were added to the sample (5 µl of protein lysate) and combined with 200 µl reagent B. After 15 min incubation at RT absorbance was measured at 750 nm in a plate reader. Pure Laemmli buffer was measured as a blank. The protein concentration was determined using a calibration curve measured with increasing concentrations of BSA (bovine serum albumin). Afterwards sample buffer (see section 6.1.12) was added to the protein lysate in a ratio 1:3 and the sample heated at 95 °C for 5 min to denature the proteins.

6.3.3.3 SDS-PAGE (Sodium-Dodecyl-Sulfate-Poly Acrylamide Gel Electrophoresis)/Western Blot

The principle behind this method lies in separation of proteins according to their size. Due to binding of SDS, proteins have identical charge per unit mass, which leads to a size depending fractionation. Electrophoresis was carried out by standard discontinuous SDS-polyacrylamide denaturing gel electrophoresis in Mini-Protean Tetra cells (BIO-RAD). Depending on the size of the protein being analysed 8 % or 12 % separating gels were prepared (see section 6.1.12). Separated proteins were transferred electrophoretically to PVDF membranes (Hybond ECL, Amersham) at 100 mA per gel for 2 h using the Wet Blot System from BioRad. Membranes were incubated for 1 h in 5 % milk blocking buffer (PBS, 0.1 % Tween-20, 5 % milk powder) to prevent unspecific antibody binding followed by primary antibody incubation in the blocking buffer at 4°C overnight. Blots were rinsed 3 times (15 min each) in washing buffer (PBS, 0.1 % Tween 20) and incubated for 1 h at RT with the appropriate secondary HRP-conjugated antibody diluted in blocking buffer. After three times washing with washing buffer and once with PBS (each 15 min), chemiluminescent signal was produced using ECL Western Blotting Detection System (Thermo Scientific), ECL plus System (Perkin Elmer) or ECL Pico/Femto System (Thermo Scientific) depending on the abundance of the protein and peroxidase activity of the secondary antibody. The membrane was put into a developing cassette and the luminescent signals developed on a radiographic film (Thermo Scientific) with exposure times of 1 sec to 1 h, depending on the signal strength.

6.3.3.4 Western blot membrane stripping

To re-incubate the membrane with another primary antibody, the membrane was incubated in stripping buffer (see section 6.1.12) for 1 h at RT and subsequently blocked with 5 % blocking buffer (see section 6.1.12) again for 1 h. Then the new primary antibody was added and incubated over night at 4 °C. The rest of the procedure was carried out as described above.

6.4.4 Cell culture

6.4.4.1. Isolation of primary glioblastoma cells from human tumor specimen

To isolate and culture primary glioblastoma cells from human tumor specimen the following detailed protocol was used (based on (Seidel, 2015 #226)). All steps of the tissue dissociation were carried out under sterile conditions in a laminar flow cell culture hood to reduce the risk of contamination of the primary culture.

For tissue dissociation and cell isolation the tumour specimen was transferred to a sterile petri dish using autoclaved forceps and washed with PBS 2 times. Hereafter the tissue was cut into small fragments using a sterile scalpel. The fragments were further chopped with a sterile single edged razor blade until the tissue was well minced. The tumour tissue was transferred to a sterile 15 ml tube by flushing the dish with 5 ml activated Dissociation medium 1 and pipetting it with a sterile pipette. The tissue suspension was incubated at 37 °C for 30 min. Every 5 min during the incubation the suspension was mixed with a 5 ml pipette. After incubation the tube was centrifuged at 300 g for five min and the supernatant carefully removed. The pellet was resuspended in 5 ml Dissociation medium 2 and the tube incubated for another 30 min at 37 °C. Again, the suspension was triturated every 5 min during the incubation. After 5 min centrifugation at 300 g the supernatant was removed carefully and the pellet resuspended in 2 ml of Red Blood Cell Lysis Buffer (Roche) and incubated 10 min at RT. 5 ml of PBS were added and the suspension centrifuged again for 5 min at 300 g. Subsequently the pellet was resuspended in 10 ml PBS and the solution filtered over a 70 µm cell strainer (BD Bioscience) into a sterile 50 ml tube. Following another round of centrifugation, the cell pellet was resuspended in 10 ml tumour sphere medium with growth factors. The cells were cultured until there were enough spheres to freeze several cryo vials.

6.4.4.2 Cell culture conditions for established cell lines

All glioblastoma cell lines were cultured in DMEM containing 10 % fetal calf serum on 10 cm tissue culture dishes under adherent conditions. For several experiments glioblastoma cell lines were cultured under tumour sphere conditions: to prevent

attachment of the cells to the plate surface the cell culture dishes were coated with 10 mg/ml pHEMA in 95 % ethanol, dried, rinsed with PBS and plated in tumour sphere medium supplemented with 20 ng/ml EGF and bFGF.

HEK 293 cells were cultured in DMEM supplemented with 10 % fetal calf serum on tissue culture dishes or flasks.

6.4.4.3 Subculturing cells

Tumour sphere cultures of primary glioblastoma cells were split, depending on their size, every 7 to 10 days. The spheres were centrifuged for 3 min at 900 rpm, the supernatant discarded and the pellet was incubated with 1 ml of accutase solution at 37 °C for 15 min. The cell suspension was triturated gently with a 1000 µl pipette tip, 9 ml tumour sphere medium added and filtered over a 40 µm cell strainer. After another round of centrifugation the cells were resuspended in fresh TSM medium including growth factors.

Adherent cells were washed with PBS and covered with 3 ml Trypsin-EDTA solution and incubated at 37 °C for 3 min until the cells detached from the plate. Hereafter 10ml of complete growth medium were added and the cells aspirated by gently pipetting. The cell suspension was centrifuged at 1000 rpm for 3 min, the supernatant discarded and the cells resuspended in fresh complete growth medium and subcultured in ratios between 1:5 and 1:20 depending on the cell line.

6.4.4.4 Cryopreservation of cells

The primary glioblastoma cells should be used at low passage number, as there is a risk of genetic alterations and phenotypic shifts over the course of prolonged culture with multiple passaging. Therefore, a substantial number of aliquots should be cryopreserved at the earliest passage when they can be sufficiently expanded. Subsequently, fresh frozen aliquots should be periodically thawed and cultured for a limited number of passages and new fresh aliquots at low passages should be frozen.

For cryopreservation the primary glioblastoma cells were centrifuged for 3 min at 900 rpm. The pellet of 1 petri dish was resuspended in 2 ml of Cryo-SFM cryopreservation medium and distributed to 2 cryo vials, which were placed into a commercial available cryo-container (#5100-0001, Thermo) used to control the freezing rate of cells. The container was filled with isopropyl alcohol at room temperature, which leads to a freezing rate of 1 °C/min when placed at -80 °C. The following day the vials were transferred to liquid nitrogen for long-term storage.

For adherent cells dishes with 70-90% cell confluence were trypsinized, centrifuged for 3 min at 1000 rpm and resuspended in 2 ml DMEM, 20 % FCS, 10 % DMSO, transferred to 2 cryo vials and frozen as described above.

Cryopreserved cells were rapidly thawed in a water bath at 37 °C and mixed with 10 ml of the corresponding culture medium and seeded on the respective culture dishes. The following day the medium was changed and, if necessary, replaced with medium containing antibiotics for transgene expression or selection.

6.4.4.5 Determining cell number

Cell number was determined using the CASY Cell Counter and Analyzer System Model TT (# 05651697001, Roche Diagnostics GmbH), which works via electronic pulse area analysis and measures cell number, size distribution and viability of a sample. Cell counting was performed by diluting 100µl cell suspension in 10ml CASY ton solution (# 05651808001, Roche Diagnostics GmbH) and analysed according to the manufacturer's instructions.

6.4.4.6 Producing lentiviruses in HEK 293T cells using calcium phosphate transfection

All steps were carried out in a S2 (biosafety level 2) laboratory.

Expression Arrest pGIPZ lentiviral shRNA vectors, as well as the pGIPZ non silencing control were purchased from Open Biosystems. Viral particles were

produced through calcium phosphate co-transfection with lentiviral vector and packaging vectors.

For the calcium phosphate transfection method HEK 293T cells were seeded at a density of 4 x 10^6 cells per T75 tissue culture flask in full medium (DMEM/10 % FCS) the day before transfection. The following day a medium change was performed 2 h before transfection using 9 ml of serum containing medium. For each transfection 25 µg specific lentiviral vector, 12.5 µg of ENV plasmid (p-CL2-VSV-G) and 12.5 µg of core packaging plasmid (pS-PAX2) were added to 450 µl sterile filtered water in a 50 ml tube. Additionally 50 µl of 2.5 M $CaCl_2$ were added. DNA was precipitated by dropwise addition 500 µl of 2x HBS to the DNA/$CaCl_2$ mixture while vortexing the mixture vigorously. After additional vortexing for one min, the mixture was incubated at RT for 30 min. In the meantime 10 µl of 10 mM chloroquine stock (final concentration 10 µM, #C6628-25g, Sigma) was added to the flask. 1 ml of precipitated DNA solution was slowly pipetted into the dish and cells were placed at 37 °C for up to 16 h. The transfection mixture was aspirated and replaced by 10 ml of standard culture medium. The virus containing supernatant was collected 48 and 72 h post-transfection into a sterile tube, which was stored at 4 °C. Addition of 10 ml fresh standard culture medium was carried out by pipetting slowly at the rim of the flask as HEK293T cells easily detach. Transfection efficiency could be monitored microscopically for expression of EmGFP.

Before concentrating the virus, the supernatant was filtered through a sterile, 0.45 µm low protein binding filter (Millex-HV 0.45 µm PVDF filters, Millipore #SLHVR25LS) to remove any remaining cellular debris. Viral supernatant was pipetted into a sterile 38.5 ml ultracentrifuge tube (PA thick-walled-UC-tube, Herolab), which was already placed in the centrifuge bucket on a balance under the tissue culture hood. Tubes were balanced to 0.1 g exactly and ultracentrifugation was performed at 20000 g for 4 h at 4 °C in a Sorvall Pro 80 Ultracentrifuge and an AH-629 swinging bucket rotor. The supernatant was discarded by decanting and residual liquid was removed by placing the tube upside down on a beforehand UV-lighted paper for a few min. The desired resuspension volume (100 µl-250 µl) of DMEM (no serum) was pipetted at the bottom of the tube. In order to dislodge the viral particles from the protein pellet the suspension was incubated for 5-10 min at 4 °C and then gently pipetted about 30 times up and down trying to avoid formation of air bubbles. The resuspended pellet

was transferred to a sterile 1.5 ml tube and centrifuged in a microfuge at full speed for 5 min at 4 °C. The supernatant was placed in a new, sterile 1,5 ml tube, aliquoted into multiple vials at 10-20 µl and stored at -80 °C. Usually the virus production per lentiviral vector was performed at least in duplicates and the concentrated virus was combined at the end to obtain higher viral titers.

6.4.4.7 Titration of lentiviral particles

For determining the virus titer 2,5 x 10^4 G55TL cells were seeded in 24 wells and titration was performed according to the manufacturer's directions including the addition of 8 µg/ml polybrene (#H9268-5g, Sigma) (Manual: Trans-Lentiviral shRNA Bulk Packaging System). Transduced cells were counted as described in the manual and transducing units per ml determined using the following formula:

Number of TurboGFP positive colonies counted x dilution factor x 40 = # TU/ml

The final TU/ml was obtained by assessing the average from the number of TU/ml of the successive dilutions.

6.4.4.8 Lentiviral transduction of cells

All steps were carried out in a S2 (biosafety level 2) laboratory.

6.4.4.8.1 Stable transduction of primary glioblastoma cell lines

Depending on the cell line and desired multiplicity of infection (MOI), primary glioblastoma cells were seeded at a density between 5x10^4 (12-well plate, 400 µl total volume including medium, polybrene and virus stock) and 1x10^6 (6-well plate, 800 µl total volume including medium, polybrene and virus stock) cells on cell culture multiwell plates coated with laminin (Sigma-Aldrich # L2020 solution in PBS (10 µg/ml), incubated at 37 °C for 3-5 h) in serum free tumour sphere medium without antibiotics, containing 8 µg/ml polybrene.

Lentiviral particles were added according to the desired MOI and the cells were incubated overnight. The following day the cells were washed with PBS and new tumor sphere medium was added. Selection was started with the corresponding antibiotic two days after transduction. Five days after viral transduction, cells were detached from the monolayer on laminin using accutase and seeded as sphere cultures in 6-well suspension culture plates in tumour sphere medium.

6.4.4.8.2 Stable transduction of glioblastoma cell lines

Depending on the cell line and desired MOI cells were seeded at a density of 5 x 10^3 and 5 x 10^5 cell per well in a 24-well cell culture plate (600 µl total volume including medium, polybrene and virus stock) in DMEM/10 % FCS containing 8 µg/ml polybrene. Lentiviral particles were added according to the desired MOI and the cells were incubated overnight. The following day cells were washed with PBS and new medium was added. In the presence of a selection marker, selection was started with the corresponding antibiotic. When the cells reached a confluence of around 80 % they were split to larger cell culture dishes.

6.4.4.9 Hypoxic incubation of cells

Before cells were cultured under hypoxic conditions medium was changed in all corresponding samples of the experiment to be compared. For hypoxic treatment cells were grown at 1 % O_2 and 5 % CO_2 for the indicated time points in an O_2 control Hypoxic Workstation (Coy Lab, Grass Lake, USA).

6.4.4.10 Sphere formation assay

For the determination of secondary sphere formation (sphere forming units (SFU)) cells were seeded at a density of 1x10^6 cells on either petri dishes (primary glioblastoma cells) or pHEMA coated tissue culture dishes (glioblastoma cell lines) in tumour sphere medium for 7 days. The cells were then split to suspension 6-well

plates (primary glioblastoma cells, 1000 cells per well) or pHEMA coated 6-well tissue culture plates (glioblastoma cell lines, 1000 cells per well) with 6 wells per condition. Spheres consisting of 4 or more cells were counted and presented as the percentage of sphere forming cells after 7 days.

6.4.4.11 Fluorescence activated cell sorting (FACS)

Cells were seeded 3 days before performing the FACS experiment into 6 well dishes (100.000 cells per well). Cells were seeded in six replicates. In addition three additional wells were seeded for IgG control, unstained control and GFP control.

The cells were dissociated with accutase containing 100 U/ml DNase I for 15 min at 37 °C. Afterwards the cells were cooled down on ice and 9ml staining buffer added and the cells were triturated and centrifuged at 4 °C for 3 min at a speed of 900 rpm.

The supernatant was discarded by inverting the tube and the cells were resuspended in 3.5 ml staining buffer. A cell strainer was placed on a FACS tube (# 55.1579, Sarstedt) and the cells were passed through it. Again the cells were centrifuged at 4 °C at 900 rpm for 3 min. The centrifugation was followed by two washing steps. The supernatant was discarded by inverting the tube. Approximately 100 µl buffer were left in the tube. 20 µl (60 µg) of normal mouse IgG (# 10400C, Invitrogen) was added to block unspecific binding. Cells were incubated on ice in the fridge for 20 min. The fluorophore-coupled antibody against CD15 (# 642917, BD Horizon) or IgG control (# 561286, BD Horizon) was added (5 µg/ml) and incubated, protected from light, for 30 min on ice in the fridge. After the antibody incubation the cells were washed 2 times with staining buffer.

For data acquisition with the BD FACS Canto the first step was to perform the compensation measurements and to find the right settings for SSC (side scatter) and FSC (forward scatter) and the suitable voltage values to detect the fluorophores. Following compensation samples were analysed: non-stained cells, dead cells (incubated shortly before measuring with 1 µl of SYTOX red (# S34859, Molecular Probes), GFP control (cells were expressing GFP) and compensation beads (# 01-1111-42, eBioscience) coupled with IgG + used fluorophore. Afterwards the normal

samples were analysed, also incubated with SYTOX to detect the dead cell population.

The acquired data was analysed with FlowJo software to gate the dead cell populations and the CD15 positive cells. The obtained percentages of populations were exported to EXCEL to generate graphs. Dot Plots were exported directly from FlowJo V2.2.

6.4.4.12 Modified Boyden Chamber assay

To assess the ability of cells to migrate through filters with defined pore sizes and/or to invade through a basement membrane matrix such as matrigel a modified Boyden chamber assay was performed. 24 well transwell plates (with 12 polycarbonate membrane inserts with a pore size of 8.0 µm; # 3422 Corning/Costar) were used.

100 µl matrigel (Matrigel # 356234; BD) were mixed with 900 µl TSM (containing EGF and FGF). 700 µl of this mixture was used to resuspend a cell pellet of a particular cell number (for G55 100.000 cells per well, for 46x 200.000 cells per well). For each condition 6 wells were prepared. 100 µl of the matrigel/cells suspension was pipetted carefully onto the filter in the upper compartment of the insert. The plate was incubated for 1h at 37 °C to allow polymerization of the matrigel. Afterwards 600 µl of TSM containing EGF/FGF and 1 % FCS were added to the lower compartment of the well and 100 µl of TSM containing only EGF/FGF were added to the upper compartment on top of the matrigel. After 18 h incubation at 37 °C the cells were fixed for 10 min by replacing the medium of the lower compartment with 70 % ethanol. The cells were rehydrated by a washing step with 1x PBS and the nuclei of the cells were stained with DAPI (1:5000 in 1x PBS; 10 min incubation). After one last washing step with 1x PBS pictures of the DAPI signal of the upper compartment were taken with a fluorescence microscope using the 2.5x objective (LEICA BM IL LED, camera: LEICA DFC420C). 1 picture of the whole compartment was taken. Afterwards the upper side of the filter was cleaned with a q-tip to remove all cells. The filter of the insert was removed and mounted with the lower side facing upwards to microscope slides with fluorescence mounting medium (Dako). After drying the slides over night at room temperature pictures were taken of the filters as described

above. The amount of cells was analysed with the program ImageJ (http://imagej.nih.gov/ij/). The number of cells that had moved through the filter was divided by the number of cells in the upper compartment and later on normalized to the control cells.

6.4.4.13 Collagen Invasion assay

To assess the invasion ability of a tumour sphere a collagen invasion assay was performed.

A 12 well plate was coated with 300 µl per well of the collagen solution and incubated for 30 min at 37 °C to allow polymerisation of the collagen. 48-72 h old single tumour spheres were picked with a 10 µl pipet tip and placed in the middle of the well. The spheres were covered with 360 µl of the collagen solution and again incubated for 30min for polymerisation. Subsequently pictures of the spheres were taken with a light microscope to record the size of the spheres at time point 0. Afterwards every 24 h pictures were taken to document the invasion of the spheres. The last time point was reached after 96 h. The invasion of the spheres was analysed with the programmes Adobe Photoshop and ImageJ. The invasion was calculated with the formula of the Invasion Index $(Perimeter)^2/Area$

6.4.5 In vivo tumour models

6.4.5.1 Intracranial tumour xenograft models

For intracranial tumour xenograft transplantations mice were anesthetized (through intraperitoneal injection of 150 µl/20 g bodyweight of 2 ml 10 % ketamine, 0.5 ml 2 % xylazine in 9 ml 0.9 % saline) and placed into a stereotactic apparatus (Kopf Instruments). The scalp was disinfected with a swab dipped in 70% ethanol and opened with a type 15 scalpel. A burr hole was made 2mm left of the sagittal suture and 0.5 mm anterior to the bregma using a micro drill 0.7 mm in diameter. The cells, resuspended in cold CO_2 independent medium, were slowly implanted at a depth of 3 mm from the dura using a 2.5 µl Hamilton syringe equipped with an unbeveled 33G

needle. The mice were kept until the development of neurological symptoms and, in case of comparative experiments, sacrificed at the same time point.

Cell lines used for intracranial tumour implantations: G55 nsc (5000 cells in 1µl), G55shSnail/shSlug (5000 cells in 1 µl), 46x nsc (200.000 cell in 2 µl), 46x shSnail/shSlug (200.000 cells in 2 µl)

6.4.5.2 Perfusion and tissue preparation

Intracranial tumor bearing mice were anesthetized (through intraperitoneal injection of 250 µl/20 g bodyweight of 2ml 10% ketamine, 1 ml 2 % xylazine in 9 ml 0.9 % saline) the chest was opened and vascular perfusion was performed using 0.9% saline for 3 min and 4 % PFA as a fixative for 6 min via a 13 gauge needle inserted through the left ventricle. The brains were dissected and additionally fixed in 4 % PFA at 4 °C over night. The brains were dehydrated in 30 % sucrose for about 4 days at 4 °C and subsequently rapidly frozen on dry ice for sectioning with a sliding microtome (Leica # SM2010R). The whole brain was sectioned by collecting 10 x 40 µm sections followed by 4 x 20 µm sections in 14 sequential microcentrifuge tubes containing cryoprotection solution. When the last section was stored in the tube, collection of sections was performed in the first tube again, resulting in brain sections of a 480 µm interval in every microcentrifuge tube. The sections were stored at -20 °C.

6.4.5.3 Quantification of tumour volume and hematoxylin an eosin (HE) staining

The tumour volume of intracranial tumours was quantified on HE stainings.

The hematoxylin solution (# A4840-500, Applichem) consists of an oxidizing agent, most commonly sodium iodide that converts hematoxylin to hematein and a mordent usually aluminium or iron compounds. The hematoxylin-metal complex acts as a basic dye, staining nucleic acids in the nucleus and cytoplasm blue. On the contrary eosin (1% eosin in 70 % EtOH, add 1 drop of concentrated acetic acid per 100 ml),

acting as an alcohol-based acidic dye, stains more basic proteins within the cytoplasm pink.

A series of brain sections covering the whole brain in 480 µm intervals was mounted on microscope slides and dried at room temperature overnight. The slides were fit into a removable glass slide rack and rehydrated in PBS for two min followed by a rinse in ultrapure aqua dest. Hematoxylin staining was performed for 8-10 min in a staining jar. The slides were rinsed in ultrapure aqua dest. and blued in tap water for 2 min, followed by an additional rinse in ultrapure aqua dest. Cytoplasmic eosin staining was performed for 6 min followed by dehydration in an ascending alcohol series (2 times 70 % and 96 % ethanol for 30 s and 2 times for 5 min in 100 % ethanol). Finally the slides were transferred to xylol 2 times for 5 min each and subsequently mounted with Cytoseal™ XYL (Richard-Allen Scientific) and dried under the chemical fume hood.

The tumour volume was calculated by tracing the tumour area using the semi-automated stereological system Stereo Investigator 4.34 (MicroBrightField Inc.) or ImageJ and calculating the volume with the following formula:

V [mm^3] = total tumour area [mm^2] x12 x 0.04 mm (thickness of sections)

6.4.5.4 Analysis of invasiveness of xenograft tumours

The invasive area of the xenograft tumours was analyses with the help of the GFP signal of the injected cells. 10 pictures of the tumour rim and the invasive area per tumour were taken with a fluorescence microscope (LEICA TCS SPE, camera: LEICA DFC420C; 20x objective). With the program ImageJ the length of the tumour rim and the area of the invading tumour cells was measured. The ratio of the invasive front to the initial perimeter of the tumour rim was calculated with the formula *area of the invasive front / length of the tumour rim*.

6.4.6 Immunofluorescence stainings

6.4.6.1 BrdU labelling and staining of cells

5-bromo-2-deoxy-uridine (BrdU) is a synthetic nucleoside and analogue of thymidine that can be incorporated into DNA during DNA synthesis. By using monoclonal antibodies directed against BrdU and enzyme- or fluorochrome-conjugated secondary antibodies, cell proliferation can be assessed.

Cells were cultured as spheres in TSM medium. For each condition triplets were prepared. The cells were separated with accutase and washed with 1x PBS. BrdU was added to the cells to a final concentration of 10 µm and incubated for 10 min at 37 °C. In parallel a control without BrdU treatment was prepared. After the incubation the cells were put directly on ice and 100000 cells transferred on microscope slides using a cytospin centrifuge (Sakura Finetek) (800 rpm, 3min). The cells on the microscope slides were fixed with 4 % PFA for 30 min at 4 °C followed by a short rinse in 1x PBS. Afterwards antigen retrieval was performed by boiling the slides for 5 min in 0.01 M sodium citrate buffer (1.47 g tri sodium citrate in 500 ml H_2O, adjust pH with 1 M HCl), pH 6.0 (before boiling the slides preheat the buffer for 20 min). The slides were cooled down in the buffer for 15min at room temperature followed by 3 washing steps of 2 min each in 1x PBS. After the washing steps the slides were incubated for 30 min in 2 N HCl to denature the BrdU-labelled DNA in the nucleus and make it accessible for antibody binding. Afterwards the slides were immersed 2 times for 5 min in 0.1 M borate buffer (3.8 g di-sodium tetra borate decahydrate in 100ml H_2O), pH 8.5 to neutralize the acid from the step before. Again the slides were washed 3 times 2 min in 1x PBS. For 1h the slides were blocked with 20 % normal goat serum/1xPBS. The primary anti-BrdU antibody (1:200 in 10% normal goat serum/1x PBS) was incubated over night at 4 °C. The next day the slides were washed 3 times 5 min with 1x PBS followed by incubation with the Alexa-568 secondary antibody (1:500 in 10 % normal goat serum/PBS) for 1 h at room temperature. Afterwards the cells were counterstained with DAPI (1:5000 in 1x PBS) to visualize the nuclei. Again the slides were washed with 1x PBS 3 times for 2 min. The cells were mounted with Dako Fluorescence mounting medium. The proliferation was analysed as a percentage of BrdU positive cells in 5 randomly selected 20x fields per slide (3 replicates per condition).

6.4.6.2 Free-floating endomucin staining of 40µm brain sections

Endomucin (endothelial sialomucin) is a protein expressed on endothelial cells. To analyse the vasculature of xenograft tumours a monoclonal anti-mouse Endomucin antibody was used.

The 40 µm brain sections were put in a 24-well plate (per well maximum 3 sections) and permeabilized for 1 h in 1 % Triton X-100/1x PBS at room temperature while shaking on an orbital shaker. Afterwards the sections were blocked with 0.5 % Triton X-100/1x PBS/5 % normal goat serum at room temperature. The primary endomucin antibody (1:500 in blocking buffer (20% normal goat serum/1x PBS/0.01 % Triton X-100)) was added to the sections and incubated for two night at 4 °C while shaking on an orbital shaker.

After the incubation with the primary antibody the sections were washed 3 times for 15 min in 1x PBS/0.01 % Triton X-100 and once with 1x PBS for 15 min. The secondary antibody (goat anti rat Alexa Fluor 568, 1:200 in blocking buffer) was added and incubated over night at 4 °C. The next day the sections were washed 3 times for 15 min with 1x PBS/0.01 % Triton X-100, followed by one washing step with 1x PBS for 15 min. The sections were counterstained with DAPI (1:5000 in 1x PBS) to visualize the nuclei. Afterwards, the sections were washed again 2 times for 5 min with 1x PBS and mounted with fluorescence mounting medium (#S3023 Dako).

The vessel area was analysed as percentage of the total tumour area in 10 pictures per tumour.

6.4.6.3 Phospho-histone 3 staining of 40µm brain sections

To assess the proliferation of tumour cells in xenografts a staining of phospho-histone 3 was performed.

The brain sections were mounted on microscope slides and dried over night at room temperature. The sections were encircled with Cytomation pen (#S2002). Sections were boiled in TE buffer for 5 min, the slides were cooled down for 20 min at room temperature. Afterwards the sections were washed 2 times 5 min in 1x PBS/0.01 %

Triton X-100 followed by one washing step in 1x PBS. To permeabilise the sections they were incubated for 4 h at room temperature in blocking buffer. The primary antibody against human-phospho Histone 3 was diluted 1:200 in incubation buffer (10% normal goat serum/1xPBS/0.01% TritonX-100) and the slices were incubated for two nights at 4°C in a humidified chamber.

After the incubation with the primary antibody the slices were washed in 1x PBS/0.01 % Triton X-100 several h (changed 2 times). The rest of the day the slices were washed in 1x PBS. The secondary antibody was diluted in 1:500 in incubation buffer and the slices were incubated over night at room temperature in a humidified chamber. The next day the slices were washed several h in 1x PBS/0.01 % Triton X-100 (two changes) followed by washing once in 1x PBS for the rest of the day. The slices were counterstained with DAPI (1:5000 in PBS) to visualize the nuclei. Afterwards the slices were washed again 3 times 5min in PBS and then mounted with fluorescence mounting medium (#S3023 Dako). The amount of proliferating cells was analysed by taking 10 pictures per slice with a 10x objective and calculating the number of phospho-histone 3 positive cells per mm^2.

6.4.6.4 Staining of apoptotic cells

To stain apoptotic cells in vitro and in vivo the apoptosis detection kit ApopTag Red *in situ* from Millipore was used. This kit is based on the TUNEL assay and detects double- and single-stranded DNA breaks by labelling the free 3'OH ends of the damaged DNA with fluorescent nucleotides. The procedure was performed according to the manual of the manufacturer.

6.4.7 Statistical analysis

Results are presented as mean + standard error of mean. Statistical comparisons of values were made using the Student's t-test or Mann-Whitney U-test. Statistical significance was assumed at $p < 0.05$ *, $p < 0.01$ **, $p < 0.001$ ***.

7. Literature

Al-Hajj, M., Wicha, M.S., Benito-Hernandez, A., Morrison, S.J., and Clarke, M.F. (2003). Prospective identification of tumorigenic breast cancer cells. Proc Natl Acad Sci U S A *100*, 3983-3988.

Alberga, A., Boulay, J.L., Kempe, E., Dennefeld, C., and Haenlin, M. (1991). The snail gene required for mesoderm formation in Drosophila is expressed dynamically in derivatives of all three germ layers. Development *111*, 983-992.

Anido, J., Saez-Borderias, A., Gonzalez-Junca, A., Rodon, L., Folch, G., Carmona, M.A., Prieto-Sanchez, R.M., Barba, I., Martinez-Saez, E., Prudkin, L.*, et al.* (2010). TGF-beta Receptor Inhibitors Target the CD44(high)/Id1(high) Glioma-Initiating Cell Population in Human Glioblastoma. Cancer Cell *18*, 655-668.

Bao, S., Wu, Q., Li, Z., Sathornsumetee, S., Wang, H., McLendon, R.E., Hjelmeland, A.B., and Rich, J.N. (2008). Targeting cancer stem cells through L1CAM suppresses glioma growth. Cancer Res *68*, 6043-6048.

Bao, S., Wu, Q., McLendon, R.E., Hao, Y., Shi, Q., Hjelmeland, A.B., Dewhirst, M.W., Bigner, D.D., and Rich, J.N. (2006a). Glioma stem cells promote radioresistance by preferential activation of the DNA damage response. Nature *444*, 756-760.

Bao, S., Wu, Q., Sathornsumetee, S., Hao, Y., Li, Z., Hjelmeland, A.B., Shi, Q., McLendon, R.E., Bigner, D.D., and Rich, J.N. (2006b). Stem cell-like glioma cells promote tumor angiogenesis through vascular endothelial growth factor. Cancer Res *66*, 7843-7848.

Bar, E.E. (2011). Glioblastoma, cancer stem cells and hypoxia. Brain Pathol *21*, 119-129.

Barbera, M.J., Puig, I., Dominguez, D., Julien-Grille, S., Guaita-Esteruelas, S., Peiro, S., Baulida, J., Franci, C., Dedhar, S., Larue, L.*, et al.* (2004). Regulation of Snail transcription during epithelial to mesenchymal transition of tumor cells. Oncogene *23*, 7345-7354.

Barrallo-Gimeno, A., and Nieto, M.A. (2005). The Snail genes as inducers of cell movement and survival: implications in development and cancer. Development *132*, 3151-3161.

Bates, R.C., and Mercurio, A.M. (2003). Tumor necrosis factor-alpha stimulates the epithelial-to-mesenchymal transition of human colonic organoids. Mol Biol Cell *14*, 1790-1800.

Batlle, E., Sancho, E., Franci, C., Dominguez, D., Monfar, M., Baulida, J., and Garcia De Herreros, A. (2000). The transcription factor snail is a repressor of E-cadherin gene expression in epithelial tumour cells. Nat Cell Biol *2*, 84-89.

Bhat, K.P., Balasubramaniyan, V., Vaillant, B., Ezhilarasan, R., Hummelink, K., Hollingsworth, F., Wani, K., Heathcock, L., James, J.D., Goodman, L.D.*, et al.* (2013). Mesenchymal differentiation mediated by NF-kappaB promotes radiation resistance in glioblastoma. Cancer Cell *24*, 331-346.

Birchmeier, W., and Behrens, J. (1994). Cadherin expression in carcinomas: role in the formation of cell junctions and the prevention of invasiveness. Biochim Biophys Acta *1198*, 11-26.

Black, K.L. (1997). The Cure for Cancer: Not If but When. Oncologist *2*, IX-X.

Bolos, V., Peinado, H., Perez-Moreno, M.A., Fraga, M.F., Esteller, M., and Cano, A. (2003). The transcription factor Slug represses E-cadherin expression and induces epithelial to mesenchymal transitions: a comparison with Snail and E47 repressors. J Cell Sci *116*, 499-511.

Bonnet, D., and Dick, J.E. (1997). Human acute myeloid leukemia is organized as a hierarchy that originates from a primitive hematopoietic cell. Nat Med *3*, 730-737.

Brabletz, T., Jung, A., Hermann, K., Gunther, K., Hohenberger, W., and Kirchner, T. (1998). Nuclear overexpression of the oncoprotein beta-catenin in colorectal cancer is localized predominantly at the invasion front. Pathol Res Pract *194*, 701-704.

Bradley, C.K., Norton, C.R., Chen, Y., Han, X., Booth, C.J., Yoon, J.K., Krebs, L.T., and Gridley, T. (2013). The snail family gene snai3 is not essential for embryogenesis in mice. PLoS One *8*, e65344.

Brat, D.J., Castellano-Sanchez, A.A., Hunter, S.B., Pecot, M., Cohen, C., Hammond, E.H., Devi, S.N., Kaur, B., and Van Meir, E.G. (2004). Pseudopalisades in glioblastoma are hypoxic, express extracellular matrix proteases, and are formed by an actively migrating cell population. Cancer Res *64*, 920-927.

Brecher, G., Pallavicini, M.G., and Cronkite, E.P. (1993). Competitive repopulation in leukemic and normal bone marrow. Blood Cells *19*, 691-697; discussion 698-707.

Brown, D.V., Daniel, P.M., D'Abaco, G.M., Gogos, A., Ng, W., Morokoff, A.P., and Mantamadiotis, T. (2015). Coexpression analysis of CD133 and CD44 identifies proneural and mesenchymal subtypes of glioblastoma multiforme. Oncotarget *6*, 6267-6280.

Burk, U., Schubert, J., Wellner, U., Schmalhofer, O., Vincan, E., Spaderna, S., and Brabletz, T. (2008). A reciprocal repression between ZEB1 and members of the miR-200 family promotes EMT and invasion in cancer cells. EMBO Rep *9*, 582-589.

Calabrese, C., Poppleton, H., Kocak, M., Hogg, T.L., Fuller, C., Hamner, B., Oh, E.Y., Gaber, M.W., Finklestein, D., Allen, M.*, et al.* (2007). A perivascular niche for brain tumor stem cells. Cancer Cell *11*, 69-82.

Cano, A., Perez-Moreno, M.A., Rodrigo, I., Locascio, A., Blanco, M.J., del Barrio, M.G., Portillo, F., and Nieto, M.A. (2000). The transcription factor snail controls epithelial-mesenchymal transitions by repressing E-cadherin expression. Nat Cell Biol *2*, 76-83.

Canoll, P., and Goldman, J.E. (2008). The interface between glial progenitors and gliomas. Acta Neuropathol *116*, 465-477.

Caussinus, E., and Gonzalez, C. (2005). Induction of tumor growth by altered stem-cell asymmetric division in Drosophila melanogaster. Nat Genet *37*, 1125-1129.

Cavallaro, U., and Christofori, G. (2004). Cell adhesion and signalling by cadherins and Ig-CAMs in cancer. Nat Rev Cancer *4*, 118-132.

Charles, N., Ozawa, T., Squatrito, M., Bleau, A.M., Brennan, C.W., Hambardzumyan, D., and Holland, E.C. (2010). Perivascular nitric oxide activates notch signaling and promotes stem-like character in PDGF-induced glioma cells. Cell Stem Cell *6*, 141-152.

Chinot, O.L., Wick, W., Mason, W., Henriksson, R., Saran, F., Nishikawa, R., Carpentier, A.F., Hoang-Xuan, K., Kavan, P., Cernea, D.*, et al.* (2014). Bevacizumab plus radiotherapy-temozolomide for newly diagnosed glioblastoma. N Engl J Med *370*, 709-722.

Cho, R.W., Wang, X., Diehn, M., Shedden, K., Chen, G.Y., Sherlock, G., Gurney, A., Lewicki, J., and Clarke, M.F. (2008). Isolation and molecular characterization of cancer stem cells in MMTV-Wnt-1 murine breast tumors. Stem Cells *26*, 364-371.

Ciruna, B., and Rossant, J. (2001). FGF signaling regulates mesoderm cell fate specification and morphogenetic movement at the primitive streak. Dev Cell *1*, 37-49.

Claes, A., Idema, A.J., and Wesseling, P. (2007). Diffuse glioma growth: a guerilla war. Acta Neuropathol *114*, 443-458.

Collins, A.T., Berry, P.A., Hyde, C., Stower, M.J., and Maitland, N.J. (2005). Prospective identification of tumorigenic prostate cancer stem cells. Cancer Res *65*, 10946-10951.

Comijn, J., Berx, G., Vermassen, P., Verschueren, K., van Grunsven, L., Bruyneel, E., Mareel, M., Huylebroeck, D., and van Roy, F. (2001). The two-handed E box binding zinc finger protein SIP1 downregulates E-cadherin and induces invasion. Mol Cell *7*, 1267-1278.

Cooper, L.A., Gutman, D.A., Chisolm, C., Appin, C., Kong, J., Rong, Y., Kurc, T., Van Meir, E.G., Saltz, J.H., Moreno, C.S.*, et al.* (2012). The tumor microenvironment

strongly impacts master transcriptional regulators and gene expression class of glioblastoma. Am J Pathol *180*, 2108-2119.

Covello, K.L., Kehler, J., Yu, H., Gordan, J.D., Arsham, A.M., Hu, C.J., Labosky, P.A., Simon, M.C., and Keith, B. (2006). HIF-2alpha regulates Oct-4: effects of hypoxia on stem cell function, embryonic development, and tumor growth. Genes Dev *20*, 557-570.

Delic, S., Lottmann, N., Jetschke, K., Reifenberger, G., and Riemenschneider, M.J. (2012). Identification and functional validation of CDH11, PCSK6 and SH3GL3 as novel glioma invasion-associated candidate genes. Neuropathol Appl Neurobiol *38*, 201-212.

Demuth, T., and Berens, M.E. (2004). Molecular mechanisms of glioma cell migration and invasion. J Neurooncol *70*, 217-228.

Derynck, R., and Zhang, Y.E. (2003). Smad-dependent and Smad-independent pathways in TGF-beta family signalling. Nature *425*, 577-584.

Dirks, P.B. (2006). Cancer: stem cells and brain tumours. Nature *444*, 687-688.

Dominguez, D., Montserrat-Sentis, B., Virgos-Soler, A., Guaita, S., Grueso, J., Porta, M., Puig, I., Baulida, J., Franci, C., and Garcia de Herreros, A. (2003). Phosphorylation regulates the subcellular location and activity of the snail transcriptional repressor. Mol Cell Biol *23*, 5078-5089.

Dong, Q., Cai, N., Tao, T., Zhang, R., Yan, W., Li, R., Zhang, J., Luo, H., Shi, Y., Luan, W*., et al.* (2014). An axis involving SNAI1, microRNA-128 and SP1 modulates glioma progression. PLoS One *9*, e98651.

Du, J., Sun, B., Zhao, X., Gu, Q., Dong, X., Mo, J., Sun, T., Wang, J., Sun, R., and Liu, Y. (2014). Hypoxia promotes vasculogenic mimicry formation by inducing epithelial-mesenchymal transition in ovarian carcinoma. Gynecol Oncol *133*, 575-583.

Eger A, Aigner K, Sonderegger S, Dampier B, Oehler S, Schreiber M, Berx G, Cano A, Beug H, and R., F. (2005). DeltaEF1 is a transcriptional repressor of E-cadherin and regulates epithelial plasticity in breast cancer cells. Oncogene *14*, 2375-2385.

Francescone, R.A., Scully, S., Faibish, M., Taylor, S.L., Oh, D., Moral, L., Yan, W., Bentley, B., and Shao, R. (2011). Role of YKL-40 in the angiogenesis, radioresistance, and progression of glioblastoma. J Biol Chem *286*, 15332-15343.

Franco, D.L., Mainez, J., Vega, S., Sancho, P., Murillo, M.M., de Frutos, C.A., Del Castillo, G., Lopez-Blau, C., Fabregat, I., and Nieto, M.A. (2010). Snail1 suppresses TGF-beta-induced apoptosis and is sufficient to trigger EMT in hepatocytes. J Cell Sci *123*, 3467-3477.

Freije, W.A., Castro-Vargas, F.E., Fang, Z., Horvath, S., Cloughesy, T., Liau, L.M., Mischel, P.S., and Nelson, S.F. (2004). Gene expression profiling of gliomas strongly predicts survival. Cancer Res *64*, 6503-6510.

Galli, R., Binda, E., Orfanelli, U., Cipelletti, B., Gritti, A., De Vitis, S., Fiocco, R., Foroni, C., Dimeco, F., and Vescovi, A. (2004). Isolation and characterization of tumorigenic, stem-like neural precursors from human glioblastoma. Cancer Res *64*, 7011-7021.

Galliher, A.J., Neil, J.R., and Schiemann, W.P. (2006). Role of transforming growth factor-beta in cancer progression. Future Oncol *2*, 743-763.

Giese, A., and Westphal, M. (1996). Glioma invasion in the central nervous system. Neurosurgery *39*, 235-250; discussion 250-232.

Gilbert, M.R., Sulman, E.P., and Mehta, M.P. (2014). Bevacizumab for newly diagnosed glioblastoma. N Engl J Med *370*, 2048-2049.

Ginestier, C., Hur, M.H., Charafe-Jauffret, E., Monville, F., Dutcher, J., Brown, M., Jacquemier, J., Viens, P., Kleer, C.G., Liu, S.*, et al.* (2007). ALDH1 is a marker of normal and malignant human mammary stem cells and a predictor of poor clinical outcome. Cell Stem Cell *1*, 555-567.

Godard, S., Getz, G., Delorenzi, M., Farmer, P., Kobayashi, H., Desbaillets, I., Nozaki, M., Diserens, A.C., Hamou, M.F., Dietrich, P.Y.*, et al.* (2003). Classification of human astrocytic gliomas on the basis of gene expression: a correlated group of genes with angiogenic activity emerges as a strong predictor of subtypes. Cancer Res *63*, 6613-6625.

Gras, B., Jacqueroud, L., Wierinckx, A., Lamblot, C., Fauvet, F., Lachuer, J., Puisieux, A., and Ansieau, S. (2014). Snail family members unequally trigger EMT and thereby differ in their ability to promote the neoplastic transformation of mammary epithelial cells. PLoS One *9*, e92254.

Grau, Y., Carteret, C., and Simpson, P. (1984). Mutations and Chromosomal Rearrangements Affecting the Expression of Snail, a Gene Involved in Embryonic Patterning in DROSOPHILA MELANOGASTER. Genetics *108*, 347-360.

Grego-Bessa, J., Diez, J., Timmerman, L., and de la Pompa, J.L. (2004). Notch and epithelial-mesenchyme transition in development and tumor progression: another turn of the screw. Cell Cycle *3*, 718-721.

Haines, I.E., and Gabor Miklos, G.L. (2014). Bevacizumab for newly diagnosed glioblastoma. N Engl J Med *370*, 2048.

Han, S.P., Kim, J.H., Han, M.E., Sim, H.E., Kim, K.S., Yoon, S., Baek, S.Y., Kim, B.S., and Oh, S.O. (2011). SNAI1 is involved in the proliferation and migration of glioblastoma cells. Cell Mol Neurobiol *31*, 489-496.

Hanahan, D., and Weinberg, R.A. (2011). Hallmarks of cancer: the next generation. Cell *144*, 646-674.

Harris, M.A., Yang, H., Low, B.E., Mukherjee, J., Guha, A., Bronson, R.T., Shultz, L.D., Israel, M.A., and Yun, K. (2008). Cancer stem cells are enriched in the side population cells in a mouse model of glioma. Cancer Res *68*, 10051-10059.

Heddleston, J.M., Li, Z., McLendon, R.E., Hjelmeland, A.B., and Rich, J.N. (2009). The hypoxic microenvironment maintains glioblastoma stem cells and promotes reprogramming towards a cancer stem cell phenotype. Cell Cycle *8*, 3274-3284.

Herranz, N., Pasini, D., Diaz, V.M., Franci, C., Gutierrez, A., Dave, N., Escriva, M., Hernandez-Munoz, I., Di Croce, L., Helin, K.*, et al.* (2008). Polycomb complex 2 is required for E-cadherin repression by the Snail1 transcription factor. Mol Cell Biol *28*, 4772-4781.

Hitoshi, S., Alexson, T., Tropepe, V., Donoviel, D., Elia, A.J., Nye, J.S., Conlon, R.A., Mak, T.W., Bernstein, A., and van der Kooy, D. (2002). Notch pathway molecules are essential for the maintenance, but not the generation, of mammalian neural stem cells. Genes Dev *16*, 846-858.

Hjelmeland, A.B., Wu, Q., Heddleston, J.M., Choudhary, G.S., MacSwords, J., Lathia, J.D., McLendon, R., Lindner, D., Sloan, A., and Rich, J.N. (2011). Acidic stress promotes a glioma stem cell phenotype. Cell Death Differ *18*, 829-840.

Hou, Z., Peng, H., Ayyanathan, K., Yan, K.P., Langer, E.M., Longmore, G.D., and Rauscher, F.J., 3rd (2008). The LIM protein AJUBA recruits protein arginine methyltransferase 5 to mediate SNAIL-dependent transcriptional repression. Mol Cell Biol *28*, 3198-3207.

Hynes, R.O. (2002). Integrins: bidirectional, allosteric signaling machines. Cell *110*, 673-687.

Ikushima, H., Todo, T., Ino, Y., Takahashi, M., Miyazawa, K., and Miyazono, K. (2009). Autocrine TGF-beta signaling maintains tumorigenicity of glioma-initiating cells through Sry-related HMG-box factors. Cell Stem Cell *5*, 504-514.

Jakowlew, S.B. (2006). Transforming growth factor-beta in cancer and metastasis. Cancer Metastasis Rev *25*, 435-457.

Janda, E., Lehmann, K., Killisch, I., Jechlinger, M., Herzig, M., Downward, J., Beug, H., and Grunert, S. (2002). Ras and TGF[beta] cooperatively regulate epithelial cell plasticity and metastasis: dissection of Ras signaling pathways. J Cell Biol *156*, 299-313.

Jin, X., Yin, J., Kim, S.H., Sohn, Y.W., Beck, S., Lim, Y.C., Nam, D.H., Choi, Y.J., and Kim, H. (2011). EGFR-AKT-Smad signaling promotes formation of glioma stem-like

cells and tumor angiogenesis by ID3-driven cytokine induction. Cancer Res *71*, 7125-7134.

Joseph, J.V., Conroy, S., Pavlov, K., Sontakke, P., Tomar, T., Eggens-Meijer, E., Balasubramaniyan, V., Wagemakers, M., den Dunnen, W.F., and Kruyt, F.A. (2015). Hypoxia enhances migration and invasion in glioblastoma by promoting a mesenchymal shift mediated by the HIF1alpha-ZEB1 axis. Cancer Lett *359*, 107-116.

Julien, S., Puig, I., Caretti, E., Bonaventure, J., Nelles, L., van Roy, F., Dargemont, C., de Herreros, A.G., Bellacosa, A., and Larue, L. (2007). Activation of NF-kappaB by Akt upregulates Snail expression and induces epithelium mesenchyme transition. Oncogene *26*, 7445-7456.

Kalluri, R., and Weinberg, R.A. (2009). The basics of epithelial-mesenchymal transition. J Clin Invest *119*, 1420-1428.

Kang, Y., and Massague, J. (2004). Epithelial-mesenchymal transitions: twist in development and metastasis. Cell *118*, 277-279.

Kaufhold, S., and Bonavida, B. (2014). Central role of Snail1 in the regulation of EMT and resistance in cancer: a target for therapeutic intervention. J Exp Clin Cancer Res *33*, 62.

Kaur, H., Phillips-Mason, P.J., Burden-Gulley, S.M., Kerstetter-Fogle, A.E., Basilion, J.P., Sloan, A.E., and Brady-Kalnay, S.M. (2012). Cadherin-11, a marker of the mesenchymal phenotype, regulates glioblastoma cell migration and survival in vivo. Mol Cancer Res *10*, 293-304.

Kim, K., Lu, Z., and Hay, E.D. (2002). Direct evidence for a role of beta-catenin/LEF-1 signaling pathway in induction of EMT. Cell Biol Int *26*, 463-476.

Kondo, M., Wagers, A.J., Manz, M.G., Prohaska, S.S., Scherer, D.C., Beilhack, G.F., Shizuru, J.A., and Weissman, I.L. (2003). Biology of hematopoietic stem cells and progenitors: implications for clinical application. Annu Rev Immunol *21*, 759-806.

Korpal, M., Lee, E.S., Hu, G., and Kang, Y. (2008). The miR-200 family inhibits epithelial-mesenchymal transition and cancer cell migration by direct targeting of E-cadherin transcriptional repressors ZEB1 and ZEB2. J Biol Chem *283*, 14910-14914.

Lapidot, T., Sirard, C., Vormoor, J., Murdoch, B., Hoang, T., Caceres-Cortes, J., Minden, M., Paterson, B., Caligiuri, M.A., and Dick, J.E. (1994). A cell initiating human acute myeloid leukaemia after transplantation into SCID mice. Nature *367*, 645-648.

Lathia, J.D., Gallagher, J., Heddleston, J.M., Wang, J., Eyler, C.E., Macswords, J., Wu, Q., Vasanji, A., McLendon, R.E., Hjelmeland, A.B.*, et al.* (2010). Integrin alpha 6 regulates glioblastoma stem cells. Cell Stem Cell *6*, 421-432.

Leong, K.G., Niessen, K., Kulic, I., Raouf, A., Eaves, C., Pollet, I., and Karsan, A. (2007). Jagged1-mediated Notch activation induces epithelial-to-mesenchymal transition through Slug-induced repression of E-cadherin. J Exp Med *204*, 2935-2948.

Li, Z., Bao, S., Wu, Q., Wang, H., Eyler, C., Sathornsumetee, S., Shi, Q., Cao, Y., Lathia, J., McLendon, R.E.*, et al.* (2009). Hypoxia-inducible factors regulate tumorigenic capacity of glioma stem cells. Cancer Cell *15*, 501-513.

Liao, H., Bai, Y., Qiu, S., Zheng, L., Huang, L., Liu, T., Wang, X., Liu, Y., Xu, N., Yan, X.*, et al.* (2015). MiR-203 downregulation is responsible for chemoresistance in human glioblastoma by promoting epithelial-mesenchymal transition via SNAI2. Oncotarget *6*, 8914-8928.

Liebner, S., Cattelino, A., Gallini, R., Rudini, N., Iurlaro, M., Piccolo, S., and Dejana, E. (2004). Beta-catenin is required for endothelial-mesenchymal transformation during heart cushion development in the mouse. J Cell Biol *166*, 359-367.

Lin, Y., Wu, Y., Li, J., Dong, C., Ye, X., Chi, Y.I., Evers, B.M., and Zhou, B.P. (2010). The SNAG domain of Snail1 functions as a molecular hook for recruiting lysine-specific demethylase 1. EMBO J *29*, 1803-1816.

Liu, L., Salnikov, A.V., Bauer, N., Aleksandrowicz, E., Labsch, S., Nwaeburu, C., Mattern, J., Gladkich, J., Schemmer, P., Werner, J.*, et al.* (2014a). Triptolide reverses hypoxia-induced epithelial-mesenchymal transition and stem-like features in pancreatic cancer by NF-kappaB downregulation. Int J Cancer *134*, 2489-2503.

Liu, Y., Liu, Y., Yan, X., Xu, Y., Luo, F., Ye, J., Yan, H., Yang, X., Huang, X., Zhang, J.*, et al.* (2014b). HIFs enhance the migratory and neoplastic capacities of hepatocellular carcinoma cells by promoting EMT. Tumour Biol *35*, 8103-8114.

Louis, D.N., Ohgaki, H., Wiestler, O.D., Cavenee, W.K., Burger, P.C., Jouvet, A., Scheithauer, B.W., and Kleihues, P. (2007). The 2007 WHO classification of tumours of the central nervous system. Acta Neuropathol *114*, 97-109.

Lu, K.V., Chang, J.P., Parachoniak, C.A., Pandika, M.M., Aghi, M.K., Meyronet, D., Isachenko, N., Fouse, S.D., Phillips, J.J., Cheresh, D.A.*, et al.* (2012). VEGF inhibits tumor cell invasion and mesenchymal transition through a MET/VEGFR2 complex. Cancer Cell *22*, 21-35.

Lu, Z., Ghosh, S., Wang, Z., and Hunter, T. (2003). Downregulation of caveolin-1 function by EGF leads to the loss of E-cadherin, increased transcriptional activity of beta-catenin, and enhanced tumor cell invasion. Cancer Cell *4*, 499-515.

Mahabir, R., Tanino, M., Elmansuri, A., Wang, L., Kimura, T., Itoh, T., Ohba, Y., Nishihara, H., Shirato, H., Tsuda, M.*, et al.* (2014). Sustained elevation of Snail promotes glial-mesenchymal transition after irradiation in malignant glioma. Neuro Oncol *16*, 671-685.

Mahesparan, R., Read, T.A., Lund-Johansen, M., Skaftnesmo, K.O., Bjerkvig, R., and Engebraaten, O. (2003). Expression of extracellular matrix components in a highly infiltrative in vivo glioma model. Acta Neuropathol *105*, 49-57.

Mani, S.A., Guo, W., Liao, M.J., Eaton, E.N., Ayyanan, A., Zhou, A.Y., Brooks, M., Reinhard, F., Zhang, C.C., Shipitsin, M.*, et al.* (2008). The epithelial-mesenchymal transition generates cells with properties of stem cells. Cell *133*, 704-715.

Massague, J. (2008). TGFbeta in Cancer. Cell *134*, 215-230.

Massague, J., and Wotton, D. (2000). Transcriptional control by the TGF-beta/Smad signaling system. EMBO J *19*, 1745-1754.

Meidhof, S., Brabletz, S., Lehmann, W., Preca, B.T., Mock, K., Ruh, M., Schuler, J., Berthold, M., Weber, A., Burk, U.*, et al.* (2015). ZEB1-associated drug resistance in cancer cells is reversed by the class I HDAC inhibitor mocetinostat. EMBO Mol Med *7*, 831-847.

Mikheeva, S.A., Mikheev, A.M., Petit, A., Beyer, R., Oxford, R.G., Khorasani, L., Maxwell, J.P., Glackin, C.A., Wakimoto, H., Gonzalez-Herrero, I.*, et al.* (2010). TWIST1 promotes invasion through mesenchymal change in human glioblastoma. Mol Cancer *9*, 194.

Molofsky, A.V., Pardal, R., Iwashita, T., Park, I.K., Clarke, M.F., and Morrison, S.J. (2003). Bmi-1 dependence distinguishes neural stem cell self-renewal from progenitor proliferation. Nature *425*, 962-967.

Mu, D., Cambier, S., Fjellbirkeland, L., Baron, J.L., Munger, J.S., Kawakatsu, H., Sheppard, D., Broaddus, V.C., and Nishimura, S.L. (2002). The integrin alpha(v)beta8 mediates epithelial homeostasis through MT1-MMP-dependent activation of TGF-beta1. J Cell Biol *157*, 493-507.

Myazono, K. (2009). Transforming growth factor-beta signaling in epithelial-mesenchymal transition and progression of cancer. Proc Jpn Acad Ser B Phys Biol Sci *85*, 314-323.

Myung, J.K., Choi, S.A., Kim, S.K., Wang, K.C., and Park, S.H. (2014). Snail plays an oncogenic role in glioblastoma by promoting epithelial mesenchymal transition. Int J Clin Exp Pathol *7*, 1977-1987.

Nagano, O., Murakami, D., Hartmann, D., De Strooper, B., Saftig, P., Iwatsubo, T., Nakajima, M., Shinohara, M., and Saya, H. (2004). Cell-matrix interaction via CD44 is independently regulated by different metalloproteinases activated in response to extracellular Ca(2+) influx and PKC activation. J Cell Biol *165*, 893-902.

Nakada, M., Nakada, S., Demuth, T., Tran, N.L., Hoelzinger, D.B., and Berens, M.E. (2007). Molecular targets of glioma invasion. Cell Mol Life Sci *64*, 458-478.

Nieto, M.A. (2002). The snail superfamily of zinc-finger transcription factors. Nat Rev Mol Cell Biol *3*, 155-166.

Norden, A.D., and Wen, P.Y. (2006). Glioma therapy in adults. Neurologist *12*, 279-292.

Noushmehr, H., Weisenberger, D.J., Diefes, K., Phillips, H.S., Pujara, K., Berman, B.P., Pan, F., Pelloski, C.E., Sulman, E.P., Bhat, K.P.*, et al.* (2010). Identification of a CpG island methylator phenotype that defines a distinct subgroup of glioma. Cancer Cell *17*, 510-522.

Nutt, C.L., Mani, D.R., Betensky, R.A., Tamayo, P., Cairncross, J.G., Ladd, C., Pohl, U., Hartmann, C., McLaughlin, M.E., Batchelor, T.T.*, et al.* (2003). Gene expression-based classification of malignant gliomas correlates better with survival than histological classification. Cancer Res *63*, 1602-1607.

Ogden, A.T., Waziri, A.E., Lochhead, R.A., Fusco, D., Lopez, K., Ellis, J.A., Kang, J., Assanah, M., McKhann, G.M., Sisti, M.B.*, et al.* (2008). Identification of A2B5+CD133- tumor-initiating cells in adult human gliomas. Neurosurgery *62*, 505-514; discussion 514-505.

Ohgaki, H., and Kleihues, P. (2005). Epidemiology and etiology of gliomas. Acta Neuropathol *109*, 93-108.

Okamoto, I., Kawano, Y., Matsumoto, M., Suga, M., Kaibuchi, K., Ando, M., and Saya, H. (1999). Regulated CD44 cleavage under the control of protein kinase C, calcium influx, and the Rho family of small G proteins. J Biol Chem *274*, 25525-25534.

Ouyang, G., Wang, Z., Fang, X., Liu, J., and Yang, C.J. (2010). Molecular signaling of the epithelial to mesenchymal transition in generating and maintaining cancer stem cells. Cell Mol Life Sci *67*, 2605-2618.

Ozdamar, B., Bose, R., Barrios-Rodiles, M., Wang, H.R., Zhang, Y., and Wrana, J.L. (2005). Regulation of the polarity protein Par6 by TGFbeta receptors controls epithelial cell plasticity. Science *307*, 1603-1609.

Ozes, O.N., Mayo, L.D., Gustin, J.A., Pfeffer, S.R., Pfeffer, L.M., and Donner, D.B. (1999). NF-kappaB activation by tumour necrosis factor requires the Akt serine-threonine kinase. Nature *401*, 82-85.

Paez-Ribes, M., Allen, E., Hudock, J., Takeda, T., Okuyama, H., Vinals, F., Inoue, M., Bergers, G., Hanahan, D., and Casanovas, O. (2009). Antiangiogenic therapy elicits malignant progression of tumors to increased local invasion and distant metastasis. Cancer Cell *15*, 220-231.

Park, S.M., Gaur, A.B., Lengyel, E., and Peter, M.E. (2008). The miR-200 family determines the epithelial phenotype of cancer cells by targeting the E-cadherin repressors ZEB1 and ZEB2. Genes Dev *22*, 894-907.

Peinado, H., Ballestar, E., Esteller, M., and Cano, A. (2004). Snail mediates E-cadherin repression by the recruitment of the Sin3A/histone deacetylase 1 (HDAC1)/HDAC2 complex. Mol Cell Biol *24*, 306-319.

Peinado, H., Olmeda, D., and Cano, A. (2007). Snail, Zeb and bHLH factors in tumour progression: an alliance against the epithelial phenotype? Nat Rev Cancer *7*, 415-428.

Peinado, H., Quintanilla, M., and Cano, A. (2003). Transforming growth factor beta-1 induces snail transcription factor in epithelial cell lines: mechanisms for epithelial mesenchymal transitions. J Biol Chem *278*, 21113-21123.

Peiro, S., Escriva, M., Puig, I., Barbera, M.J., Dave, N., Herranz, N., Larriba, M.J., Takkunen, M., Franci, C., Munoz, A.*, et al.* (2006). Snail1 transcriptional repressor binds to its own promoter and controls its expression. Nucleic Acids Res *34*, 2077-2084.

Penuelas, S., Anido, J., Prieto-Sanchez, R.M., Folch, G., Barba, I., Cuartas, I., Garcia-Dorado, D., Poca, M.A., Sahuquillo, J., Baselga, J.*, et al.* (2009). TGF-beta increases glioma-initiating cell self-renewal through the induction of LIF in human glioblastoma. Cancer Cell *15*, 315-327.

Perego, C., Vanoni, C., Massari, S., Raimondi, A., Pola, S., Cattaneo, M.G., Francolini, M., Vicentini, L.M., and Pietrini, G. (2002). Invasive behaviour of glioblastoma cell lines is associated with altered organisation of the cadherin-catenin adhesion system. J Cell Sci *115*, 3331-3340.

Perl, A.K., Wilgenbus, P., Dahl, U., Semb, H., and Christofori, G. (1998). A causal role for E-cadherin in the transition from adenoma to carcinoma. Nature *392*, 190-193.

Phillips, H.S., Kharbanda, S., Chen, R., Forrest, W.F., Soriano, R.H., Wu, T.D., Misra, A., Nigro, J.M., Colman, H., Soroceanu, L.*, et al.* (2006). Molecular subclasses of high-grade glioma predict prognosis, delineate a pattern of disease progression, and resemble stages in neurogenesis. Cancer Cell *9*, 157-173.

Pietras, A., Hansford, L.M., Johnsson, A.S., Bridges, E., Sjolund, J., Gisselsson, D., Rehn, M., Beckman, S., Noguera, R., Navarro, S.*, et al.* (2009). HIF-2alpha maintains an undifferentiated state in neural crest-like human neuroblastoma tumor-initiating cells. Proc Natl Acad Sci U S A *106*, 16805-16810.

Ping, Y.F., Yao, X.H., Jiang, J.Y., Zhao, L.T., Yu, S.C., Jiang, T., Lin, M.C., Chen, J.H., Wang, B., Zhang, R.*, et al.* (2011). The chemokine CXCL12 and its receptor

CXCR4 promote glioma stem cell-mediated VEGF production and tumour angiogenesis via PI3K/AKT signalling. J Pathol *224*, 344-354.

Pouyssegur, J., Dayan, F., and Mazure, N.M. (2006). Hypoxia signalling in cancer and approaches to enforce tumour regression. Nature *441*, 437-443.

Pries, A.R., Hopfner, M., le Noble, F., Dewhirst, M.W., and Secomb, T.W. (2010). The shunt problem: control of functional shunting in normal and tumour vasculature. Nat Rev Cancer *10*, 587-593.

Purow, B.W., Haque, R.M., Noel, M.W., Su, Q., Burdick, M.J., Lee, J., Sundaresan, T., Pastorino, S., Park, J.K., Mikolaenko, I.*, et al.* (2005). Expression of Notch-1 and its ligands, Delta-like-1 and Jagged-1, is critical for glioma cell survival and proliferation. Cancer Res *65*, 2353-2363.

Read, T.A., Fogarty, M.P., Markant, S.L., McLendon, R.E., Wei, Z., Ellison, D.W., Febbo, P.G., and Wechsler-Reya, R.J. (2009). Identification of CD15 as a marker for tumor-propagating cells in a mouse model of medulloblastoma. Cancer Cell *15*, 135-147.

Reya, T., Morrison, S.J., Clarke, M.F., and Weissman, I.L. (2001). Stem cells, cancer, and cancer stem cells. Nature *414*, 105-111.

Rickman, D.S., Bobek, M.P., Misek, D.E., Kuick, R., Blaivas, M., Kurnit, D.M., Taylor, J., and Hanash, S.M. (2001). Distinctive molecular profiles of high-grade and low-grade gliomas based on oligonucleotide microarray analysis. Cancer Res *61*, 6885-6891.

Romashkova, J.A., and Makarov, S.S. (1999). NF-kappaB is a target of AKT in anti-apoptotic PDGF signalling. Nature *401*, 86-90.

Sahlgren, C., Gustafsson, M.V., Jin, S., Poellinger, L., and Lendahl, U. (2008). Notch signaling mediates hypoxia-induced tumor cell migration and invasion. Proc Natl Acad Sci U S A *105*, 6392-6397.

Sakisaka, T., and Takai, Y. (2005). Cell adhesion molecules in the CNS. J Cell Sci *118*, 5407-5410.

Sasaki, H., Yoshida, K., Ikeda, E., Asou, H., Inaba, M., Otani, M., and Kawase, T. (1998). Expression of the neural cell adhesion molecule in astrocytic tumors: an inverse correlation with malignancy. Cancer *82*, 1921-1931.

Savary, K., Caglayan, D., Caja, L., Tzavlaki, K., Bin Nayeem, S., Bergstrom, T., Jiang, Y., Uhrbom, L., Forsberg-Nilsson, K., Westermark, B.*, et al.* (2013). Snail depletes the tumorigenic potential of glioblastoma. Oncogene *32*, 5409-5420.

Schmalhofer, O., Brabletz, S., and Brabletz, T. (2009). E-cadherin, beta-catenin, and ZEB1 in malignant progression of cancer. Cancer Metastasis Rev *28*, 151-166.

Schulte, J.D., Srikanth, M., Das, S., Zhang, J., Lathia, J.D., Yin, L., Rich, J.N., Olson, E.C., Kessler, J.A., and Chenn, A. (2013). Cadherin-11 regulates motility in normal cortical neural precursors and glioblastoma. PLoS One *8*, e70962.

Seidel, S., Garvalov, B.K., Wirta, V., von Stechow, L., Schanzer, A., Meletis, K., Wolter, M., Sommerlad, D., Henze, A.T., Nister, M.*, et al.* (2010). A hypoxic niche regulates glioblastoma stem cells through hypoxia inducible factor 2 alpha. Brain *133*, 983-995.

Sekiya, S., and Suzuki, A. (2011). Glycogen synthase kinase 3 beta-dependent Snail degradation directs hepatocyte proliferation in normal liver regeneration. Proc Natl Acad Sci U S A *108*, 11175-11180.

Sell, S. (2004). Stem cell origin of cancer and differentiation therapy. Crit Rev Oncol Hematol *51*, 1-28.

Sell, S. (2006). Potential gene therapy strategies for cancer stem cells. Curr Gene Ther *6*, 579-591.

Sell, S., and Pierce, G.B. (1994). Maturation arrest of stem cell differentiation is a common pathway for the cellular origin of teratocarcinomas and epithelial cancers. Lab Invest *70*, 6-22.

Shaikh, D., Zhou, Q., Chen, T., Ibe, J.C., Raj, J.U., and Zhou, G. (2012). cAMP-dependent protein kinase is essential for hypoxia-mediated epithelial-mesenchymal transition, migration, and invasion in lung cancer cells. Cell Signal *24*, 2396-2406.

Shen, Q., Goderie, S.K., Jin, L., Karanth, N., Sun, Y., Abramova, N., Vincent, P., Pumiglia, K., and Temple, S. (2004). Endothelial cells stimulate self-renewal and expand neurogenesis of neural stem cells. Science *304*, 1338-1340.

Shimono, Y., Zabala, M., Cho, R.W., Lobo, N., Dalerba, P., Qian, D., Diehn, M., Liu, H., Panula, S.P., Chiao, E.*, et al.* (2009). Downregulation of miRNA-200c links breast cancer stem cells with normal stem cells. Cell *138*, 592-603.

Siebzehnrubl, F.A., Silver, D.J., Tugertimur, B., Deleyrolle, L.P., Siebzehnrubl, D., Sarkisian, M.R., Devers, K.G., Yachnis, A.T., Kupper, M.D., Neal, D.*, et al.* (2013). The ZEB1 pathway links glioblastoma initiation, invasion and chemoresistance. EMBO Mol Med *5*, 1196-1212.

Siegel, P.M., and Massague, J. (2003). Cytostatic and apoptotic actions of TGF-beta in homeostasis and cancer. Nat Rev Cancer *3*, 807-821.

Singh, S.K., Clarke, I.D., Terasaki, M., Bonn, V.E., Hawkins, C., Squire, J., and Dirks, P.B. (2003). Identification of a cancer stem cell in human brain tumors. Cancer Res *63*, 5821-5828.

Soeda, A., Park, M., Lee, D., Mintz, A., Androutsellis-Theotokis, A., McKay, R.D., Engh, J., Iwama, T., Kunisada, T., Kassam, A.B.*, et al.* (2009). Hypoxia promotes

expansion of the CD133-positive glioma stem cells through activation of HIF-1alpha. Oncogene *28*, 3949-3959.

Son, M.J., Woolard, K., Nam, D.H., Lee, J., and Fine, H.A. (2009). SSEA-1 is an enrichment marker for tumor-initiating cells in human glioblastoma. Cell Stem Cell *4*, 440-452.

Spaderna, S., Schmalhofer, O., Hlubek, F., Berx, G., Eger, A., Merkel, S., Jung, A., Kirchner, T., and Brabletz, T. (2006). A transient, EMT-linked loss of basement membranes indicates metastasis and poor survival in colorectal cancer. Gastroenterology *131*, 830-840.

Sturm, D., Witt, H., Hovestadt, V., Khuong-Quang, D.A., Jones, D.T., Konermann, C., Pfaff, E., Tonjes, M., Sill, M., Bender, S*., et al.* (2012). Hotspot mutations in H3F3A and IDH1 define distinct epigenetic and biological subgroups of glioblastoma. Cancer Cell *22*, 425-437.

Subramanian, A., Harris, A., Piggott, K., Shieff, C., and Bradford, R. (2002). Metastasis to and from the central nervous system--the 'relatively protected site'. Lancet Oncol *3*, 498-507.

Sullivan, D.E., Ferris, M., Nguyen, H., Abboud, E., and Brody, A.R. (2009). TNF-alpha induces TGF-beta1 expression in lung fibroblasts at the transcriptional level via AP-1 activation. J Cell Mol Med *13*, 1866-1876.

Thiery, J.P. (2002). Epithelial-mesenchymal transitions in tumour progression. Nat Rev Cancer *2*, 442-454.

Thiery, J.P. (2003). Epithelial-mesenchymal transitions in development and pathologies. Curr Opin Cell Biol *15*, 740-746.

Thiery, J.P., Acloque, H., Huang, R.Y., and Nieto, M.A. (2009). Epithelial-mesenchymal transitions in development and disease. Cell *139*, 871-890.

Thuault, S., Valcourt, U., Petersen, M., Manfioletti, G., Heldin, C.H., and Moustakas, A. (2006). Transforming growth factor-beta employs HMGA2 to elicit epithelial-mesenchymal transition. J Cell Biol *174*, 175-183.

Toyota, M., Ahuja, N., Suzuki, H., Itoh, F., Ohe-Toyota, M., Imai, K., Baylin, S.B., and Issa, J.P. (1999). Aberrant methylation in gastric cancer associated with the CpG island methylator phenotype. Cancer Res *59*, 5438-5442.

Trepant, A.L., Bouchart, C., Rorive, S., Sauvage, S., Decaestecker, C., Demetter, P., and Salmon, I. (2015). Identification of OLIG2 as the most specific glioblastoma stem cell marker starting from comparative analysis of data from similar DNA chip microarray platforms. Tumour Biol *36*, 1943-1953.

van den Boom, J., Wolter, M., Kuick, R., Misek, D.E., Youkilis, A.S., Wechsler, D.S., Sommer, C., Reifenberger, G., and Hanash, S.M. (2003). Characterization of gene

expression profiles associated with glioma progression using oligonucleotide-based microarray analysis and real-time reverse transcription-polymerase chain reaction. Am J Pathol *163*, 1033-1043.

Venere, M., Fine, H.A., Dirks, P.B., and Rich, J.N. (2011). Cancer stem cells in gliomas: identifying and understanding the apex cell in cancer's hierarchy. Glia *59*, 1148-1154.

Verhaak, R.G., Hoadley, K.A., Purdom, E., Wang, V., Qi, Y., Wilkerson, M.D., Miller, C.R., Ding, L., Golub, T., Mesirov, J.P.*, et al.* (2010). Integrated genomic analysis identifies clinically relevant subtypes of glioblastoma characterized by abnormalities in PDGFRA, IDH1, EGFR, and NF1. Cancer Cell *17*, 98-110.

Vinas-Castells, R., Beltran, M., Valls, G., Gomez, I., Garcia, J.M., Montserrat-Sentis, B., Baulida, J., Bonilla, F., de Herreros, A.G., and Diaz, V.M. (2010). The hypoxia-controlled FBXL14 ubiquitin ligase targets SNAIL1 for proteasome degradation. J Biol Chem *285*, 3794-3805.

Visvader, J.E., and Lindeman, G.J. (2008). Cancer stem cells in solid tumours: accumulating evidence and unresolved questions. Nat Rev Cancer *8*, 755-768.

Visvader, J.E., and Lindeman, G.J. (2012). Cancer stem cells: current status and evolving complexities. Cell Stem Cell *10*, 717-728.

Wellner, U., Schubert, J., Burk, U.C., Schmalhofer, O., Zhu, F., Sonntag, A., Waldvogel, B., Vannier, C., Darling, D., zur Hausen, A.*, et al.* (2009). The EMT-activator ZEB1 promotes tumorigenicity by repressing stemness-inhibiting microRNAs. Nat Cell Biol *11*, 1487-1495.

Wen, P.Y., and Kesari, S. (2008). Malignant gliomas in adults. N Engl J Med *359*, 492-507.

Wenk, M.B., Midwood, K.S., and Schwarzbauer, J.E. (2000). Tenascin-C suppresses Rho activation. J Cell Biol *150*, 913-920.

Wicha, M.S., Liu, S., and Dontu, G. (2006). Cancer stem cells: an old idea--a paradigm shift. Cancer Res *66*, 1883-1890; discussion 1895-1886.

Wipff, P.J., Rifkin, D.B., Meister, J.J., and Hinz, B. (2007). Myofibroblast contraction activates latent TGF-beta1 from the extracellular matrix. J Cell Biol *179*, 1311-1323.

Wu, Y., Deng, J., Rychahou, P.G., Qiu, S., Evers, B.M., and Zhou, B.P. (2009a). Stabilization of snail by NF-kappaB is required for inflammation-induced cell migration and invasion. Cancer Cell *15*, 416-428.

Wu, Y., Evers, B.M., and Zhou, B.P. (2009b). Small C-terminal domain phosphatase enhances snail activity through dephosphorylation. J Biol Chem *284*, 640-648.

Yang, H.W., Menon, L.G., Black, P.M., Carroll, R.S., and Johnson, M.D. (2010). SNAI2/Slug promotes growth and invasion in human gliomas. BMC Cancer *10*, 301.

Yang, Z., Rayala, S., Nguyen, D., Vadlamudi, R.K., Chen, S., and Kumar, R. (2005). Pak1 phosphorylation of snail, a master regulator of epithelial-to-mesenchyme transition, modulates snail's subcellular localization and functions. Cancer Res *65*, 3179-3184.

Yilmaz, M., and Christofori, G. (2009). EMT, the cytoskeleton, and cancer cell invasion. Cancer Metastasis Rev *28*, 15-33.

Yook, J.I., Li, X.Y., Ota, I., Fearon, E.R., and Weiss, S.J. (2005). Wnt-dependent regulation of the E-cadherin repressor snail. J Biol Chem *280*, 11740-11748.

Zheng, H., Shen, M., Zha, Y.L., Li, W., Wei, Y., Blanco, M.A., Ren, G., Zhou, T., Storz, P., Wang, H.Y.*, et al.* (2014). PKD1 phosphorylation-dependent degradation of SNAIL by SCF-FBXO11 regulates epithelial-mesenchymal transition and metastasis. Cancer Cell *26*, 358-373.

Zhou, B.P., Deng, J., Xia, W., Xu, J., Li, Y.M., Gunduz, M., and Hung, M.C. (2004). Dual regulation of Snail by GSK-3beta-mediated phosphorylation in control of epithelial-mesenchymal transition. Nat Cell Biol *6*, 931-940.

Zhou, B.P., Hu, M.C., Miller, S.A., Yu, Z., Xia, W., Lin, S.Y., and Hung, M.C. (2000). HER-2/neu blocks tumor necrosis factor-induced apoptosis via the Akt/NF-kappaB pathway. J Biol Chem *275*, 8027-8031.

Zhou, Y., Wu, S., Liang, C., Lin, Y., Zou, Y., Li, K., Lu, B., Shu, M., Huang, Y., Zhu, W.*, et al.* (2015). Transcriptional upregulation of microtubule-associated protein 2 is involved in the protein kinase A-induced decrease in the invasiveness of glioma cells. Neuro Oncol.

Index of Figures and Tables

3. Introduction

4. Results

Abbreviations

° C: degree Celsius

µg: microgram

µl: microlitre

µm: micrometre

A2B5: antigen

ADAM: a disintegrin and metalloproteinase

APS: ammoniumpersulfate

ASPHD2: aspartate beta-hydroxylase domain containing 2

BMP7: bone morphogenic protein 7

BrdU: bromodeoxyuridine

BTSC: brain tumour stem cell

C/EBP-β/ δ: CAAT enhancer binding protein

CD133: prominin 1 glycoprotein

CD15: 3-fucosyl-N-acetyl-lactosamine antigen cluster

CD24: cluster of differentiation 24 antigen

CD44: cell surface glycoprotein

CDKN2A: cyclin-dependent kinase inhibitor 2A

CNS: central nervous system

Co: control

coREST: co-repressor of REST (RE1-Silencing Transcription factor)

CPS: cryo-protection solution

CRISPR/Cas9: clustered regularly interspaced short palindromic repeats/caspase 9

CSC: cancer stem cell

CXCR4: CXC-motif chemokine receptor 4

DAPI: 4′,6-Diamidin-2-phenylindol

DEPC: di-ethylpyrocarbonate

DKFZ: Deutsches Krebsforschungszentrum

DLL3: Notch ligand delta like 3

DNA: deoxyribonucleic acid

E-cadherin: epithelial cadherin

ECM: extracellular matrix

EGF: epidermal growth factor

EGFR: epidermal growth factor receptor

EMT: epithelial to mesenchymal transition

FACS: fluorescence activated cell sorting

FBXL14: F-box protein 14

FCS: fetal calf serum

FGF: fibroblast growth factor

g: gram

G34: glycine 34

GABA: gamma-aminobutyric acid

GABRA1: gamma-aminobutyric acid receptor A 1

GBM: glioblastoma multiforme

G-CIMP: CpG-island methylator phenotype

GFP/eGFP: (enhanced) green fluorescence protein

GMT: glial to mesenchymal transition

GSK3β: glycogen synthase kinase 3 beta

h: hour

H&E: haematoxylin and eosin

H3F3A: histone 3 family 3A

HBS: HEPES buffered saline

HDAC: histone deacetylase

HEY1: Hes-related family BHLH transcription factor with YRPW motif 1

HGF: hepatocyte growth factor

HIF: hypoxia inducible factor

Id1: DNA-binding protein inhibitor

IDH1: isocitrate dehydrogenase

IgG:	immunoglobulin G
IKKα:	IκB (inhibitor of kappa B) kinase α
IL:	interleukin
JNK:	c-Jun N-terminal kinase
K27:	lysine 27
l:	litre
LB:	Luria-Bertani
LOX:	lysyl oxidase
LSD:	lysine specific demethylase
LTBP:	latent TGFβ-binding proteins
M:	molar
MAML3:	mastermind-like protein 3
MAP2:	microtubule associated protein 2
Mes:	mesenchymal
mg:	milligram
min:	minute
miRNA:	micro ribonucleic acid
ml:	milliltre
mm:	millimetre
mM:	millimolar
MMP:	matrix metalloproteinase
MOI:	multiplicity of infection
MRI:	magnetic resonance imaging
mRNA:	messenger ribonucleic acid
N-cadherin:	neural cadherin
NCAM:	neural cell adhesion molecule 1
NEFL:	neurofilament, light polypeptide
NES:	nuclear export sequence
NF1:	neurofibromin 1
NFATc2:	nuclear factor of activated T cells 2

NF-κB: nuclear factor kappa B

ng: nanogram

nm: nanometre

Oct4: octamer-binding transcription factor 4

Olig2: oligodendroglial marker 2

p53 or TP53: cellular tumour antigen p53

PAK1: p21 activated kinase 1

PB: phosphate buffer

PBS: phosphate buffered saline

PCAM1: Platelet endothelial cell adhesion molecule

PCNA: proliferating cell nuclear antigen

PCR: polymerase chain reaction

PDGF: platelet derived growth factor

PDGFRA: platelet derived growth factor receptor A

PFA: paraformaldehyde

PI3K-Akt: Phosphatidylinositol 3-kinase-Akt pathway

PKD1 polycystin 1

PN: proneural

PRC2: polycomb repressor complex 2

PRMT5: protein Arginine Methyltransferase 5

Prolif: proliferative

PTEN: phosphatase and tensin homologue

q-RT PCR: quantitative real time polymerase chain reaction

Ras/ERK: rat sarcoma G-protein/Extracellular Signal-regulated Kinase-1 pathway

RAS-MAPK: rat sarcoma G-protein/ Mitogen-activated protein kinases

RB: retinoblastoma protein

RNA: ribonucleic acid

RT: room temperature

RTK: receptor tyrosine kinase

sec: second

Ser-10: serine 10

SFU: sphere forming units

shRNA: short hairpin ribonucleic acid

SLC12A5: potassium/chloride transporter

SNAG: Snail/Gfi domain

Sox2: sex determining region Y-box 2

SRD: serine rich domain

STAT3: signal transducer and activator of transcription 3

SVZ: subventricular zome

SYT1: synaptotagmin I

TCGA: The Cancer Genome Atlas

TGFβ1: transforming growth factor β1

TNFα: tumour necrosis factor alpha

TOP2A: topoisomerase 2A

TU: transducing units

TUNEL: TdT mediated dUTP-biotin nick end labelling

uPA: urokinase-type plasminogene activator

uPAR: urokinase-type plasminogene activator receptor

VEGF: vascular endothelial growth factor

VHL: von Hippel-Lindau

WHO: world health organisation

Wnt: wingless gene from drosophila melanogaster

YKL40: human chitinase 3 like

ZEB: Zinc finger E-box binding homeobox 1

β-TrCP: beta-transducin repeat containing protein

Acknowledgements

First of all I would like to thank Prof. Till Acker for giving me this interesting Ph.D.-project and the opportunity to work in his institute. Thank you and the head of the research lab Dr. Boyan Garvalov for the excellent guidance, helpful discussions and overall support.

Thanks also to the Ph.D. program of the veterinary medical and human medical faculty to include me into the program. As well I would like to thank the GGL (Giessen Graduate School for the Life Sciences) for giving me excellent training, good support and motivation.

A very important support was also the encouragement and assistance of all current and former members of the Institute for Neuropathology in Giessen. THANK YOU Sabine, Annette, Marion, Conny, Anne, Nuray, Sascha, Manuela, Miao, Alina and Omelyan (especially for the help with the animal experiments). It is indescribable how much it means to have colleagues who support you, who share happiness and anger or desperation with you. I will never forget all of you!

Natürlich möchte ich auch meiner Familie und Benny danken, die mich immer in jeglicher Form unerlässlich unterstützen. Vielen, vielen Dank dafür!

Der Lebenslauf wurde aus der elektronischen Version der Arbeit entfernt.

The curriculum vitae was removed from the electronic version of the paper.